Aus der

Medizinischen Universitätsklinik und Poliklinik Tübingen

Abteilung Innere Medizin I

(Schwerpunkt: Gastroenterologie, Gastrointestinale Onkologie, Hepatologie, Infektiologie und Geriatrie)

Characterization of FGFR2 fusions in cholangiocarcinoma of patients from the Molecular Tumor Board Tuebingen

Inaugural-Dissertation
zur Erlangung des Doktorgrades
der Medizin

der Medizinischen Fakultät
der Eberhard Karls Universität
zu Tübingen

vorgelegt von

Kleinhenz, Fabian

2025

Dekan:	Professor Dr. B. Pichler
1. Berichterstatter:	Professor Dr. med. M. Bitzer
2. Berichterstatter:	Professor Dr. med. A. L. Mihaljevic
3. Berichterstatter:	Professor Dr. med. H. Becker

Tag der Disputation: 18.03.2025

Meinen Eltern

Table of contents

Abbreviations

AC – ampullary cancer
ATP – adenosine triphosphate
BTC – biliary tract cancer
BSA – bovine serum albumin
CA19-9 – carbohydrate antigen 19-9
CCA – cholangiocarcinoma
cfDNA – cell-free DNA
CR – complete response
dCCA – distal cholangiocarcinoma
DMEM – Dulbecco's Modified Eagle's Medium
DMSO – dimethyl sulfoxide
eCCA – extrahepatic cholangiocarcinoma
FBS – fetal bovine serum
FDA – food and drug administration
FGF – fibroblast growth factor
FGFR – fibroblast growth factor receptor
FRS2 – fibroblast growth factor receptor substrate 2
GBC – gallbladder cancer
GFP – green fluorescence protein
iCCA – intrahepatic cholangiocarcinoma
Ig – immunoglobulin
MTB – molecular tumor board
ORR – overall response rate
OS – overall survival
PBS – phosphate-buffered saline
pCCA – perihilar cholangiocarcinoma
PFS – progression-free survival
PD – progressive disease
PI3K/AKT – phosphatidylinositol 3-kinase/protein kinase B
PLCγ – phospholipase Cγ

PR – partial response

RAS/MAPK – rat sarcoma/mitogen activated protein kinases

rpm – rotations per minute

SNV – single nucleotide variant

SD – stable disease

SRB – sulforhodamine B

STAT – signal transducer and activator of transcription

TACE – trans

TBS – tris-buffered saline

TBS-T – tris-buffered saline with Tween20

TCA – trichloroacetic acid

TKI – tyrosine kinase inhibitor

TRIS – tris(hydroxy)aminomethane

1. Introduction

1.1 Clinical background of cholangiocarcinoma

1.1.1 Tumor classification

Cholangiocarcinoma represents an epithelial malignancy of the biliary tract. About 90 % of the tumors are adenocarcinomas (Valle et al., 2016). Cholangiocarcinoma can be classified according to anatomical localization with cancers of the intrahepatic (iCCA) and extrahepatic (eCCA) bile ducts. Extrahepatic tumors can be further subdivided into a perihilar (pCCA) and distal (dCCA) subtype. A broader definition of biliary tract cancers (BTCs) comprises cholangiocarcinoma (CCA), gallbladder cancer (GBC) and tumors of the ampulla of Vater (major duodenal papilla), ampullary cancer (AC) (**Fig. 1**). Although they are summarized as BTCs, each subgroup has its own specific molecular characteristics and treatment options (Rizvi et al., 2018).

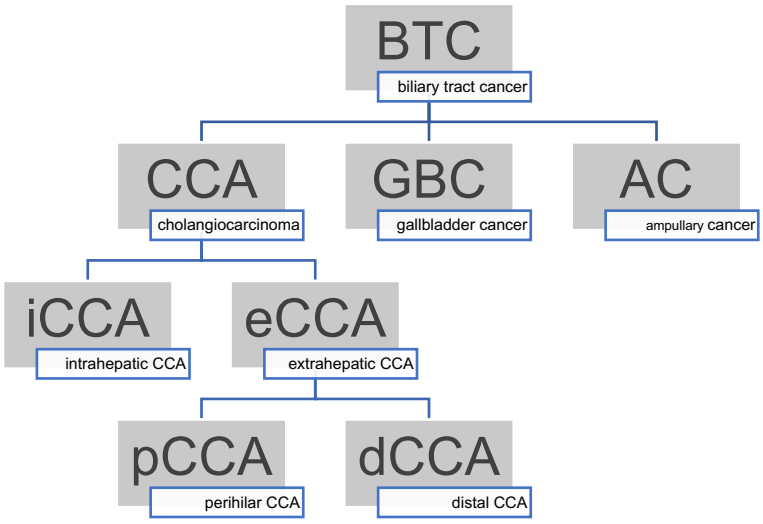

Figure 1: *Classification of cholangiocarcinoma according to anatomical location.* Overview of the classification and the abbreviations used consistently in this thesis. The term biliary tract cancer (BTC) includes the tumor entities cholangiocarcinoma (CCA), gallbladder cancer (GBC) and ampullary cancer (AC). Cholangiocarcinoma (CCA) can be further divided into an intrahepatic (iCCA) and an extrahepatic (eCCA) type, which in turn comprises a perihilar (pCCA) and a distal (dCCA) subtype.

1.1.2 Epidemiology

Considering all entities of CCA, it accounts for about 3 % of all gastrointestinal malignancies and represents 10-25 % of all hepatobiliary cancers (Belfiore et al., 2020). A closer look at the subtypes reveals a frequency of 60 % for perihilar (pCCA), 30 % for distal (dCCA) and about 10 % for intrahepatic (iCCA) localization (Esnaola et al., 2016). Worldwide, CCAs are rare, with an incidence of 2/100.000, and yet they cause 20 % of deaths from hepatobiliary malignancies (Kirstein and Vogel, 2016).

Reviewing various studies over the last decade, there is a steady increase in incidence of the intrahepatic subtype. Overall incidence of iCCA has increased up to 10-fold, while for eCCA it has declined over the past 30 years (Rizvi et al., 2018). Marked regional differences in iCCA incidence exist, due to genetic variations and regional risk factors, such as liver fluke, leading to much higher rates in Thailand with an incidence of up to 90/100.000 (Valle et al., 2016).

1.1.3 Etiology and risk factors

Even if most CCAs are regarded to develop without an identified reason, there are a few well-known risk factors (Banales et al., 2016).

Established risk factors for CCA include especially choledochal cysts, choledocholithiasis, primary sclerosing cholangitis (PSC) and parasitic infections (e.g. liver fluke such as *Opisthorchis viverrini*) (Tyson and El-Serag, 2011).

Regarding iCCA in particular, chronic liver diseases, such as hepatitis (especially hepatitis B and C) or cirrhosis, as well as metabolic diseases or liver toxins are associated risk factors (Bitzer et al., 2022).

1.1.4 Clinical manifestation and diagnostics

Unfortunately, CCA, especially iCCA, is often asymptomatic in early stages. While eCCA may cause cholestatic symptoms like icterus, stool discoloration, darkening of urine, pruritus and epigastric pain, iCCA can be very heterogeneous and often manifests only in commonly known unspecific symptoms of cancer (i.e. loss of weight, night sweats, fatigue).

Because of the above mentioned sparse or unspecific symptoms, diagnosis of CCA is in 20-25 % an incidental finding (Alvaro et al., 2011).
Diagnostically, hints for CCA can be found in anamnesis and clinical examination. Moreover, imaging techniques such as MRI, CT, sonography or magnetic resonance cholangiopancreaticography (MRCP) are used to detect these tumors. In laboratory examinations, increased cholestasis parameters can sometimes be found. Increased serum levels of carbohydrate antigen 19-9 (CA19-9) can also be indicative of a cholangiocellular malignancy, whereas sensitivity and specificity are only about 60 % respectively (Rizvi and Gores, 2013). In addition to its function as a progression parameter, CA19-9 is also attributed a prognostic meaning (Juntermanns et al., 2018).

1.1.5 Current systemic treatment options for cholangiocarcinoma

The only curative treatment option for CCA is a complete surgical tumor resection, which is only possible in early stages of disease (Banales et al., 2016). However, less than one-third of the tumors are diagnosed at a resectable stage (Khan et al., 2012). Among patients who have undergone surgical resection, the risk of recurrence is 40-80 % (Bitzer et al., 2022). In case of an advanced unresectable or already metastatic tumor, a palliative systemic therapy consisting of gemcitabine and cisplatin is used as first-line treatment (Valle et al., 2010). Recently, the combination of durvalumab in addition to gemcitabine and cisplatin reached a significantly improved overall survival (OS) compared to gemcitabine and cisplatin alone (Oh et al., 2022). The only randomized phase III trial comparing systemic therapy to placebo in the second-line setting was the ABC-06 trial of FOLFOX. This study showed a small but statistically significant improvement in OS (Primrose et al., 2019).
Interestingly, multiple genomic alterations have been discovered in cholangiocarcinoma in recent years that can be therapeutically targeted (Valle et al., 2021, Bitzer et al., 2022). In this context, *fibroblast growth factor receptor (FGFR) 2* fusion genes have become the focus of routinely applied molecular diagnostics. (Vogel et al., 2023).

1.2 Fundamentals of the FGFR signaling pathway

1.2.1 Function, structure and signaling of FGFR

The physiological function of FGFR and its signaling is very diverse. Already in an early phase of human development, FGFR signaling contributes to the formation of the epiblast and plays furthermore a major role in organogenesis (Ornitz and Itoh, 2015). In adult age, the signaling pathway has an essential role in response to injury and tissue repair (Eswarakumar et al., 2005).

FGFR is a receptor tyrosine kinase and is activated through phosphorylation by binding of different fibroblast growth factors (FGF) as ligands. Receptors were first detected to be phosphorylated by FGF1 and FGF2 in NIH/3T3 cells (Coughlin et al., 1988). While the FGF family nomenclature describes 23 members, only 18 different FGF glycoproteins are known to lead to activation of the signaling pathway (Turner and Grose, 2010).

The FGFR family comprises four different types of receptors, whose basic structure is always quite similar. FGFRs have three extracellular immunoglobulin(Ig)-like domains, one transmembrane domain and two intracellular tyrosine kinases (**Fig. 2**) (Ornitz and Itoh, 2015). Ligand binding specificity of the four receptor types is regulated by the Ig-like domains II and III and the linker region in between (Plotnikov et al., 2000).

Binding of FGFs triggers receptor dimerization and subsequent trans-autophosphorylation of the kinase domains leads to activation of various intracellular pathways (Touat et al., 2015). These activations mainly include rat sarcoma/mitogen activated protein kinases (RAS/MAPK), phosphatidylinositol 3-kinase/protein kinase B (PI3K/AKT), phospholipase Cγ (PLCγ) and signal transducer and activator of transcription (STAT) pathways. While PLCγ and STAT signaling is directly triggered by respective phosphorylation by the tyrosine kinase domain of FGFR, RAS/MAPK and PI3K/AKT pathway require an additional adapter protein called fibroblast growth factor receptor substrate 2 (FRS2) (Ornitz and Itoh, 2015). This signal-transducing FRS2 adapter protein is anchored to the cell membrane next to FGFRs through myristoylation. When phosphorylated, it binds growth factor receptor-bound 2 (GRB2), which afterwards activates RAS/MAPK and PI3K/AKT signaling (Valencia et al., 2011).

These four mentioned intracellular pathways, in turn, are known to increase cell proliferation, migration, and survival and thus have a decisive role for carcinogenesis (Turner and Grose, 2010).

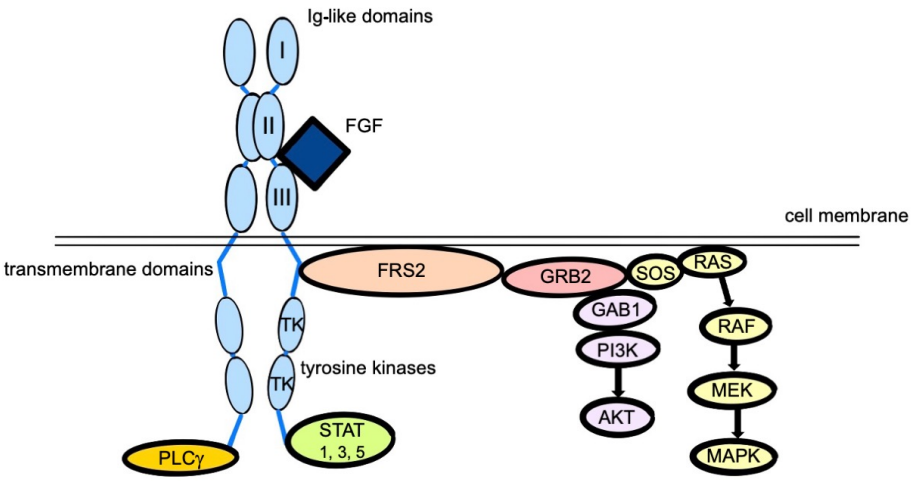

Figure 2: *Schematic simplified representation of FGFR and its most important downstream signaling pathways.* Binding of FGF leads to dimerization of FGFR, followed by auto-transphosphorylation of its kinase domains. Presented in a simplified way, PLCγ and STAT signaling is directly initiated by tyrosine kinase domains of FGFR. By contrast, activation of PI3K-AKT and MAPK pathways require activated FRS2 as an additional intermediate step (Touat et al., 2015).

1.2.2 Role of *FGFR* alterations in cancer

The significance of the FGFR signaling pathway for tumor pathogenesis was highlighted by a screening of more than 1000 somatic mutations in coding exons of over 500 protein kinase genes (Greenman et al., 2007). These protein kinase genes were examined in 210 different cancer entities and, of note, the FGFR pathway was found to be the most common with non-synonymous mutations (Greenman et al., 2007). Besides numerous somatic changes, also some germline variations were detected playing a role in carcinogenesis (Turner and Grose, 2010). FGFR and its altered versions are thought to have both oncogenic

potential and tumor suppressive properties in certain contexts (Ahmad et al., 2012). However, most publications report that cancerous diseases are caused by a gain of function modification of FGFR leading to activation of the signaling pathway (Katoh, 2016).

In descending order, most alterations of *FGFR* are caused by gene amplifications (66 %), point mutations (26 %) or chromosomal rearrangements leading to a fusion gene (8 %) (Roskoski, 2020). Gene amplifications can be found in various malignancies, but are most widely known for *FGFR2* in gastric and *FGFR1* in breast cancer (Turner and Grose, 2010). Translocations in *FGFR3* can cause hematologic malignancies and somatic point mutations of this receptor subtype result in *FGFR3* being one of the most frequently mutated genes in urothelial carcinoma (Ahmad et al., 2012). Considering these heterogeneous tumor entities, the essential role of this pathway in carcinogenesis and the need to find therapeutic options becomes evident.

1.2.3 FGFR inhibition in cancer treatment

In principle, inhibition of the FGFR signaling pathway is addressed mainly by three different mechanisms in *in vitro* and *in vivo* studies (Touat et al., 2015).

First, there are monoclonal antibodies, which bind to the extracellular domain of the receptor. They represent competitive inhibitors that block the FGF binding site or receptor dimerization (Touat et al., 2015). The most advanced of these is the FGFR2b antibody bemarituzumab, which has shown promising efficacy in a phase II trial as first-line treatment for advanced gastric cancer (Wainberg et al., 2021).

Second, FGF ligand trap molecules sequester FGF ligands and prevent their binding to FGFRs by acting as decoy receptors (Chae et al., 2017). FGF-ligand trap molecule FP-1039 is the best-studied to date and was well tolerated in a phase I and Ib trial (Tolcher et al., 2016, van Brummelen et al., 2020).

Third and most investigated, there are small molecules, called tyrosine kinase inhibitors (TKIs). TKIs in contrast to the above-mentioned therapeutic principles, do not target the extracellular part of the receptor, but bind to the intracellular tyrosine kinase and thus inhibit autophosphorylation of tyrosine residues (Chae

et al., 2017). These FGFR kinase inhibitors can be further subdivided into an unselective and a selective subtype. On the one hand, unselective inhibitors have effects on FGFR as well as on other tyrosine kinases and are thus also named multikinase inhibitors (Chae et al., 2017). On the other hand, selective TKIs bind almost exclusively to FGFRs and besides are asserted to be more potent and to cause less adverse events (Facchinetti et al., 2019). Yet, they cause a unique assortment of clinical adverse events, of which hyperphosphatemia, ocular and dermatologic toxicities are the most notable (Mahipal et al., 2020).

In 2019, erdafitinib became the first selective FGFR-targeting TKI, that has been approved by the U.S. Food and Drug Administration (FDA) for the treatment of urothelial carcinoma (U.S. Food and Drug Administration, 2019). In addition to the much-studied and partially approved FGFR inhibitors for CCA, which will be addressed later, several FGFR kinase inhibitors are currently being tested in clinical trials for various other types of cancer (Weaver and Bossaer, 2021).

1.3 Pathogenesis of cholangiocarcinoma

1.3.1 Cholangiocarcinogenesis in general

Considering the risk factors mentioned above, it is reasonable that inflammation plays a key role in the development of malignant cholangiocellular tumors. In this context, inflammatory signaling pathways involving cytokines and growth factors are thought to be responsible for the development of DNA damage (Rizvi and Gores, 2013). In recent years, tumor genome sequencing has led to detection of various DNA changes that contribute to cholangiocarcinogenesis. The genetic landscape of CCAs varies according to different studies. Nevertheless, eCCA exhibits alterations especially for *HER2/3* and *KRAS* genes (Lamarca et al., 2020). For iCCA, which is increasing in incidence, mainly alterations in *IDH* and especially *FGFR* genes were found (Mahipal et al., 2019).

1.3.2 *FGFR* alterations in cholangiocarcinoma

Considering all alterations of the *FGFR* gene detected in CCA, the frequency range is 8-25 %, with these alterations almost exclusively detected in the intrahepatic subtype (Tariq et al., 2019).

More specifically, most of FGFR changes identified in iCCA were *FGFR2* fusion genes (Nakamura et al., 2015). Fusion genes, in general, are hybrid genes that result from a rearrangement of two previously independent genes. This rearrangement can be caused by a translocation, chromosomal inversion, duplication or deletion (Touat et al., 2015). Occurrence of *FGFR2* fusion genes in iCCA varies in different cohorts from 11-45 %, but is usually assumed to be about 15 % in reviews (Javle et al., 2016, Sia et al., 2015, Mahipal et al., 2019, Tariq et al., 2019).

Wu et al. were the first to describe a fusion gene in iCCA. More precisely, they discovered the intrachromosomal *FGFR2-BICC1* fusion in two cases of advanced tumors and could demonstrate enhanced proliferation in a cell model (Wu et al., 2013). Furthermore, Arai et al. identified not only *FGFR2-BICC1* but also a novel translocation leading to the *FGFR2-AHCYL1* fusion and demonstrated that these fusions were mutually exclusive with *KRAS* and *BRAF* mutations. For both FGFR2 fusions, they demonstrated anchorage-independent growth, activation of downstream signaling and sensitivity to FGFR selective inhibitors when expressed in a NIH/3T3 cell model (Arai et al., 2014). Corroborating the oncogenic potential of *FGFR2* fusion genes, similar findings were made for *FGFR2-PPHLN1* with additional evidence of permanent fusion protein activation (Sia et al., 2015). So far, several different fusion partners of *FGFR2* were identified that have oncogenic potential. The FGFR2 fusions all appear to share a common mechanism for triggering oncogenic activation despite different molecular characteristics of their fusion partners (Vogel et al., 2023). They all have in common that N-terminal kinase domain of FGFR2 is intact and that ligand-independent dimerization and subsequent activation is caused by fusion partners at the C-terminal site of the protein (Li et al., 2019). It appears that the replacement and consequent loss of certain gene sequences of the C-terminal site, which normally mediate a negative feedback mechanism on the kinase activity of wild type proteins, leads to constitutive receptor dimerization in FGFR2 fusion proteins (Vogel et al., 2023).

1.3.3 Clinical features of *FGFR*-altered cholangiocarcinoma

Although there is no consensus in the literature as to whether there are clinical differences between CCAs with FGFR alteration and those without, several authors suggested at least some special characteristics of the FGFR-altered tumors. Median cancer-specific survival and disease-free intervals were longer in patients with CCA harboring FGFR2 translocations and therefore suggest a better prognosis (Graham et al., 2014). Moreover, Javle et al. performed comprehensive genomic profiling on 412 iCCA and could present improved OS for patients with FGFR2 alteration (Javle et al., 2016). These findings are further supported by a study by Jain et al., who compared 95 patients with CCA harboring FGFR changes (including 63 *FGFR2* fusion genes) with 282 patients without FGFR alterations. They demonstrated, that tumors with FGFR aberrations were more common in younger patients (<40) and were related to longer OS, even after cases treated with FGFR inhibitors were excluded (Jain et al., 2018). However, no significant difference in OS was found when comparing FGFR2 fusions with other FGFR2 alterations (Jain et al., 2018).

To improve prognosis, FGFR-inhibiting drugs are considered a promising therapeutic option for FGFR2-altered cholangiocarcinoma.

1.3.4 FGFR inhibition in cholangiocarcinoma treatment

Regarding FGFR inhibition in cholangiocarcinoma treatment, both unselective and selective TKIs have shown encouraging results (Goyal et al., 2021).

First, unselective TKIs pazopanib and especially ponatinib have offered the potential to improve outcomes for patients with FGFR-altered iCCA showing antitumor activity in three cases (Borad et al., 2014). The unselective inhibitor ponatinib was initially approved for chronic myeloid leukemia or Philadelphia chromosome-positive acute lymphoblastic leukemia targeting BCR-ABL (Tan et al., 2019). Multikinase inhibitors with FGFR-inhibitory activity, like ponatinib, are of special interest for iCCA since they have already been approved safe for other purposes.

Following the discovery of numerous FGFR changes in a variety of cancer types, several selective FGFR inhibitors have been developed (Kelley et al., 2020).

Several of these TKIs have been and are currently being tested in advanced stages of iCCA, and to date three of them have been approved for this purpose (Vogel et al., 2023).

PanFGFR (FGFR1-4) inhibiting infigratinib (BGJ398) was tested in a phase II study by Javle et al. in 108 patients with advanced iCCA with FGFR alterations (88 patients with FGFR2 fusions). The study revealed promising results with an overall response rate (ORR) of 23.1 %, a disease control rate of 84.3 % and a median progression-free survival (PFS) of 7.3 months (Javle et al., 2021). In 2021, infigratinib received FDA approval for FGFR2 fusion-positive or rearranged, previously treated, locally advanced or metastatic cholangiocarcinoma (U.S. Food and Drug Administration, 2021, Kang, 2021).

Furthermore, the selective FGFR1-3 effective TKI pemigatinib acquired an FDA and EMA approval for patients with previously treated and advanced CCA with FGFR2 fusions or other rearrangements as second-line therapy (U.S. Food and Drug Administration, 2020, European Medicines Agency, 2021, Hoy, 2020). In the phase II study preceding approval, pemigatinib led to an ORR of 35.5 % and a median PFS of 6.9 months for FGFR2 fusions or rearrangements (Abou-Alfa et al., 2020).

In contrary to other FGFR2 inhibitors, futibatinib binds covalently to the receptor's ATP pocket leading to irreversibly inhibition (Tan et al., 2014). Updated results from the phase II FOENIX-CCA2 study, published in June 2022, showed an ORR of 42 % and a median PFS of 8.9 months for futibatinib treatment in 103 patients with progressive disease of advanced or metastatic FGFR2-altered iCCA (Goyal et al., 2022). These results led to FDA approval in September 2022 for patients with iCCA harboring FGFR2 fusions or rearrangements in advanced or therapy-refractory stages (U.S. Food and Drug Administration, 2022). In the recently published final results of the phase II study of futibatinib, the median PFS was updated to 9.0 months (Goyal et al., 2023).

Moreover, infigratinib, pemigatinib and futibatinib are currently tested in phase III studies as first-line therapy for cholangiocarcinoma with altered FGFR2 receptors (Vogel et al., 2023).

Although FGFR inhibitors have exposed promising results, there is great concern that over time patients will suffer tumor progression despite treatment due to acquired resistance (Javle et al., 2018). A detailed analysis of three patients enrolled in the phase II study of infigratinib, whose tumors progressed despite therapy, demonstrated recurrent point mutations in the FGFR2 kinase domain (Goyal et al., 2017). They elucidated, that the recurrent point mutations emerged as a mechanism of secondary resistance under treatment pressure with the selective FGFR inhibitor. Additionally, they presented, that all three patients examined, exhibited the point mutation p.V564F in post-progression cell-free DNA (cfDNA) analysis, which acts as a gatekeeper mutation altering the accessibility of the ATP-binding pocket for TKIs (Goyal et al., 2017). Other discovered resistance-mediating point mutations like p.E565A, p.N549H and p.K641R stabilize the kinase domain in an activated state (Chen et al., 2007, Byron et al., 2013).
Subsequently, studies were able to present ways of overcoming the developed resistance by changing the applied FGFR inhibitor, reflecting that such tumors still depend on FGFR2 signaling events, but not for p.V564F mutation (Goyal et al., 2019). For mutation p.E565A, found in the kinase domain of FGFR2 fusion-positive tumors, the aforementioned unselective TKI ponatinib as well as futibatinib (TAS-120) were capable to overcome resistance *in vitro* as well as *in vivo* (Goyal et al., 2019, Krook et al., 2020). Nevertheless, emergence of secondary acquired resistance to FGFR selective drugs remains a major challenge (Krook et al., 2019).

1.4 Summary, own findings and aims of this study

1.4.1 Summary of the introduction

Although cholangiocarcinoma is a rather rare malignancy, incidence of iCCA increases and prognosis remains very poor despite several available therapies (Rizvi et al., 2018). Recent studies have unraveled FGFR2 fusions as a particular promising novel target for patients with iCCA and have led to approval of pemigatinib, infigratinib and futibatinib, FGFR selective TKIs, as second-line in advanced iCCA with FGFR2 fusions or rearrangements (U.S. Food and Drug Administration, 2020, European Medicines Agency, 2021, U.S. Food and Drug

Administration, 2021, U.S. Food and Drug Administration, 2022). A variety of TKIs is currently tested in ongoing clinical trials as second-line but also first-line therapy (Chmiel et al., 2022). Despite promising results of FGFR-inhibiting TKIs, the development of resistant subclones under therapeutic pressure limits response durations, which range between 6-9 months (median PFS: infigratinib 7.3 months; pemigatinib 6,9 months; futibatinib 9.0 months) (Javle et al., 2021, Abou-Alfa et al., 2020, Goyal et al., 2023).

1.4.2 Own findings

Within the framework of the Molecular Tumor Board (MTB) of Tuebingen University Hospital, tumor biopsies were taken from patients with advanced iCCA who had progressed under standard treatment and tumor genetic analyses were performed. These analyses included the review of numerous known potentially oncogenic gene alterations (Heining et al., 2018, Bitzer et al., 2020). In this context, various FGFR2 alterations, were identified, including the *FGFR2-BICC1* fusion gene, which has been described several times in the literature (Wu et al., 2013, Arai et al., 2014). Furthermore, a gene fusion between *FGFR2* and the gene *SH3GLB1* (*FGFR2-SH3GLB1*) was detected, which has been described, but not yet characterized (Jain et al., 2018). In addition, the previously unknown *FGFR2-AHCYL2* gene fusion has been discovered.

Subsequently, the MTB suggested therapies with FGFR-targeting TKIs. As no FGFR inhibiting drugs were approved for iCCA at treatment decisions and clinical trials were initially not available, the patients were treated off-label with the multikinase inhibitors ponatinib, lenvatinib or nintedanib that target FGFR and are approved for other indications (Borad et al., 2014, Yamamoto et al., 2014, Dai et al., 2019, King and Javle, 2021). Further on, some patients could be enrolled in a trial to be treated with the selective FGFR inhibitor infigratinib. Response to treatment varied among the compounds tested. Interestingly, the multikinase inhibitor lenvatinib showed promising efficacy with durable responses of up to 12 months in heavily pretreated patients. Unfortunately, after a good initial response for some of the TKIs, tumor progress was observed and studies on resistance mechanisms were followed up.

1.4.3 Aims of this study

As already highlighted, numerous studies have identified several *FGFR2* fusion genes in iCCA (Li et al., 2019). The molecular characteristics and subsequent malignant potential of several FGFR2 fusions (*FGFR2-BICC1*, *FGFR2-AHCYL1*, *FGFR2-PPHLN1*) have been demonstrated by *in vitro* studies (Wu et al., 2013, Arai et al., 2014, Sia et al., 2015). However, it remains unclear, whether all *FGFR2* fusion genes can act as oncogenic drivers and whether the fusion partner affects molecular characteristics and function (Babina and Turner, 2017). Influence of the different FGFR2 fusion partners should therefore be examined individually.

Furthermore, a lot of *in vitro* and *in vivo* trials confirmed the important role of TKIs with FGFR-inhibitory effects for treatment, especially because of the lack of palliative second-line treatment (Mahipal et al., 2019). Nevertheless, it is not sufficiently clarified yet whether promising results apply to all FGFR2 fusions or whether there are differences concerning the response to various TKIs. In addition, the problem of secondary developed resistance is increasing in relevance and therefore needs to be urgently addressed (Krook et al., 2020).

The first aim of this thesis was to analyze the disease course of selected patients with iCCA bearing FGFR alterations who received therapies based on recommendations of the MTB of Tuebingen University Hospital.

Using a “bed to benchside” approach, the second aim was to generate and characterize novel patient-analogue cellular models, that stably express the FGFR2 fusions identified.

Using these cell lines, the third aim was to test and compare the efficacy of different FGFR-targeting TKIs *in vitro*. Particular attention should be paid to differences between unselective and selective TKIs.

The fourth aim of this thesis was to investigate the impact of additional kinase mutations in *FGFR2* fusion genes on cellular characteristics and on drug effects.

2. Materials and methods

2.1 Processing of patient cases and genetic tumor analyses

Seven patients with CCA (n = 7) were included in this study. All of these patients signed the broad consent form “Einwilligungserklärung zur Verwendung von Biomaterial und Daten in der Forschungsdatenbank und Biobank der Medizinischen Fakultät & des Universitätsklinikums Tübingen (MFT/UKT Biobank)”. Before starting the study, the project was reviewed and accepted by the local ethics committee on 10/10/2019 (714/2019B02). All studies were conducted in accordance with the Declaration of Helsinki.

All patient cases were presented and discussed at the MTB of Tuebingen University Hospital. The MTB is an interdisciplinary, multi-professional conference, which plans special individual and targeted therapies based on molecular characteristics of malignant tumors. The members are composed of experts in the fields of clinical and translational oncology, pathology, radiology, human genetics and molecular biology (Bitzer et al., 2020). The main recommendations included off-label therapies or clinical studies. Treatment efficacy assessment was performed every 4-12 weeks using CT or MRI scans evaluated by experienced radiologists oriented along the established RECIST 1.1 criteria (Eisenhauer et al., 2009). Clinical courses were categorized for best response based on imaging into complete (CR) and partial response (PR), stable disease (SD) or progressive disease (PD).

For comparison of two different types of therapy, the Von Hoff model was used, where patients are considered as their own control group (Von Hoff, 1998). Here, a ratio between the PFS of the treatment under study and the PFS of the previous treatment is calculated and considered clinically significant if it is > 1.3-1.5 (Rodon et al., 2019, Hoff et al., 2010).

Before genetic tumor analyses, patients were consulted by a specialist in clinical genetics. Genetic tumor analyses, including liquid biopsy, next generation sequencing (NGS), transcriptome sequencing or whole exome sequencing (WES) were performed by CeGaT (CeGaT GmbH, Tuebingen, Germany), the Institute of Medical Genetics and Applied Genomics in Tuebingen, or within the Molecularly Aided Stratification for Tumor Eradication Research (MASTER) precision

oncology program at the National Center for Tumor Diseases/German Cancer Consortium (NCT/DKTK) as previously described (Heining et al., 2018, Bitzer et al., 2020).

2.2 Cell culture of NIH/3T3 and novel generated cells

The NIH/3T3 cell line was a kind gift by Wolfgang Neubert (Max Planck Institute for Biochemistry, Martinsried, Germany). Authentication of the NIH/3T3 cell line was confirmed by the Mouse Short Tandem Repeat (STR) Profile Report Cell Line Authentication Service (ATCC, Manassas, VA, USA) in 2020. Cells were grown in Dulbecco's Modified Eagle's Medium (DMEM) – high glucose (Sigma-Aldrich, Taufkirchen, Germany) complemented with 10 % FBS and 1 % penicillin-streptomycin (Thermo Fisher Scientific, Schwerte, Germany). Cells were cultured in a humidified atmosphere at 37 °C in 5 % CO_2 and routinely tested for mycoplasma using a DAPI test (Thermo Fisher Scientific, Schwerte, Germany). To guarantee sufficient nutrient supply, a medium change was performed every 2-3 days. Cells were passaged before reaching 90 % confluence by washing with PBS and short incubation at 37 °C with trypsin until cells detached. Afterwards, the growth medium was used to stop trypsinization and resuspension of the cells. When carrying out experiments, no antibiotics were used.

2.3 Cryoconservation – freezing and thawing of cells

To preserve the cells for a longer period of time, they were frozen according to the following procedure. After reaching a confluence of approximately 90 % in a cell culture flask, the cells were first washed with phosphate-buffered saline (PBS) (Sigma-Aldrich, Taufkirchen, Germany), detached with trypsin (Sigma-Aldrich, Taufkirchen, Germany), next resuspended with their required medium and then put in a 15 ml tube. The tubes containing the cells were then centrifuged at 1200 rotations per minute for 5 minutes. After discard of the supernatant, the cell pellet was dissolved in freezing medium consisting of normal growth medium with 20 % fetal bovine serum (FBS) (Sigma-Aldrich, Taufkirchen, Germany) and 20 % dimethyl sulfoxide (DMSO) (Carl Roth, Karlsruhe, Germany). The cell suspension was then aliquoted and added to cryogenic storage vials (Thermo Fisher

Scientific, Schwerte, Germany) containing 1 x 10^6 – 3 x 10^6 cells. The vials were then stored at -80 °C for 2 days using the cryo-freezing container “Mr. Frosty” (Thermo Fisher Scientific, Schwerte, Germany) to freeze slowly. Finally, they were stored in a tank with liquid nitrogen at -196 °C.

After thawing, the cells were washed by resuspension with growth medium and centrifugation at 1200 rpm for 5 minutes. They were then cultivated as described below. Before the cells were used for experiments, they were passaged at least once.

2.4 Plasmid design

The plasmids were designed by Stephan Spahn (MD.) and Bui Khac Cuong (MD., PhD.) using SnapGene (GSL Biotech LLC., Chicago, IL, USA).

First, the fusion genes *FGFR2-SH3GLB1* and *FGFR2-AHCYL2* were generated according to patients’ sequencing data. Additionally, a plasmid with the *FGFR2-BICC1* fusion gene was designed according to published data in the sense of a positive control (Arai et al., 2014). In addition, two plasmids containing the *FGFR2-AHCYL2* fusion gene with previously described single point mutations leading to therapy resistance were created (Goyal et al., 2017, Krook et al., 2020). Pursuant to the chosen two single nucleotide variants (SNVs), the generated fusions resulted in *FGFR2-AHCYL2* p.E565A and *FGFR2-AHCYL2* p.V564F.

The following plasmids were bought already manufactured with the corresponding designed gene section as well as with genes for neomycin resistance (*neo*) and an enhanced green fluorescent protein (*eGFP*) (GenScript, Piscataway, NJ, USA):

- pcDNA3.1(+)P2A-eGFP
- Kozak_FGFR2-BICC1_pcDNA3.1(+)-P2A-eGFP
- Kozak_FGFR2-SH3GLB1_pcDNA3.1(+)-P2A-eGFP
- FGFR2-AHCYL2_pcDNA3.1(+)-P2A-eGFP

- FGFR2-AHCYL2_E585A_mutation_pcDNA3.1(+)-P2a-eGFP

(corresponding to p.E565A)

- FGFR2-AHCYL2_V584F_mutation_pcDNA3.1(+)-P2A-eGFP

(corresponding to p.V564F)

An example of the plasmid design is displayed in the results section below (see **Figure 4**). The included P2A sequence ensures that the FGFR2 fusions and the eGFP expressed in the plasmid are split in two (Szymczak and Vignali, 2005). Furthermore, this allows equimolar expression of both proteins from their common promoter (Liu et al., 2017). Thus, the eGFP signal can be used to draw conclusions about transfection success.

2.5 Transfection of NIH/3T3 cells with different fusion genes

To generate a cell culture model of the divergent FGFR2 fusions to be examined, cells were transfected using chemical transfection. NIH/3T3 cell line was selected as a suitable cell line for this purpose because they do not express endogenous FGFR, they are easy to transfect and several FGFR pathway-related discoveries were made using them (Arai et al., 2014, Sia et al., 2015, Turner and Grose, 2010).

Transfection of cells

Transfection was conducted according to manufacturer's instructions. First, the above-mentioned plasmids were added respectively 10µl (c = 200 ng/µl, m = 2µg) to the Effectene transfection reagent substances (Qiagen, Hilden, Germany) at a ratio of 1/30 (µl transfection reagent/µg DNA). Next, substance was admixed to a cell culture flask containing $5x10^5$ NIH/3T3 cells. After 48 hours of incubation with those reagents, cells were checked for GFP signal using fluorescence microscopy (Axio Observer Z1 with Fluorescence Box HXP 120 C, Zeiss, Oberkochen, Germany) and afterwards selected.

Selection of cells using G418

Afterwards, cells were transferred to 100mm TC dishes (Sarstedt, Nümbrecht, Germany) and were selected using sterile G418 (Biochrom, Berlin, Germany) with an initial concentration of 2 mg/ml.

Selection of single colonies

By checking the green fluorescence protein (GFP) signal via fluorescence microscopy, individual colonies were selected and expanded by transferring them to 6-well plates, while lowering the concentration of G418 each time of transfer. After maximum 30 days, 4 different clones were cryopreserved each.

Designation of the novel generated cell lines used in the following

For simplicity, the (novel) cell lines studied are abbreviated as shown here (**Table 1**).

Table 1: *Designation of cell lines in the following*

Cell line	Abbreviation
wild type NIH/3T3 cells	**WT-NIH/3T3**
empty vector P2A-eGFP-transfected NIH/3T3 cells	**CTL-NIH/3T3**
FGFR2-BICC1-transfected NIH/3T3 cells	**FGFR2-BICC1**
FGFR2-SH3GLB1-transfected NIH/3T3 cells	**FGFR2-SH3GLB1**
FGFR2-AHCYL2-transfected NIH/3T3 cells	**FGFR2-AHCYL2**
*FGFR2-AHCYL2 p.*E565A-transfected NIH/3T3 cells	**".E565A"**
*FGFR2-AHCYL2 p.*V564F-transfected NIH/3T3 cells	**".V564F"**

2.6 Western blot for detection of FGFR2 and different downstream signals

Western blot technique (also called Immunoblot) is a widely used procedure to identify specific proteins (Mahmood and Yang, 2012). It was first described by Towbin in 1979 (Towbin et al., 1979), but got its name two years later by Burnette (Burnette, 1981).

To analyze (altered) FGFR2 and its downstream signals in the novel cell lines, proteins were first extracted, sorted by molecular weight via gel electrophoresis, transferred to a nitrocellulose membrane and finally detected using different antibodies.

Protein extraction from cells

To isolate proteins, cells were grown on a 100mm TC dish for 3-4 days. They were then lysed on ice with RIPA buffer (EMD Millipore, Billerica, MA, USA) with additional added Proteinase and Phosphatase Inhibitor (Thermo Fisher Scientific, Schwerte, Germany) and phenylmethylsulfonyl fluoride (PMSF) (Sigma-Aldrich, Taufkirchen, Germany). Next, cells were disrupted via sonication with a SONOPULS homogenizer (Bandelin, Berlin, Germany). After slowly rotating the lysate at 4 °C for 30 minutes and centrifugation of the cell debris for 7 minutes at 1200g at 4 °C, the supernatant was preserved. Afterwards, protein concentrations of the samples were obtained by Pierce BCA Protein Assay Kit (Thermo Fisher Scientific, Schwerte, Germany) using Synergy HTX multi-mode plate reader (BioTek, Bad Friedrichshall, Germany). Proteins were denatured by adding NuPAGE LDS Sample Buffer (Thermo Fisher Scientific, Schwerte, Germany) and Dithiothreitol (DTT) (Thermo Fisher Scientific, Schwerte, Germany) and heating of the whole mixture 5 minutes at 95 °C with neoBlock Heater (neoLab, Heidelberg, Germany).

Gel electrophoresis

For gel electrophoresis, resolving gels from 7.5–10 % acrylamide and stacking gels with 4 % acrylamide were prepared using Rotiphorese NF-acrylamide/bis-solution 30 % (Carl Roth, Karlsruhe, Germany) (**Table 2**). 20 µg protein samples

were loaded and separated through electrophoresis using self-produced running buffer (25 mM TRIS, 192 mM glycine, 35 mM SDS) (all materials from Carl Roth, Karlsruhe, Germany) at 140 V and 140 mA for 1-2 hours.

Table 2: *Recipes for stacking and resolving polyacrylamide gels*

Reagent	Stacking gel – 4 %	Resolving gel – 7,5 %	Resolving gel- 10 %
30 % acrylamide	1.98 ml	3.75 ml	5 ml
0,5M TRIS-HCl	3.78 ml		
1,5M TRIS-HCl		3.75 ml	3.75 ml
H_2O	9 ml	7.28 ml	6.05 ml
10 % SDS	150 µl	150 µl	150 µl
TEMED	15 µl	7.5 µl	7.5 µl
10 % APS	75 µl	75 µl	75 µl

All listed materials are from Carl Roth (Karlsruhe, Germany)

Electroblotting (Transfer)

Proteins were transferred onto 0.2 µm thick nitrocellulose membranes with the Trans-blot Turbo Transfer System (Bio-Rad, München, Germany) using extra thick blot membrane filters (Bio-Rad, München, Germany) and a Bjerrum Schafer-Nielsen transfer buffer as recommended by Bio-Rad (48 mM TRIS, 29 mM glycine, 20 % methanol).

Blocking, antibody incubation and detection

After transfer, membranes were blocked for 1 hour in 5 % nonfat dry milk (Bio-Rad, München, Germany) diluted in TBS-T (50mM TRIS, 150mM NaCl, 0.05 % Tween20).

Membranes were then incubated at 4 °C overnight with the following antibodies diluted in 5 % nonfat dry milk (Bio-Rad, München Germany) (**Table 3**).

Table 3: *Primary antibodies for Western blotting and its used concentrations*

Antibody	Distributor	Cat. No.	Dilution
FGFR2 (Rabbit mAb)	Cell Signaling	#23328	1:1000
pFGFR (Mouse mAb)	Cell Signaling	#3476	1:1000
FRS2 (Mouse mAb)	Santa Cruz	sc-17841	1:100
pFRS2 (Rabbit mAb)	Cell Signaling	#3861	1:1000
MAPK (P44/42) (Rabbit mAb)	Cell Signaling	#4695	1:1000
pMAPK (pP44/42) (Rabbit mAb)	Cell Signaling	#9101	1:1000
STAT3 (Rabbit mAb)	Cell Signaling	#4904	1:2000
pSTAT3 (Rabbit mAb)	Cell Signaling	#9131	1:1000
AKT (pan) (Rabbit mAb)	Cell Signaling	#4685	1:1000
pAKT (1/2/3)(pan) (Mouse mAb)	Santa Cruz	sc-514032	1:500
Beta-actin (Mouse mAb)	Cell Signaling	#3700S	1:1000
Vinculin (Mouse mAb)	Sigma-Aldrich	V9131	1:5000

Antibodies were either from Cell Signaling (Frankfurt, Germany), Santa Cruz (Dallas, TX, USA) or Sigma-Aldrich (Taufkirchen, Germany)

A washing procedure of 5-10 minutes with TBS-T was reiterated 3 times after incubation. Hereafter incubation with a secondary mouse or rabbit antibody (both: Invitrogen by Thermo Fisher Scientific, Schwerte, Germany) coupled with a horseradish-peroxidase at a dilution of 1:1000 in TBS-T with 5 % nonfat dry milk was performed. Membranes were then washed again 3 times for 5 – 10 minutes. Then 500 µl of Clarity Western ECL Substrate (Bio-Rad, München, Germany) was added on top of the membranes to detect a signal in the subsequent detection with X-ray cassettes and suitable radiographic films (Thermo Fisher Scientific, Schwerte, Germany).

To obtain a loading control via Beta-actin or Vinculin, membranes were either cut into two parts after blotting or stripped after antibody detection using stripping buffer (Thermo Fisher Scientific, Schwerte, Germany).
To determine the relative protein abundance by densitometry the surface area was measured with ImageJ (developed by Wayne Rasband for the National Institutes of Health) and then normalized to the respective band of Beta-actin or Vinculin.

Investigation of drug effects on downstream signals

To investigate the effects of different substances on downstream signals, cells were treated before protein extraction according to the following procedure:
First, 150.000 cells were seeded into a 6-well plate. After incubation for 48 hours, cells were exposed to different concentrations of substances for additional 24 hours. The following substances or DMSO, as a negative control, were added for the appropriate concentrations (**Table 4).**

Table 4: *Substances and its concentrations used for Western blots of downstream signals in FGFR2 fusion protein-expressing cells after treatment*

Substance:	Distributor:	Concentration:	Unit:
Infigratinib	Selleckchem	0.5	µM
Lenvatinib	Selleckchem	1	µM
Ponatinib	Selleckchem	0.1	µM
Gemcitabine	Selleckchem	1	µM

All substances listed are from Selleckchem (Houston, TX, USA)

The experiment was always performed for WT-NIH/3T3 cells and transfected cells in parallel.
After 24 hours of incubation with drugs, the above explained protein extraction from cells was performed. The respective procedure was reiterated 3 times.

2.7 SRB assay as proliferation and cytotoxicity assay

Sulforhodamine B (SRB) assays, first described by Skehan et al. (Skehan et al., 1990), were performed to study cytotoxicity of different substances. The applied protocol comprises 4 main steps.

Seeding and treatment of the cells

3.000 cells per well were seeded on 24-well plates with 500 µl of DMEM – high glucose with 10 % FBS. Medium was changed after 24 hours and the lower described drugs were added to the wells in corresponding concentration (**Table 5**). Both for each treatment and each cell line, wells were treated in duplicate. Negative control was performed by adding an equal amount of DMSO. For comparison, WT-NIH/3T3 cells and CTL-NIH/3T3 cells were treated in the same way as the FGFR2 fusion gene-transfected ones under investigation.

Table 5: *Substances and its concentrations used for SRB assay drug testing*

Substance:	Distributor:	Concentrations:					Unit:
Infigratinib	Selleckchem		0.25	0.5	1	5	µM
Futibatinib	Cayman Chemicals		0.25	0.5	1	5	µM
Lenvatinib	Selleckchem	0.5	1	2	4	8	µM
Ponatinib	Selleckchem		0.05	0.1	0.2	0.5	µM
Nintedanib	Selleckchem	0.1	0.2	0.5	1	2	µM
Cabozantinib	Selleckchem	1	2	4	5	8	µM
Gemcitabine	Selleckchem	10	15	20	25	30	nM

Substances were either from Selleckchem (Houston, TX, USA) or Cayman Chemicals (Ann Arbor, MI, USA)

Incubation of cells with treatment substances

After treatment, cells were incubated at 37 °C with 5 % CO_2 for 7 days.

Fixation of cells

Following incubation, medium with drugs was discarded and the cells were washed with ice-cold PBS and fixed for 30 minutes at 4 °C using 200 µl cold 10 % trichloroacetic acid (TCA) (Carl Roth, Karlsruhe, Germany). TCA was then washed out with water and the 24-well plates were dried at 40 °C for 12 hours.

SRB staining and measurement

Remaining cells were stained for 20 minutes with 0.4 % Alfa Aesar Sulforhodamine B sodium salt (Thermo Fisher Scientific, Schwerte, Germany) dissolved in 1 % acetic acid. SRB solution was then discarded and afterwards rinsed with 1 % acetic acid. Next, plates were again stored at 40 °C for at least 6 hours.

For measurement, stained cells were solubilized with 500-1000 µl 10 mM TRIS for 10 minutes and transferred to a 96-well plate. Test solutions were duplicated again, to get 4 measuring fields for each concentration on the 96-well plates finally.

The optical density (OD), used as a proxy for cell mass, was conclusively measured with a Synergy HTX multi-mode plate reader at 550 nm wavelength. The two averages of the 4 wells were analyzed and used for further evaluation.

2.8 Soft agar colony formation assay for verification of anchorage-independent growth

To examine anchorage-independent growth of novel cell lines, a marker of malignant transformation, soft agar colony formation assays were executed. The experiment was performed as described by Borowicz et al. with slight modifications described below (Borowicz et al., 2014).

Whereas in normal cells loss to extracellular matrix contacts leads to anoikis, a special type of apoptotic cell death, malignant cells can grow anchorage-independently by formation of colonies (Frisch and Francis, 1994, Nguyen et al., 2009).

Preparation of bottom layer of agar

At the beginning of the assay, a 3.5 % agar was prepared by heating and mixing autoclaved water and Difco™ Noble Agar (BD Biosciences, Heidelberg, Germany). DMEM – high glucose supplemented with 20 % FBS and 1 % penicillin-streptomycin was warmed up to 45 °C in a water bath. After 3.5 % agar was melted, it was mixed with the corresponding quantity of medium to reach a final agar concentration of 0.7 %. This composite was then used for plating the bottom layer of agar and further for preparation of agar containing cells and treatment substances.

Preparation of upper layer of agar containing cells and treatment substances

For the upper layer of agar, cells were trypsinized and counted. A suspension of 2000 cells/ml was created in the required quantity, and substances or DMSO were added in the respective concentration (**Table 6**). Subsequently, the suspension was diluted and mingled 1:1 with the already described 0.7 % agar medium mix. Dilution thus produced a final 0.35 % agar concentration containing 1000 cells/ml and the tested drugs or DMSO control for the upper layer.

Table 6: *Substances and its concentrations used for soft agar colony formation assay*

Substance:	Distributor:	Concentration:	Unit:
Infigratinib	Selleckchem	0.5	µM
Lenvatinib	Selleckchem	0.25	µM

All substances used were from Selleckchem (Houston, TX, USA)

Plating the agar layers

The soft agar colony formation assay was conducted using 6-well plates.

Per well, 4 ml of the 0.7 % agar medium mix was added slowly to avoid air bubbles. Thereafter plates were left to stand at room temperature for 30 minutes so

that the agar mix could solidify. In the end, 2 ml of the 0.35 % agar containing overall 2000 cells and treatment substances were layered on top and left at room temperature for 15 minutes.
Plates were then transferred to an incubator with 37 °C and 5 % CO_2.

Staining and counting of colonies

After cells were cultivated in soft agar for 21 days, growth was stopped and colonies were stained with 1 ml Iodonitrotetrazolium chloride (violet) (Sigma-Aldrich, Taufkirchen, Germany). After incubation overnight with the dye, images of plates were taken and analyzed using Image J.

2.9 Statistical analysis

Analysis of data was realized using GraphPad Prism 8 (GraphPad Software Inc, CA, USA). The statistical test methods used were unpaired, two-tailed Student's t-test and one-way ANOVA as appropriate. The results are presented as mean ± standard deviation (± SD), whereby the Western blot analyses are shown as mean ± standard error of the mean (± SEM). IC_{50} values were generated using the nonlinear regression analysis "dose-response inhibition" comparing the inhibitor with a normalized response assuming a variable slope. Statistical significance was assumed for $P < 0.05$ and experiments were performed at least three times.

3. Results

3.1 Patient case reports with *FGFR2* alterations in cholangiocarcinoma

The clinical course of seven patients (n = 7) with iCCA and *FGFR2* alterations were evaluated in detail for this study. The patients were discussed at the MTB and FGFR-inhibiting drugs were recommended between 2017 and 2022. All of the patients received the TKI lenvatinib. The in-detail analysis of these clinical data stimulated a “bed to benchside” approach with the corresponding *in vitro* results shown in detail below (see chapter 3.2 – 3.5). The cellular *in vitro* models were mainly based on two case reports with iCCA and *FGFR2* fusion genes. These case reports are described in more detail below. The first patient had a tumor with a *FGFR2-SH3GLB1* fusion, which has been described previously but not yet characterized *in vitro* (Jain et al., 2018, Goyal et al., 2021). The second patient had a tumor harboring a previously not described *FGFR2-AHCYL2* fusion.

3.1.1 Case report 1: Patient with *FGFR2-SH3GLB1* fusion-positive iCCA (patient #1)

A 42-year-old male patient was admitted to hospital due to a hyperglycemic derailment which led to the initial diagnosis of type 2 diabetes. Within the scope of a sonographic examination, several suspected foci of liver malignancy were found. Laboratory analysis delivered an initial CA19-9 value of 1639 kU/l. After liver biopsy, he was diagnosed advanced iCCA with the CT scan showing multiple suspicious malignant liver lesions up to 10 cm, as well as enlarged lymph nodes in the upper abdomen and nodes suspected of metastasis in the lungs. Tumor material was also sent for tumor exome and transcriptome sequencing. The patient was subsequently treated with gemcitabine/cisplatin. The first follow-up CT scan after 2.2 months of gemcitabine/cisplatin displayed formally SD, yet with a rising CA19-9 value of 3234 kU/l. Therefore, the treating physicians initiated a second line therapy consisting of folinic acid, flourouracil (5-FU) and irinotecan (FOLFIRI). Unfortunately, tumor progression occurred after 7.8 months. Thus, PFS was 2.2 and 7.8 months for first- and second-line chemotherapies,

respectively. The results of the performed tumor exome and transcriptome sequencing revealed an *FGFR2-SH3GLB1* gene fusion, that has been described earlier (Jain et al., 2018). Interestingly, the SH3 domain containing GRB2 like endophilin B1 (*SH3GLB1*) gene encodes a protein possibly involved in the regulation of apoptotic signaling (Pierrat et al., 2001). Thus, after disease progression during the FOLFIRI therapy and at this time no clinical study available, the MTB recommended an off-label individual treatment with the multikinase inhibitor lenvatinib (Yamamoto et al., 2014). Under this treatment, CA19-9 serum levels decreased and SD was detected after 2 months via CT scan. Overall, a PFS of 10.4 months was achieved with lenvatinib. As the disease progressed, a combination therapy of folinic acid, flourouracil (5-FU) and oxaliplatin (FOLFOX) was started. After 2.3 months, the CT scan disclosed progress in bone lesions, while hepatic and pulmonary metastases were stable (PFS: 2.3 months). Thereupon, the patient could be enrolled in a phase II study exploring infigratinib (ClinicalTrials.gov Identifier: NCT02150967) (Javle et al., 2021). Unfortunately, staging CT scan showed progression of bone lesions but again stable results for liver and lung metastases, providing a PFS of only 2.3 months for infigratinib. Therefore, bone lesions were biopsied and confirmed iCCA with the previously detected *FGFR2-SH3GLB1* fusion. In this biopsy, no point mutation in the kinase region or other explanations for resistance were found. Afterwards, brain metastases were detected and the patient finally passed away despite neurosurgical attempts to control the intracerebral disease. OS was 29 months after the initial diagnosis of iCCA and 19 months after the first treatment with a FGFR-inhibiting TKI (**Fig. 3**).

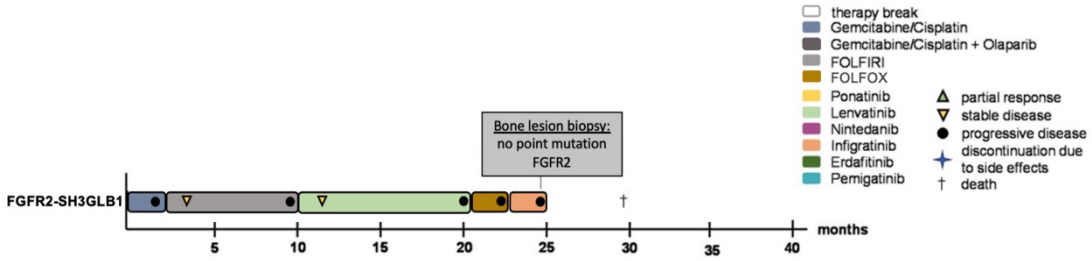

Figure 3: *Timeline of individual treatment course of patient with iCCA and FGFR2-SH3GLB1 fusion*. The patient was treated with different chemotherapeutics, selective and unselective FGFR-targeting TKIs. Timeline indicating duration of administered therapies according to the legend, staging results, and FGFR2 sequencing results of bone lesion biopsy. For ease of comparison, scale and legend are identical to figure 4.

3.1.2 Case report 2: Patient with *FGFR2-AHCYL2* fusion-positive iCCA (patient #2)

A 35-year-old female patient presented to the hospital because she had developed hyperbilirubinemia. She was diagnosed to have advanced iCCA via MRI with an initial CA19-9 value of 4790 kU/l. After 2 months of chemotherapy with gemcitabine/cisplatin, CT scans showed PR and she could subsequently undergo an extended right hemihepatectomy. Despite R0 tumor resection, multiple new liver lesions occurred 3 months after surgery. At this point, the CA19-9 value was 52 kU/l and she was subsequently again subjected to gemcitabine/cisplatin therapy. Chemotherapy led to a reduced tumor size in a MRI scan and CA19-9 serum levels returned to the normal range with 16 kU/l at follow-up examinations after 2 months. After the patient denied the option of living-donor liver transplantation, chemotherapy was continued and diagnostic tumor panel sequencing was carried out. A follow-up MRI scan after an additional 2 months displayed intrahepatic tumor progression, resulting in a PFS of 4.2 months receiving gemcitabine/cisplatin after the recurrence of the tumor. Tumor panel sequencing results revealed, among other alterations, an *FGFR2-AHCYL2* fusion gene, which has not been described previously. A more detailed analysis revealed, that the *FGFR2-AHCYL2* fusion gene developed through fusion of exon 1-17 of *FGFR2*

and exon 2-17 of *AHCYL2*. The protein encoded by the S-adenosylhomocysteine hydrolase-like 2 isoform (*AHCYL2*) gene is possibly implicated in protein metabolism in the conversion of S-adenosylhomocysteine to L-homocysteine and adenosine (Frazier-Wood et al., 2012). In the resulting fusion protein, part of the AHCYL2 sequence was attached to the C-terminal end of the FGFR kinase domain. *In silico* modelling suggested the kinase activity of the fusion protein to be most probably not affected and proposed a therapy with an FGFR inhibiting TKI. At this time, no clinical study was available for the patient, thus the MTB recommended ponatinib as off-label therapy. The multikinase inhibitor ponatinib was previously reported achieving either a response or SD in three published case reports with other tumors harboring *FGFR2* fusion genes (Borad et al., 2014). Ponatinib was administered for 1.5 months, until follow-up examinations using MRI bared progress of intrahepatic lesions, extrahepatic lymph nodes, and a new soft tissue metastasis in the right thoracic wall area (PFS: 1.5 months). At that time, CA19-9 serum levels yielded a value of 43 kU/l. Afterwards, the soft tissue lesion was again biopsied for sequencing to investigate, whether the fusion gene was still present, and chemotherapy with FOLFIRI was begun. After nearly 1 month of FOLFIRI therapy, an MRI scan exhibited slightly progressing lesions with stable CA19-9 levels with 45 kU/l. However, the patient poorly tolerated the therapy and stated that she did not want to continue the FOLFIRI regimen. At this point still there was no option for the inclusion in a clinical study. According to an MTB-initiated search for alternative treatments, lenvatinib was an available option to inhibit FGFR pathways (Yamamoto et al., 2014, King and Javle, 2021). Meanwhile the fusion gene was confirmed in the second biopsy. Upon treatment, lenvatinib achieved a partial response in the follow-up examination already after 1.5 months using a MRI scan. Besides, the drug was well tolerated by the patient and CA19-9 value decreased to 20 kU/l. Repeated staging scans confirmed a partial response to the multikinase inhibitor, until tumor progression was first detected after 9 months by PET-CT scan, resulting in a PFS for lenvatinib of 9.0 months. Another biopsy was performed, but sequencing analyses failed to find an explanation for the observed diminishing effect of lenvatinib within the *FGFR2* gene or its downstream signals. After a therapy break of 3 months, treatment with

gemcitabine/cisplatin was started again in combination with the PARP-inhibiting TKI olaparib, due to heterozygous deletions concerning DNA damage response and repair (DDR) genes *ERCC4*, *CHEK2* and *FANCA* genes (Lin et al., 2019), according to a further MTB recommendation. Yet, the patient showed PD in an MRI scan after only 1.6 months (PFS: 1.6 months). The subsequent therapy according to the FOLFOX regime was not tolerated by the patient. Next, the patient was treated with nintedanib until progress was noticed in the first staging CT scan, corresponding to a PFS of only 1.5 months. Thereafter, the patient was enrolled in a then available phase II study with infigratinib (ClinicalTrials.gov Identifier: NCT02150967) (Javle et al., 2021). Of note, infigratinib led to a partial response which was confirmed by follow-up CT scans. This was an important finding, because it showed that despite a successful previous targeting of the FGFR-alteration the tumor was still addicted to this pathway. Unfortunately, the patient was excluded from the study due to therapy interruptions caused by recurrent cholangitis and the therapy had to be stopped prior to progression, leading to a formal PFS of 5.5 months, which is far longer than the PFS of the previous treatment with Nintedanib. At the time of further tumor progression an additional liver biopsy of a tumor lesion now revealed a p.N549H point mutation, which is considered to cause resistance to FGFR-inhibitory drugs (Goyal et al., 2017, Krook et al., 2019). An additionally performed liquid biopsy of cfDNA detected further multiple *FGFR* mutations consistent with acquired resistance to TKIs, including the p.V564F gatekeeper mutation. Despite this finding, due to the lack of alternative treatment options and at that time unclear implications of these mutations for further FGFR-targeting treatments, erdafitinib and pemigatinib were subsequently administered, but without success, resulting in short PFS periods of 0.8 months, respectively. The patient died soon after due to severe cholangiosepsis. The OS after the diagnosis of tumor recurrence and numerous different systemic therapies was 38 months and remarkably 31 months after the initiation of lenvatinib as an off-label treatment for FGFR inhibition (**Fig. 4**). (Spahn et al., 2024)

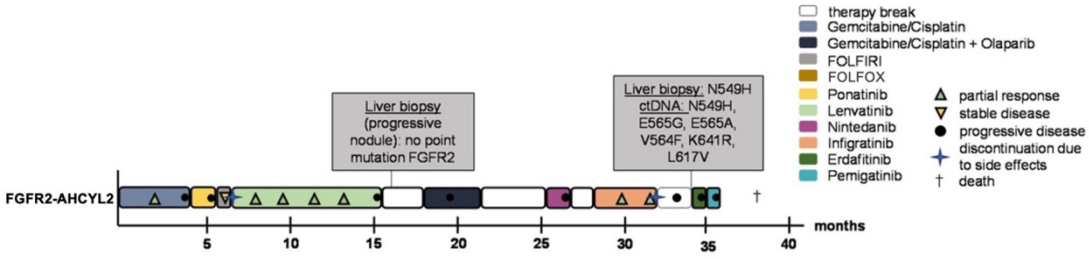

Figure 4: *Timeline of individual treatment course of patient with iCCA and FGFR2-AHCYL2 fusion*. The patient was treated with different chemotherapeutics, selective and unselective FGFR-targeting TKIs. Timeline indicating duration of administered therapies according to the legend, staging results, and FGFR2 sequencing results of liver biopsies. For ease of comparison, scale and legend are identical to figure 3.

3.1.3 Lenvatinib in further patients with CCA harboring *FGFR2* alterations

A retrospective analysis could identify five further patients in the MTB database that were treated with lenvatinib to target FGFR2 according to MTB recommendations. The detailed analysis of these patients revealed that lenvatinib led to a partial response in four of the total seven patients (**Fig. 5 A**). One of the patients (370_371delinsCys & Del) has been reported in detail previously (Bitzer et al., 2021). Two exemplary [18F]fluorodeoxyglucose (FDG) - positron emission tomography (PET) scans before and eight weeks after initiation of treatment with lenvatinib depicted apparent metabolic responses to the treatment (**Fig. 5 B**).

All seven patients received at least a “classical” first-line therapy prior to lenvatinib.

Looking at the first line therapy, although a partial response was initially observed for gemcitabine/cisplatin treatment in patient #2, the tumor progressed after 4.2 months. Patient #1 also experienced a progress, which was detected after 2.2 months. The results were similar for first-line treatment in other cases considered, resulting in a median PFS of 2.5 months for the therapies applied first. Only considering gemcitabine/cisplatin as first-line therapy the median PFS was 2.1 months.

Regarding the treatment courses with lenvatinib, patient #1 had a PFS of 10.4 months and patient #2 of 9.0 months. Furthermore, for patient #2 even a partial response was noticed, as well as in three additional cases. Considering all patient cases together, for lenvatinib, the median PFS was 7.0 months and the median OS was 12.5 months, ranging from 3.6 to 30.3 months. Comparing the two lines of therapy, median PFS was significantly lower with established gemcitabine/cisplatin therapy than with lenvatinib after gemcitabine/cisplatin application (**Fig. 5 C**). Of note, the calculated PFS ratio regarding lenvatinib calculated according to the Van Hoff model (see chapter 2.1) was favorable compared to both, previous and first-line therapies in 6 of 7 patients (**Fig. 5 A**).

Taken together, given the clinical observations that lenvatinib appears to be a promising therapeutic approach to target FGFR2-related cholangiocarcinoma, a "bed to benchside" approach was initiated to gain further insight into this potential treatment option. (Spahn et al., 2024)

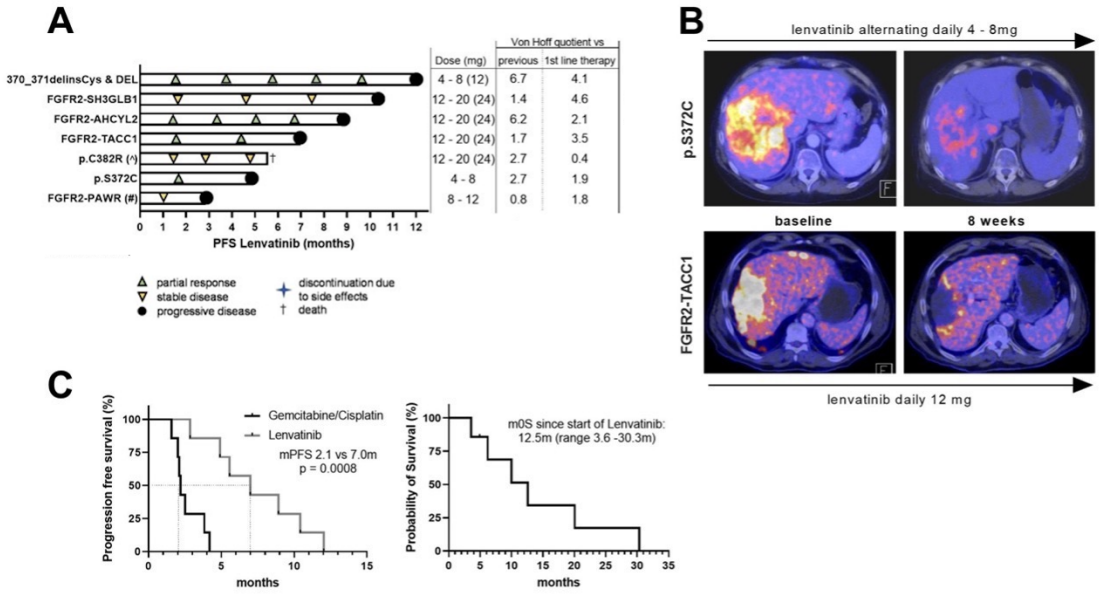

Figure 5: *Lenvatinib response in patients with FGFR2-altered iCCA*. **(A)** Swimmer plot demonstrating distinct treatment responses since initiation of treatment with lenvatinib. Depicted is the lenvatinib dose used for the majority of the treatment course with the maximum dose in brackets, as well as the Von Hoff quotient of lenvatinib compared to first-line therapy and prior therapies. First-line therapy was gemcitabine/cisplatin in all patients except one, who was treated with FOLFIRINOX (^). The first patient (370_371delinsCys & Del) has been reported in detail previously (Bitzer et al., 2021). The patient with an FGFR2-PAWR fusion (#) was treated with infigratinib prior to treatment with lenvatinib. **(B)** PET-scans after 8 weeks of Lenvatinib treatment in patients with iCCA harboring FGFR2 alterations. **(C)** Kaplan-Meier survival curves showing PFS of lenvatinib compared to prior gemcitabine/cisplatin therapy and OS since initiation of treatment with lenvatinib. Adapted from our own publication (Spahn et al., 2024).

3.2 Generation and characterization of cell lines expressing *FGFR2* fusion genes

3.2.1 Generation of NIH/3T3 cell lines expressing FGFR2 fusions

To functionally characterize the newly identified fusion gene FGFR2-AHCYL2 and compare it to the previously described fusion genes FGFR2-SH3GLB1 and FGFR2-BICC1, the first step was to generate patient-specific stable cell lines expressing these fusion genes.

Representative results for the transfection of the *FGFR2-SH3GLB1* fusion gene are shown in the following figure, whereas the results for the other *FGFR2* fusion genes were correspondingly equivalent (**Fig. 6**).

Initially, plasmid constructs were generated for the different *FGFR2* fusion genes as shown in the schematic representation (**Fig. 6 A**). Using *eGFP* gene anchored in the plasmid construct, the expression was initially checked after transfection by fluorescence microscopy. Directly after transfection, GFP signal was expressed in a high proportion of NIH/3T3 cells, but in varying degrees. After selection with G-418, four clones were selected for further studies for each *FGFR2* fusion gene, which had a slightly lower proportion of GFP-expressing cells but a moderate, uniform, and temporally stable signal (**Fig. 6 B**). As a control, WT-NIH/3T3 cells were also exposed to G-418 and were completely dead after one week.

To confirm the FGFR2 fusions at the protein level, Western blots of the four different selected clones were performed with antibodies specific for pFGFR2 after selection for each newly generated cell line and subsequently, as the antibody was then available, with FGFR2. For the FGFR2-SH3GLB1 fusion protein as an example, two bands sized 130 – 150 kDa could be detected with pFGFR antibody and “clone C” was used for all further experiments (**Fig. 6 C**). Likewise, for the other two fusion-expressing cell lines containing *FGFR2-BICC1* and *FGFR2-AHCYL2*, the cells with the strongest pFGFR expression in Western blot analyses were used as the final clone for further experiments (**Table 6**).

Table 6: *Original designation of the selected clones after transfection*

Cell line	Clones picked after G-418 selection	Final clones used in the following
empty vector P2A-eGFP-transfected NIH/3T3 cells	**A1a1**, B1a1, B5a1, B5b2	**A1a1**
FGFR2-BICC1-transfected NIH/3T3 cells	**C2b1**, B5c, B5f, D1d	**C2b1**
FGFR2-SH3GLB1 -transfected NIH/3T3 cells	C1a2, C1a3, **C8c1** *, C8c2	**C8c1** *
FGFR2-AHCYL2 -transfected NIH/3T3 cells	1b, **2b**, 2b1, 2c	**2b**

* clone C8c1 is referred to as “clone C” in Fig. 6 C

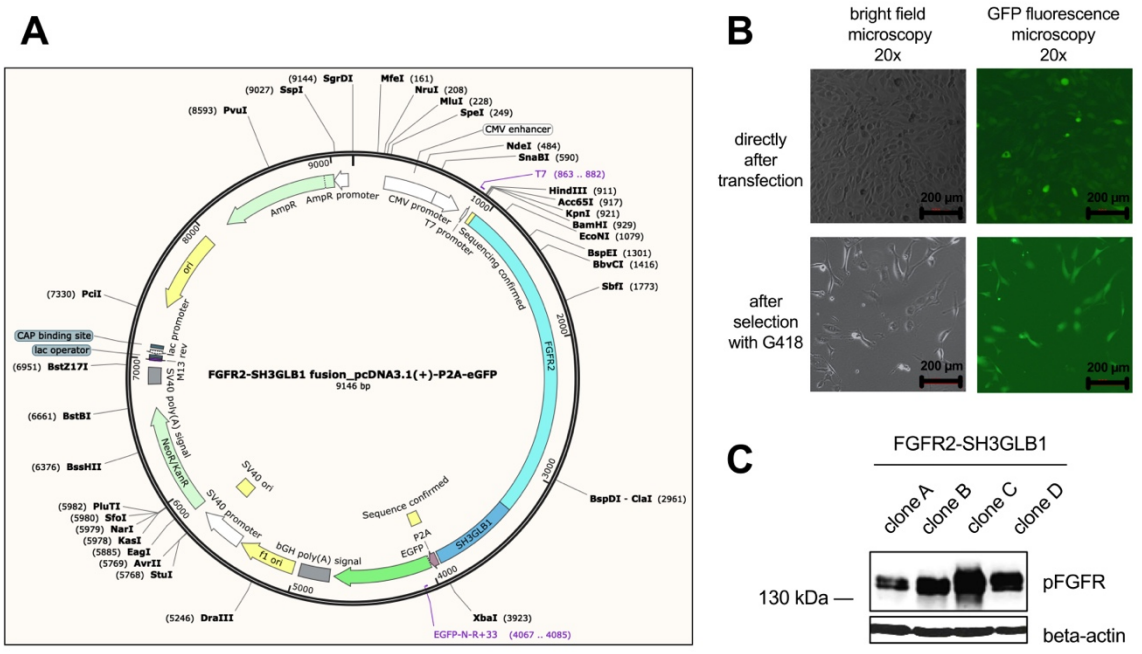

Figure 6: *Transfection and selection of FGFR2-SH3GLB1 fusion gene-transfected cells.* **(A)** Plasmid construct of the patient-analogue FGFR2-SH3GLB1 gene including eGFP- and neomycin-resistance-mediating regions. **(B)** Representative images of bright field and respective GFP fluorescence microscopy of FGFR2-SH3GLB1-transfected cells 48 hours after transfection and after 30 days of selection (scale bar = 200 µm). **(C)** Western blot analysis of pFGFR protein showing four different generated clones expressing FGFR2-SH3GLB1. “clone C” (originally “C8c1”) was picked for further investigations.

After selection of the respective final clone via Western blot, all transfected NIH/3T3 cells had a moderate and stable GFP signal in fluorescence microscopy. The GFP-positive rate was comparable between the different newly generated cell lines, though only slightly higher for empty vector-transfected CTL-NIH/3T3 cells (**Fig. 7 A**). Western blotting using FGFR2 antibodies confirmed, that only endogenous FGFR2 was expressed at about 130 kDa, both for WT-NIH/3T3 and for CTL-NIH/3T3 cells. For all *FGFR2* fusion gene-transfected cells, however, additional bands at different sizes could be recognized (**Fig. 7 B and C**). Thereby, the band size corresponded to the estimated size of the fusion gene. The 5.049 base pair (bp) long *FGFR2-BICC1* gene transfection resulted in a band at about 230 kDa, that could hardly be seen in 10 % resolving gel, but became visible using 7,5 % resolving gel. *FGFR2-SH3GLB1*, a 2.982 bp long fusion gene, led to detection of an additional band in the range of 150 kDa in respective transfected cells. Furthermore, *FGFR2-AHCYL2*-harboring cells indicated an about 180 kDa sized band in Western blot analyses, according to its 3.837 bp long fusion sequence. Taken together, the respective *FGFR2* fusion genes were stably expressed in NIH/3T3 cells and led to the formation of a corresponding fusion protein.

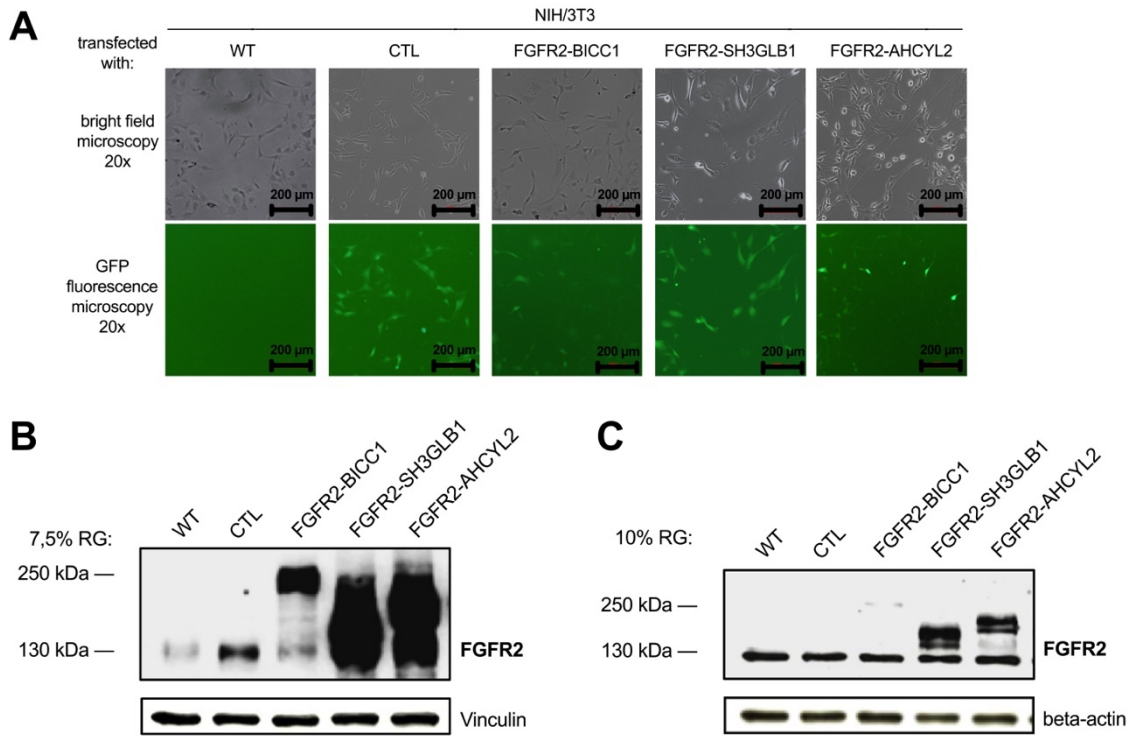

Figure 7: *Fluorescence microscopy and Western blot analysis of FGFR2 in different FGFR2 fusion gene-transfected NIH/3T3 cells.* **(A)** Representative images of bright field or GFP fluorescence microscopy of the final clones chosen for further investigation (scale bar = 200 µm). **(B)** Western blot analysis of FGFR2 protein expressed in final clones using a 7.5 % resolving gel or **(C)** a 10 % resolving gel.

3.2.2 Impact of FGFR2 fusions on different downstream signals

For further molecular analyses, the novel cell lines were examined using Western blot analysis to inspect possible oncogenesis relevant downstream activations. For that purpose, the proteins FRS2, P44/42 (MAPK), STAT3 and their phosphorylated form were investigated (**Fig. 8 A and B**). The analyses demonstrated that pFGFR was increased in FGFR2 fusion protein-positive cells compared to CTL-NIH/3T3 cells. In the Western blots using 10 % resolving gel, pFGFR could not be detected for *FGFR2-BICC1*-transfected cells, probably due to its large size. Nevertheless, other blots using 7,5 % resolving gel confirmed that there was stronger phosphorylation of FGFR in this cell line, too (**Fig. 8 C**).

Further descending in the downstream cascade, adapter protein FRS2 was investigated. While all tested cells presented the same expression of its inactivated

form, pFRS2 bands were exclusively displayed in the Western blot of fusion gene containing cells. Although a slight activation of pP44/42 (MAPK) was seen for the CTL-NIH/3T3 cells compared to WT-NIH/3T3, observed effects were even stronger for cells expressing an FGFR2 fusion gene. Stronger protein expression for pSTAT3 was exclusively found in *FGFR2-SH3GLB1* and *FGFR2-AHCYL2*-positive cells. Considering all protein analyses performed, no consistent enhanced expression of pAKT was apparent for the generated cell lines. As the fusion gene *FGFR2-AHCYL2* has not been previously described, an additional densitometric analysis of six independent Western blot analyses was performed to quantify the observed increased protein expression by transfection of the fusion gene. The evaluation confirmed a statistically higher expression for pFGFR (about 8x higher), pMAPK (about 3,5x higher) and pSTAT3 (about 4x higher) in FGFR2-AHCYL2 cells compared to WT-NIH/3T3 cells (**Fig. 8 D-G**). In conclusion, expression of an *FGFR2* fusion gene led to activation of downstream signaling pathways. (Spahn et al., 2024)

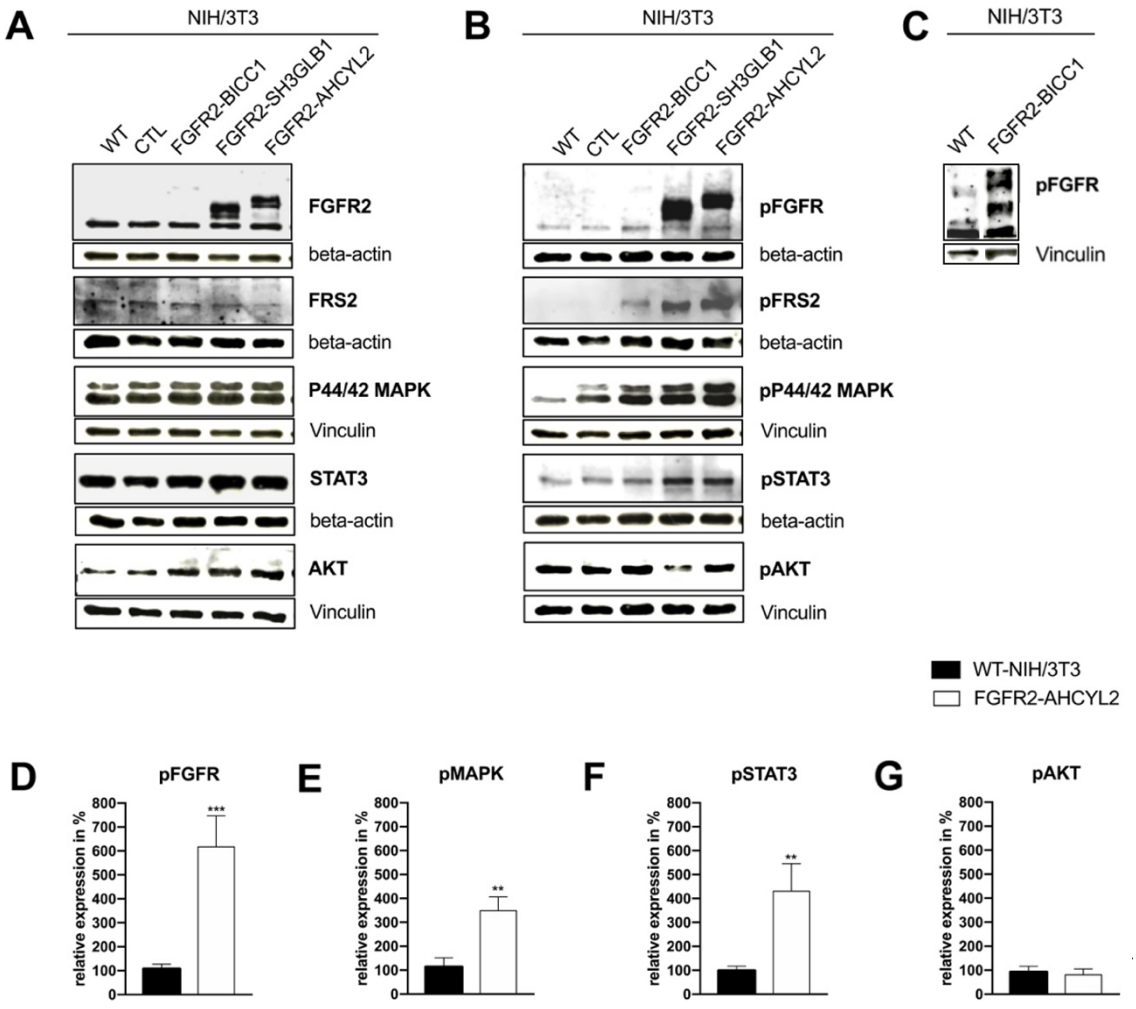

Figure 8: *Western blot analysis of FGFR2 fusion gene-transfected NIH/3T3 cells for downstream pathways.* **(A)** Western blot analysis of the unphosphorylated FGFR2 pathway proteins in NIH/3T3 cells expressing different fusion proteins and **(B)** their respective phosphorylated active forms. **(C)** Western blot with 7.5 % resolving gel for analysis of pFGFR in FGFR2-BICC1 compared with WT-NIH/3T3. Densitometric analyses of **(D)** pFGFR, **(E)** pMAPK, **(F)** pSTAT3 and **(G)** pAKT in FGFR2-AHCYL2 expressing NIH/3T3, graphs show mean ± SEM, $^{**}P \leq 0.01$, $^{***}P \leq 0.001$ in comparison to wild type NIH/3T3 cells, n = 6.

3.2.3 Functional analyses of *FGFR2* fusion gene-expressing cells

To assess the functional modifications caused by expression of *FGFR2* fusion genes, SRB assays and soft agar colony formation assays were performed.

First, cell proliferation of novel cell lines was investigated using SRB assays and cell mass was compared after 7 days.

Expression of FGFR2 fusion increased cell proliferation and cell mass was about 2.5x higher for the *FGFR2* fusion gene-expressing cells compared to CTL-NIH/3T3 cells. Similar proliferation with respect to the different fusion proteins was observed (**Fig. 9 A**).

Second, soft agar colony formation assays were performed to evaluate whether the novel fusion gene cell lines were capable of anchorage-independent growth. As *FGFR2-BICC1*-transfected NIH/3T3 cells have previously been shown to have the ability of anchorage-independent growth, only FGFR2-SH3GLB1 and FGFR2-AHCYL2 cells were assessed for this (Arai et al., 2014).

Whereas nearly no colonies were formed by CTL-NIH/3T3 cells, FGFR2-SH3GLB1 as well as FGFR2-AHCYL2 cells formed at least 100 colonies. The number of colonies of the two FGFR2 fusion cell lines examined did not differ significantly (**Fig. 9 B**). Moreover, in addition to the increased number of colonies, *FGFR2* fusion gene-expressing cells formed significantly larger colonies (**Fig. 9 C and D**). With increased proliferation and the ability of anchorage independent growth, the novel generated cell lines showed malignant potential. (Spahn et al., 2024)

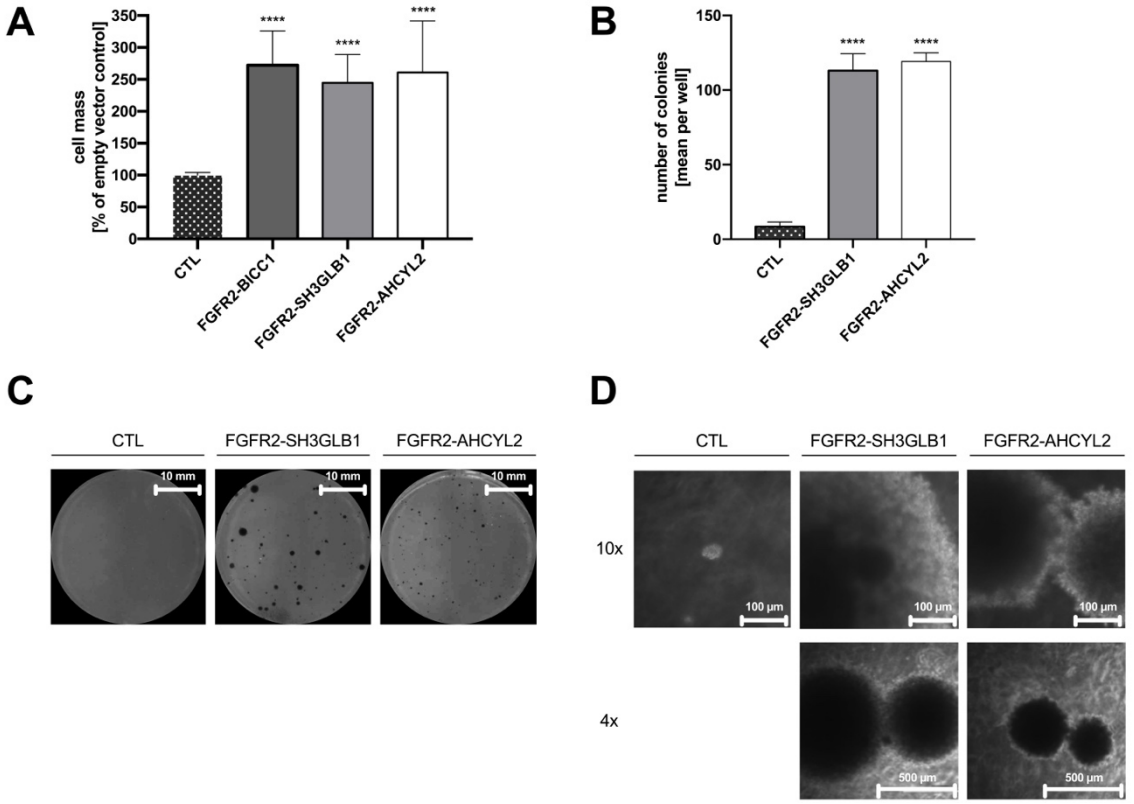

Figure 9: *Proliferation and anchorage-independent growth assays of NIH/3T3 cells expressing FGFR2 fusions.* **(A)** Proliferation analyses of FGFR2 fusion-expressing cell lines using SRB assays after 7 days in culture, graphs show mean ± SD, ****$P \leq 0.0001$ compared to control-transfected NIH/3T3 cells, n = 30. **(B)** Quantification of soft agar colony formation of NIH/3T3 expressing FGFR2-SH3GLB1 and FGFR2-AHCYL2 after 21 days, graphs show mean ± SD, ****$P \leq 0.0001$ compared to control-transfected NIH/3T3 cells, n = 8. **(C)** Representative images of soft agar wells of the indicated cell lines after 21 days of incubation (scale bar = 10 mm) and (**D)** representative images of the respective colony size using 10x (scale bar = 100 µm) or 4x (scale bar = 500 µm) bright field microscopy.

3.3 Drug assays of FGFR2 fusion-positive cells

3.3.1 Functional drug assays of NIH/3T3 cells expressing *FGFR2* fusion genes

The availability of a cell culture model with different patient-derived *FGFR2* fusion genes provided the possibility to compare different drugs in the presence of these fusion proteins. First, the FGFR inhibiting unselective TKIs lenvatinib, ponatinib and nintedanib; second, the FGFR selective TKIs infigratinib and futibatinib; third the classical chemotherapeutic drug gemcitabine; and fourth the non FGFR inhibiting multikinase inhibitor cabozantinib were studied.

Investigation of FGFR-inhibiting multikinase inhibitors in SRB assays

First, the applied unselective TKIs were investigated. In contrast to the selective FGFR-inhibiting drugs, inhibitors like lenvatinib, ponatinib and nintedanib inhibit multiple tyrosine kinase receptors, including FGFR (Dienstmann et al., 2014). In line with the observed clinical effects in the patients, treatment with lenvatinib at all concentrations tested significantly inhibited cell growth for *FGFR2* fusion gene-expressing cells compared to CTL-NIH/3T3 cells (**Fig. 10 A**). The results for ponatinib differed for the lowest concentrations between the tested cell lines. Yet, higher concentrations significantly inhibited cell growth in all fusion gene-positive cells (**Fig. 10 B**). In lower concentrations, nintedanib did not inhibit cell growth in FGFR2 fusion cell lines, compared to CTL-NIH/3T3. Only for 1 µM concentration, a consistently better proliferation-inhibiting effect could be identified, when comparing the generated *FGFR2* fusion gene-positive cells to the CTL-NIH/3T3 cells. However, the effects did not show a consistent stronger inhibition in fusion gene-positive compared to control-transfected cells (**Fig. 10 C**). (Spahn et al., 2024)

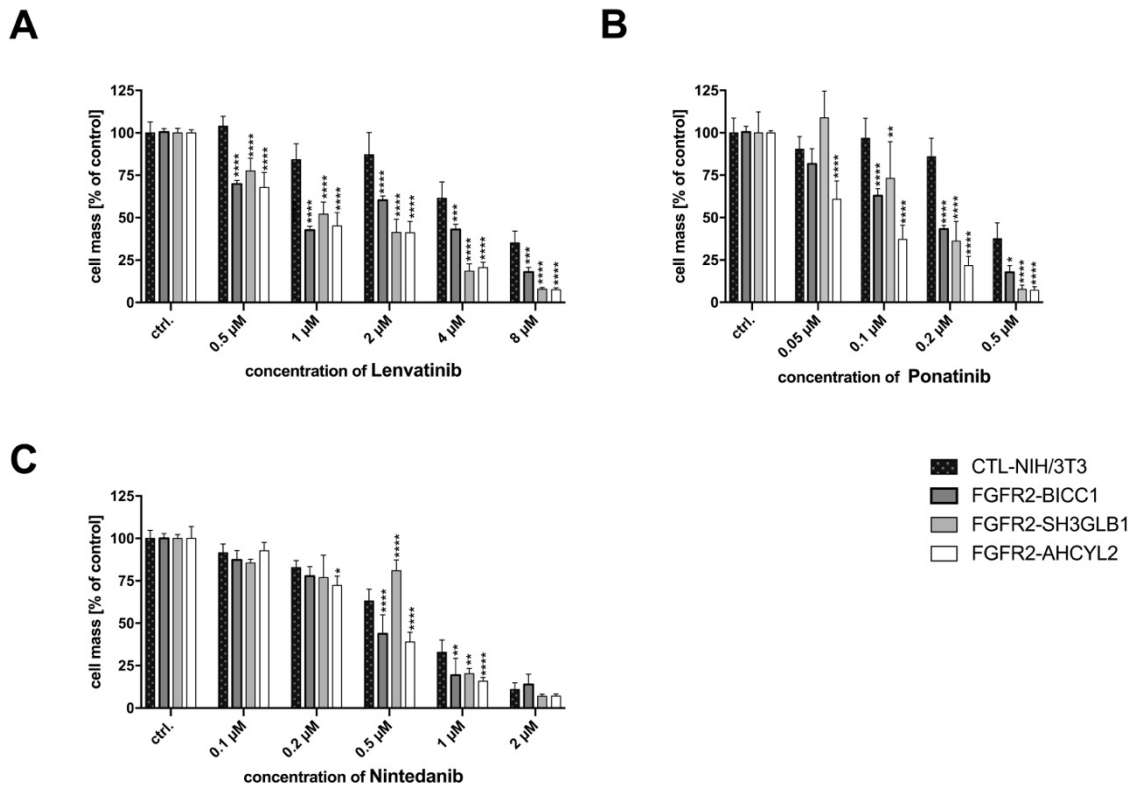

Figure 10: *Efficacy of unselective tyrosine kinase inhibitors with FGFR-inhibitory capacity in novel FGFR2 fusion-expressing cell lines.* Proliferation analyses using SRB assays after 7 days of treatment with the indicated unselective inhibitors **(A)** lenvatinib, **(B)** ponatinib and **(C)** nintedanib, graphs show mean ± SD, **P* ≤ 0.05, ***P* ≤ 0.01, ****P* ≤ 0.001, *****P* ≤ 0.0001 compared to control-transfected NIH/3T3 cells, n = 6.

Investigation of selective FGFR-inhibiting TKIs in SRB assays

The selective FGFR inhibitor infigratinib significantly inhibited proliferation of the FGFR2 fusion-expressing cell lines in comparison with CTL-NIH/3T3 cells at all concentrations tested (**Fig. 11 A**). Similar results were obtained for the covalent binding FGFR-inhibiting futibatinib, thus indicating good efficacy of both selective inhibitors (**Fig. 11 B**). (Spahn et al., 2024)

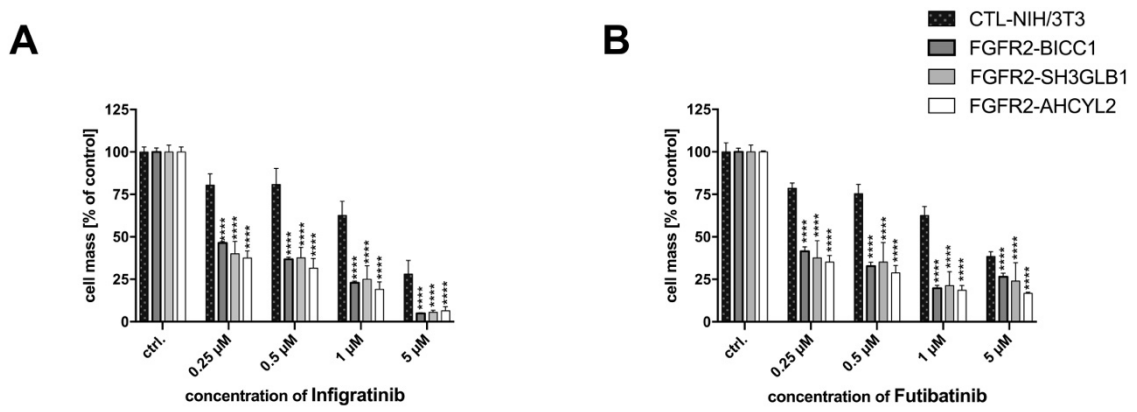

Figure 11: *Efficacy of selective FGFR inhibitors in novel FGFR2 fusion-expressing cell lines.* Proliferation analyses using SRB assays after 7 days of treatment with the indicated selective inhibitors **(A)** infigratinib and **(B)** futibatinib, graphs show mean ± SD, ****$P \leq 0.0001$ compared to control-transfected NIH/3T3 cells, n = 6.

Investigation of the multikinase inhibitor cabozantinib without FGFR-inhibitory activity and the chemotherapeutic substance gemcitabine in SRB assays

Finally, cells were treated with cabozantinib, a TKI without described FGFR inhibition, and with gemcitabine, one component of the current chemotherapeutic first-line combination treatment for advanced CCA. These treatments were intended as control experiments.

Treatment with cabozantinib did not inhibit cell proliferation of FGFR2 fusion-expressing cells (**Fig. 12 A**). Instead, the results resembled the increased proliferative activity, shown without treatment as shown above (see **Fig. 9**). These results demonstrated that the investigated cell lines did not show an unspecific antiproliferative effect during the treatment with TKIs in general, but only for those inhibitors with a relevant FGFR-inhibitory activity. For the treatment with gemcitabine, despite the higher proliferation, the drug was less effective in FGFR2 fusion cells compared to CTL-NIH/3T3 cells. Moreover, differences among the fusion gene cells were found. Cell proliferation of FGFR2-SH3GLB1 cells was more affected by gemcitabine than that of FGFR2-BICC1 and FGFR2-AHCYL2 cells (**Fig. 12 B**). Thus, gemcitabine seems not to inhibit the increased general proliferation in FGFR2 fusion-expressing cells. (Spahn et al., 2024)

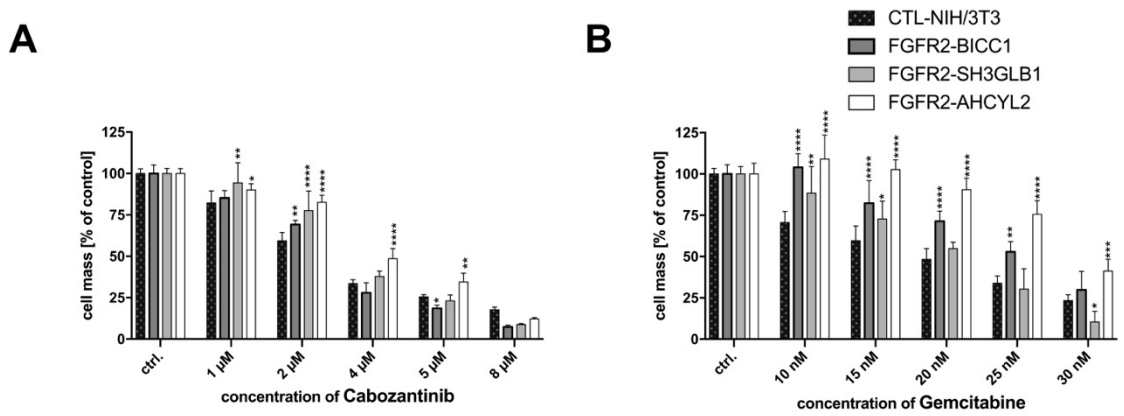

Figure 12: *Efficacy of an unselective tyrosine kinase inhibitor without FGFR inhibition capacity and gemcitabine as one component of standard CCA chemotherapy treatment in novel FGFR2 fusion-expressing cell lines.* Proliferation analyses using SRB assays after 7 days of treatment with **(A)** the non-FGFR-inhibiting multikinase inhibitor cabozantinib and **(B)** the current standard chemotherapeutic drug gemcitabine, graphs show mean ± SD, **P* ≤ 0.05, ***P* ≤ 0.01, ****P* ≤ 0.001, *****P* ≤ 0.0001 compared to control-transfected NIH/3T3 cells, n = 6.

IC_{50} values of tested drugs on FGFR2 fusion gene-expressing cells

Next, IC_{50} values of the different tested substances in SRB assays were calculated using PRISM. Furthermore, these values were compared to the values obtained for the empty vector containing CTL-NIH/3T3 cells. By this, enhanced or reduced drug sensitivity of the different cells caused by the respective FGFR2 fusion should be evaluated. Sensitivity was interpreted as increased or decreased when the IC_{50} of FGFR2 fusion gene-bearing cells was less or more than 100 %, respectively. Of note, expression of a *FGFR2* fusion gene increased sensitivity to all FGFR-inhibiting TKIs, except *FGFR2-SH3GLB1* to nintedanib (**Fig. 13**). Moreover, this increased sensitivity varied in degree. For *FGFR2-AHCYL2* and *FGFR2-BICC1* cells sensitivity to nintedanib was only enhanced to a smaller extent. The multikinase inhibitors ponatinib and especially lenvatinib showed good results regarding all cells harboring an *FGFR2* fusion gene, leading to IC_{50} values lower than 38.2 % and 29.7 %, respectively, compared to control transfected cells. Even better efficacy was observed for FGFR2-selective TKIs with IC_{50} values of less than 12.6 % for infigratinib and 1.8 % for futibatinib. In contrast,

all FGFR2 fusion-positive cells showed reduced sensitivity to multikinase inhibitor cabozantinib, with IC_{50} values up to 150.1 % compared to CTL-NIH/3T3 cells. Again, this suggests that the effects of TKIs on these cell lines were caused by inhibition of FGFR, without nonspecific effects of the TKIs themselves. Furthermore, sensitivity for gemcitabine was decreased for all FGFR2 fusion-expressing cells compared to CTL-NIH/3T3 cells (IC_{50} values up to 163.1 %). Interestingly, cells transfected with an *FGFR2* fusion gene were the least sensitive to gemcitabine using this comparison.

In conclusion, the multikinase inhibitors lenvatinib and ponatinib and the selective inhibitors infigratinib and futibatinib were effective in the cellular model, whereas the chemotherapeutic gemcitabine appeared to be inefficient.

For better visual illustration of the respective effects on IC_{50} values, additional color coding was used in the figure according to gradations of increased or decreased sensitivity. Different color intensities of green were used for increased sensitivity (% of IC_{50} value for CTL-NIH/3T3: < 50 %: bright green, 10–30 %: green, < 10 %: intense green) and different color intensities of red for decreased sensitivity (% of IC_{50} value for CTL-NIH/3T3: > 100 %: bright red, > 120 %: red). (Spahn et al., 2024)

	unselective FGFR inhibitors						selective FGFR inhibitors							
	Lenvatinib		Ponatinib		Nintedanib		Infigratinib		Futibatinib		Cabozantinib		Gemcitabine	
	IC_{50} in nmol/L SD (n)	% of IC_{50} empty vector	IC_{50} in nmol/L SD (n)	% of IC_{50} empty vector	IC_{50} in nmol/L SD (n)	% of IC_{50} empty vector	IC_{50} in nmol/L SD (n)	% of IC_{50} empty vector	IC_{50} in nmol/L SD (n)	% of IC_{50} empty vector	IC_{50} in nmol/L SD (n)	% of IC_{50} empty vector	IC_{50} in nmol/L SD (n)	% of IC_{50} empty vector
CTL-NIH/3T3	**5456** 405 (6)	**100.0**	**408** 26 (6)	**100.0**	**634** 26 (6)	**100.0**	**1815** 184 (6)	**100.0**	**2389** 203 (6)	**100.0**	**2594** 66 (6)	**100.0**	**17.6** 0,5 (6)	**100.0**
FGFR2-BICC1	**1620** 236 (6)	**29.7**	**156** 7 (6)	**38.2**	**428** 24 (6)	**67.5**	**229** 9 (6)	**12.6**	**33** 22 (6)	**1.4**	**2670** 62 (6)	**102.9**	**24.9** 0,6 (6)	**141.5**
FGFR2-SH3GLB1	**1260** 63 (6)	**23.1**	**159** 12 (6)	**39.0**	**707** 43 (6)	**111.5**	**171** 31 (6)	**9.4**	**29** 35 (6)	**1.2**	**3229** 104 (6)	**124.5**	**19.9** 0,5 (6)	**113.1**
FGFR2-AHCYL2	**1021** 69 (6)	**18.7**	**69** 4 (6)	**16.9**	**376** 13 (6)	**59.3**	**133** 19 (6)	**7.3**	**42** 14 (6)	**1.8**	**3893** 84 (6)	**150.1**	**28.7** 0,5 (6)	**163.1**

Figure 13: *IC_{50} values of selected substances in NIH/3T3 cells harboring different FGFR2 fusion genes.* Illustration shows IC_{50} values of different drugs for NIH/3T3 cells expressing the indicated construct in nmol/L ± SD and their respective percentage of the value for empty vector-transfected cells, n = 6. Additional color coding was used for the percentage of IC_{50} values of empty vector-transfected cells as follows: < 50 % bright green, 30-10 % green, < 10 % dark green; > 100 % bright red, > 120 % red.

Colony formation assays for the FGFR-selective TKI infigratinib and the FGFR-inhibiting unselective TKI lenvatinib

Drug effects of the selective FGFR inhibitor infigratinib as well as of lenvatinib as a non-selective inhibitor were additionally investigated in colony formation assays. Both inhibitors significantly reduced the colony formation for cells transfected with *FGFR2-SH3GLB1* and *FGFR2-AHCYL2* (**Fig. 14**).

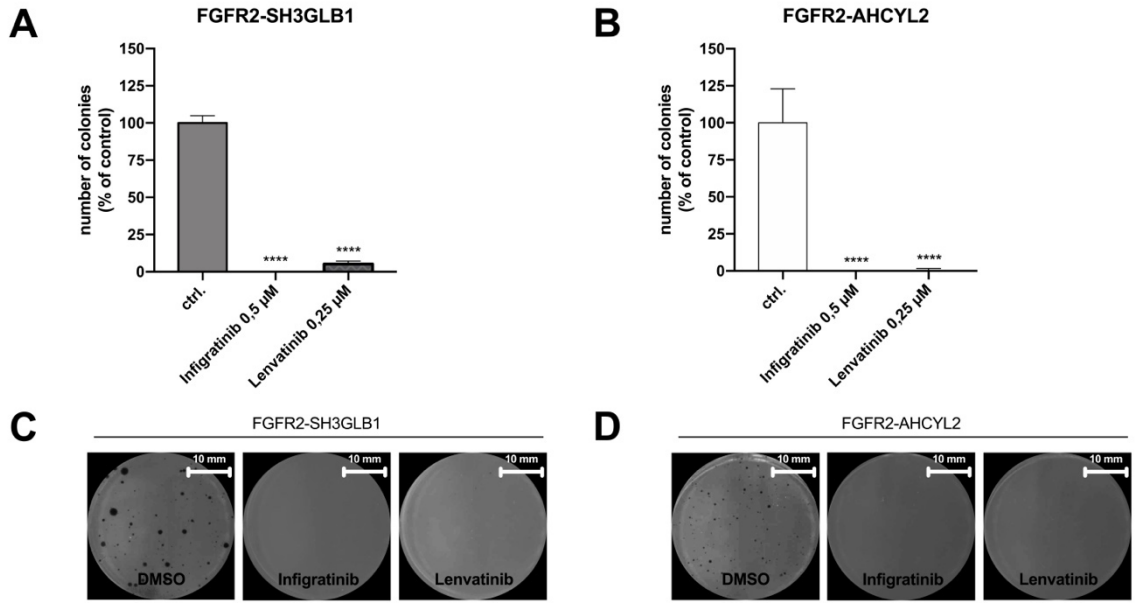

Figure 14: *Efficacy of tyrosine kinase inhibitors infigratinib and lenvatinib in novel FGFR2 fusion-expressing cell lines using soft agar colony formation assays.* Quantification of soft agar colony formation after 21 days for transfected cells with **(A)** FGFR2-SH3GLB1 and **(B)** FGFR2-AHCYL2, graphs show mean ± SD, ****$P \leq 0.0001$ compared to the respective DMSO treated cells, n = 6. Representative images of soft agar wells after 21 days of incubation for **(C)** FGFR2-SH3GLB1 and **(D)** FGFR2-AHCYL2 plasmid containing cells (scale bar = 10 mm).

3.3.2 Western blots of downstream signals in FGFR2-AHCYL2 fusion-expressing cells after treatment with various TKIs

To elucidate molecular implications of different TKIs on downstream signals, Western blot analyses were performed for hitherto undescribed FGFR2-AHCYL2 cells with or without treatment. For that purpose, the relevant concentrations of

infigratinib, lenvatinib and ponatinib were chosen that approximately led to 50 % cell mass reduction after 7 days in SRB assays (**Fig. 15 A**).

For the phosphorylated form of FGFR, a significant inhibition (about 60-90 %) was detected by treatment with all TKIs compared to DMSO exposed cells (**Fig. 15 B**). On the contrary, signal for pP44/42 (MAPK) was significantly weaker (about 85 %) only after treatment with infigratinib (**Fig. 15 C**). Analysis of pSTAT3 indicated a signal reduction after treatment for all TKIs tested, ranging from 30-65 % (**Fig. 15 D**). Of note, lenvatinib led to a weaker signal reduction of pFGFR, yet causing a stronger signal reduction for pSTAT3 (**Fig. 15 B and D**). These results suggest that nonselective FGFR inhibitors have a different effect on down-stream signaling than selective ones.

Results obtained for gemcitabine within the same test setup are shown in a following chapter below (see chapter 3.5.2, **Fig. 23 A-E**).

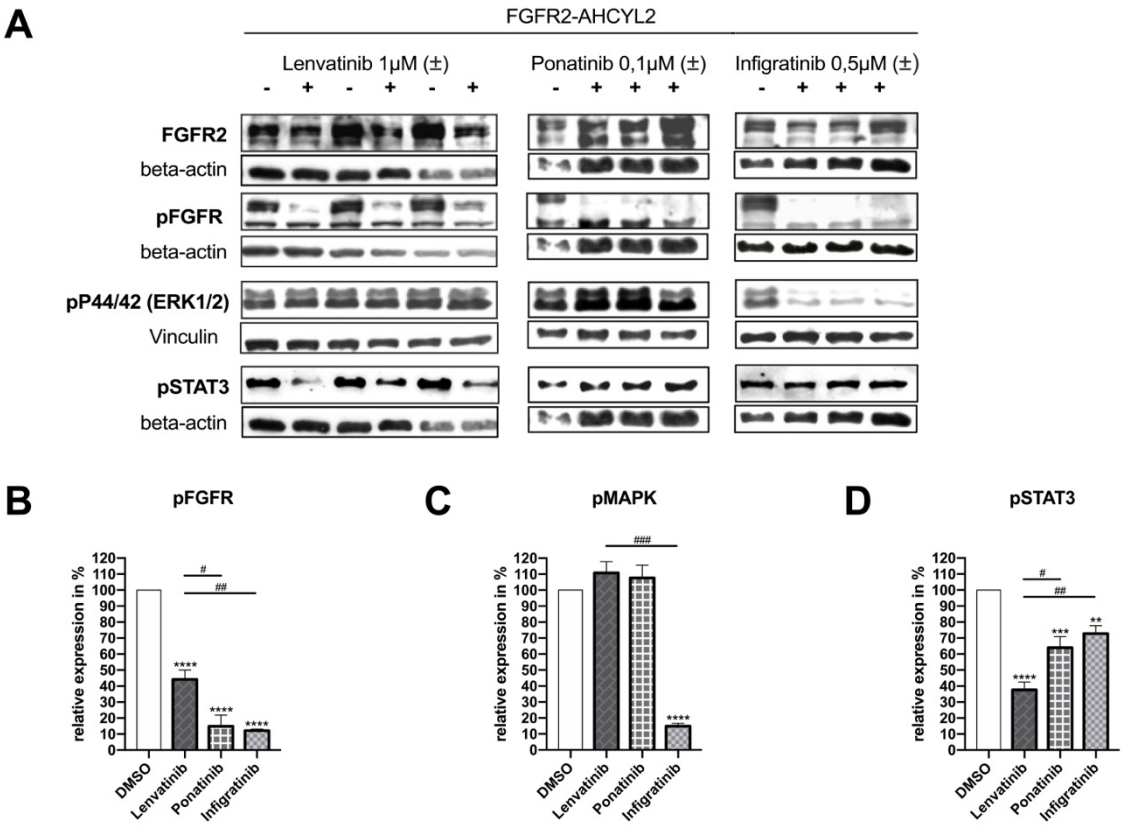

Figure 15: *Effects of the selective FGFR2 inhibitor infigratinib and the unselective TKIs lenvatinib and ponatinib on FGFR2 downstream pathways.* **(A)** Western blot analysis of the FGFR2 pathway in FGFR2-AHCYL2-transfected NIH/3T3 cells after 24h treatment with the indicated TKI using a standardized concentration that reduced cell mass to 50% after 7 days. Densitometric analyses of **(B)** pFGFR, **(C)** pMAPK and **(D)** pSTAT3 in FGFR2-AHCYL2-NIH/3T3 cells after treatment with the indicated TKI, graphs show mean ± SEM, ***P* ≤ 0.01, ****P* ≤ 0.001, *****P* ≤ 0.0001 compared to DMSO treated cells, #*P* ≤ 0.05, ##*P* ≤ 0.01, ###*P* ≤ 0.001 compared to lenvatinib treated cells, n = 3.

3.4 Generation and characterization of NIH/3T3 cell lines with *FGFR2-AHCYL2* fusion genes with point mutations in the kinase region

3.4.1 Generation of NIH/3T3 cell lines harboring FGFR2-AHCYL2 fusions with additional kinase point mutations p.E565A or p.V564F and its effect on different downstream signals

FGFR2 kinase mutations have been described as resistance factors leading to progressive disease in patients (Goyal et al., 2017, Javle et al., 2018). The two resistance mediating kinase mutations p.E565A and p.V564F were selected for further studies.

For this reason, the above described *FGFR2-AHCYL2* p.E565A (abbreviated ".E565A" in the following) and *FGFR2-AHCYL2* p.V564F (abbreviated ".V564F" in the following) fusion gene plasmids were transfected into NIH/3T3 cells. Analogous to the procedure for the previously described generated cell lines, four clones each with a moderate and temporally stable GFP signal were first identified, and in the next step the clone with the strongest pFGFR and FGFR2 expression in the Western blot was selected and used for further experiments (**Table 7**).

Table 7: *Original designation of the selected clones after transfection*

Cell line	Clones picked after G-418 selection	Final clones used in the following
FGFR2-AHCYL2 p.V564F -transfected NIH/3T3 cells	B7b, C6b1, **D4**, D4a	**D4**
FGFR2-AHCYL2 p.E565A -transfected NIH/3T3 cells	**A4a2**, C3a1, D5a1, D5a2	**A4a2**

First, these novel cell lines were characterized and compared to the FGFR2-AHCYL2 wild type-expressing cells (**Fig. 16,** also see **Fig. 7 – 8**). Western blot analyses confirmed, that the *FGFR2* fusion genes were stably overexpressed. FGFR2 proteins of ".E565A" and ".V564F" cells were detected with an equal size as their wild type fusion of approximately 180 kDa (**Fig. 16 B**). For both, ".E565A"

and “.V564F” cells, downstream signals of pFGFR, pFRS2, pP44/42 (MAPK) and pSTAT3, were enhanced in a similar manner as for their wild type fusion counterparts. Only a slightly weaker expression for pFRS2 and pP44/42 (MAPK) was found for „.E565A” in comparison to “.V564F” (**Fig. 16 C**).

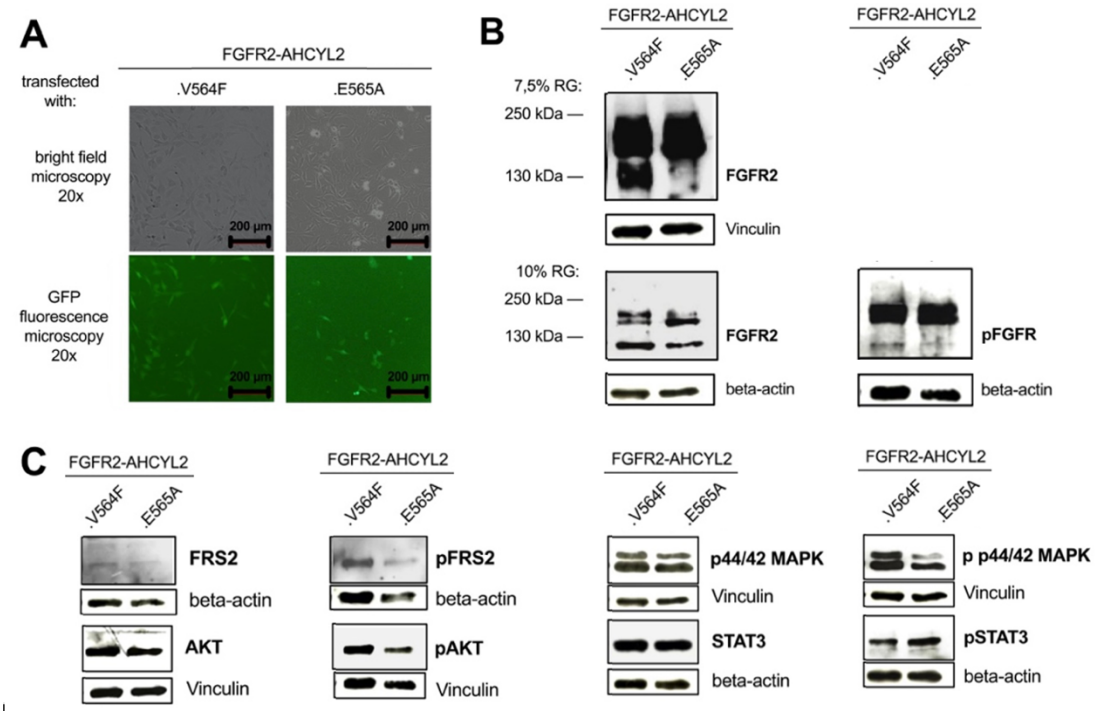

Figure 16: *Fluorescence microscopy of NIH/3T3 cells harboring FGFR2-AHCYL2 fusions with kinase point mutation p.V564F or p.E565A and Western blot analysis corresponding to the cell lines of FGFR2 and its downstream pathway proteins.* **(A)** Representative images of bright field or GFP fluorescence microscopy of stably transfected clones used for further analyses (scale bar = 200 µm). **(B)** Western blot analysis of the FGFR2 protein using a 7.5 % (upper part) or 10 % (lower part) resolving gel and the pFGFR protein using a 10 % resolving gel. **(C)** Western blot analysis of FGFR2 downstream signaling proteins in NIH/3T3 cells expressing FGFR2-AHCYL2 p.V564F or p.E565A.

3.4.2 Functional analyses of *FGFR2*-AHCYL2 fusion gene-expressing cells with additional kinase mutations p.E565A or p.V564F

Additionally, functional assays were performed for ".E565A"- and ".V564F" cells. Using SRB assays, both demonstrated a significantly increased proliferation, that was about 2x higher compared to empty vector-transfected cells (**Fig. 17,** also see **Fig. 9**).

".V564F" fusion gene-bearing cells, were exemplarily assessed by means of the soft agar colony formation assay. Findings exhibited a significantly higher number of colonies compared to CTL-NIH/3T3 cells, comparable to the wild type fusion-expressing cell line shown previously (**Fig. 17 B and C**, also see **Fig. 9**).

Taken together, these results suggest that in the assays examined, the cell lines with the additional kinase mutation behaved similarly to cells with the FGFR2-AHCYL2 wild type fusion.

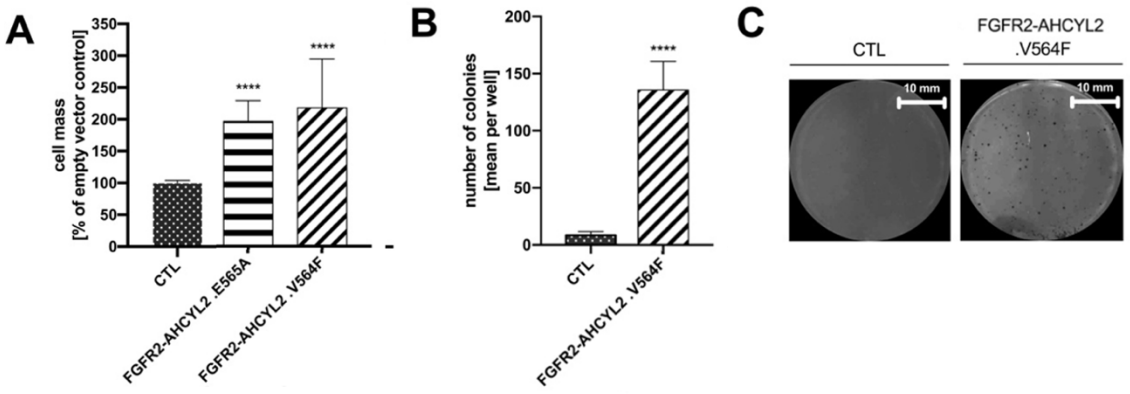

Figure 17: *Proliferation and anchorage-independent growth assays of NIH/3T3 cells harboring FGFR2-AHCYL2 fusions with kinase point mutation p.V564F or p.E565A.* **(A)** Proliferation analysis of FGFR2 fusion-expressing cell lines using SRB assays after 7 days in culture, graphs show mean ± SD, ****$P \leq 0.0001$ compared to empty vector-transfected NIH/3T3 cells, n = 30. **(B)** Quantification of soft agar colony formation after 21 days of NIH/3T3 expressing FGFR2-AHCYL2 fusion with kinase point mutation p.V564F, graphs show mean ± SD, ****$P \leq 0.0001$ compared to control-transfected NIH/3T3 cells, n = 8. **(C)** Representative images of the indicated cell lines in soft agar after 21 days of incubation (scale bar = 10 mm).

3.5 Drug Assays of FGFR2-AHCYL2-expressing cells with kinase point mutations

3.5.1 Functional drug assays of FGFR2-AHCYL2 p.E565A and p.V564F cells

After the generation of FGFR2-AHCYL2 cell lines with a kinase mutation associated with therapy resistance in patients, we assessed the inhibitory effect of various clinically applied drugs in these cells.

Investigation of selective FGFR-inhibiting TKIs in SRB assays

First, assays for inhibition of proliferation were performed with selective TKIs infigratinib and futibatinib. As already shown above, both substances indicated good efficacy in FGFR2 fusion-positive cells with the wild type kinase (see **Fig. 11**). However, both ".E565A" and ".V564F" cells showed a significantly reduced inhibitory activity to infigratinib in contrast to their FGFR2-AHCYL2 wild type analogue. Thus, expression of point mutated fusion genes led to infigratinib resistance. Yet, some inhibitory effect compared to CTL-NIH/3T3 cells was preserved. Experiments resulted in a slightly better inhibition effect for ".E565A" cells than for CTL-NIH/3T3 cells, but only for two concentrations tested. For ".V564F"-positive cells however, no better inhibitory effect of infigratinib was detected comparing them to CTL-NIH/3T3 cells (**Fig. 18 A**).

Similarly, in comparison to their wild type FGFR2-AHCYL2 cells, sensitivity to futibatinib was significantly lower for cells expressing a point mutated fusion gene.

Nevertheless, some inhibitory effect remained comparing ".E565A" and ".V564F" cells to CTL-NIH/3T3 cells. More precisely, remaining effectiveness was apparent for three concentrations tested on ".E565A" cells and two concentrations applied on ".V564F" cells (**Fig. 18 B**). (Spahn et al., 2024)

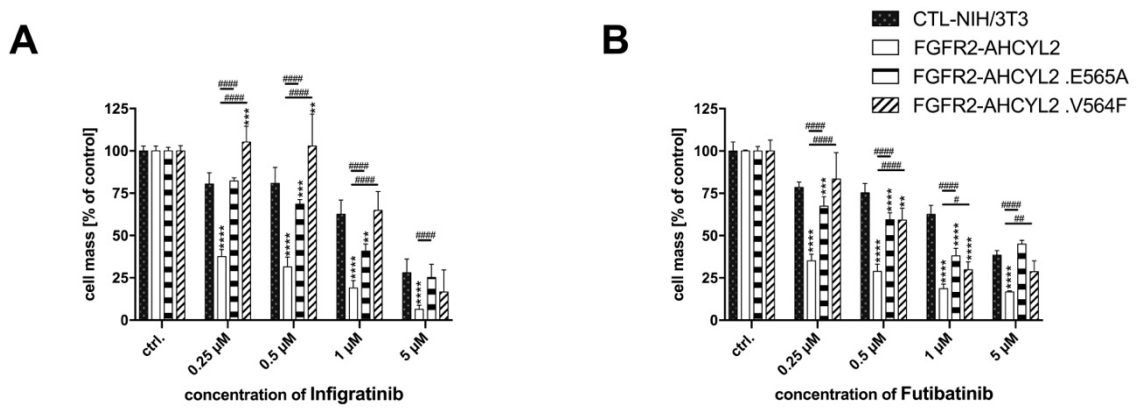

Figure 18: *Efficacy of selective FGFR inhibitors in FGFR2 fusion-expressing cell lines with kinase point mutation p.E565A or p.V564F.* Proliferation analyses using SRB assays after 7 days of treatment with the indicated selective inhibitors **(A)** infigratinib and **(B)** futibatinib, graphs show mean ± SD, ***P* ≤ 0.01, ****P* ≤ 0.001, *****P* ≤ 0.0001 compared to control-transfected NIH/3T3 cells, #*P* ≤ 0.05, ##*P* ≤ 0.01, ####*P* ≤ 0.0001 compared to FGFR2-AHCYL2 wild type-transfected cells, n = 6. Experiments were performed together with FGFR2 fusions with wild type kinase. Data of FGFR2-AHCYL2 wild type fusion-expressing cells correspond to the previously shown (Fig. 11).

Investigation of FGFR-inhibiting multikinase inhibitors in SRB assays

Next, sensitivity of ".E565A" and ".V564F" cells to multikinase inhibitors with FGFR-inhibitory activity was studied.

Both ".E565A" and ".V564F" cells displayed a lower sensitivity to lenvatinib than the wild type FGFR2-AHCYL2 cells. However, the cells with a kinase mutation showed significantly stronger inhibition at all concentrations of lenvatinib tested compared to CTL-NIH/3T3 cells (**Fig. 19 A**). Analyzing ponatinib, the experiments delivered a tendency for point mutated FGFR2-AHCYL2 cells to respond worse to the drug treatment matched to their wild type fusion cells. No differences were detected comparing ponatinib treatment of cells expressing ".E565A" with CTL-NIH/3T3 cells. On the contrary, ".V564F" cells indicated a superior drug response than CTL-NIH/3T3 cells considering high ponatinib concentrations (**Fig. 19 B**). The results of the experiments with nintedanib were mostly very similar to those for ponatinib. Again, both ".E565A" and ".V564F" cells showed a certain resistance to the multikinase inhibitor in comparison to their wild type fusion equivalent (**Fig. 19 C**). (Spahn et al., 2024)

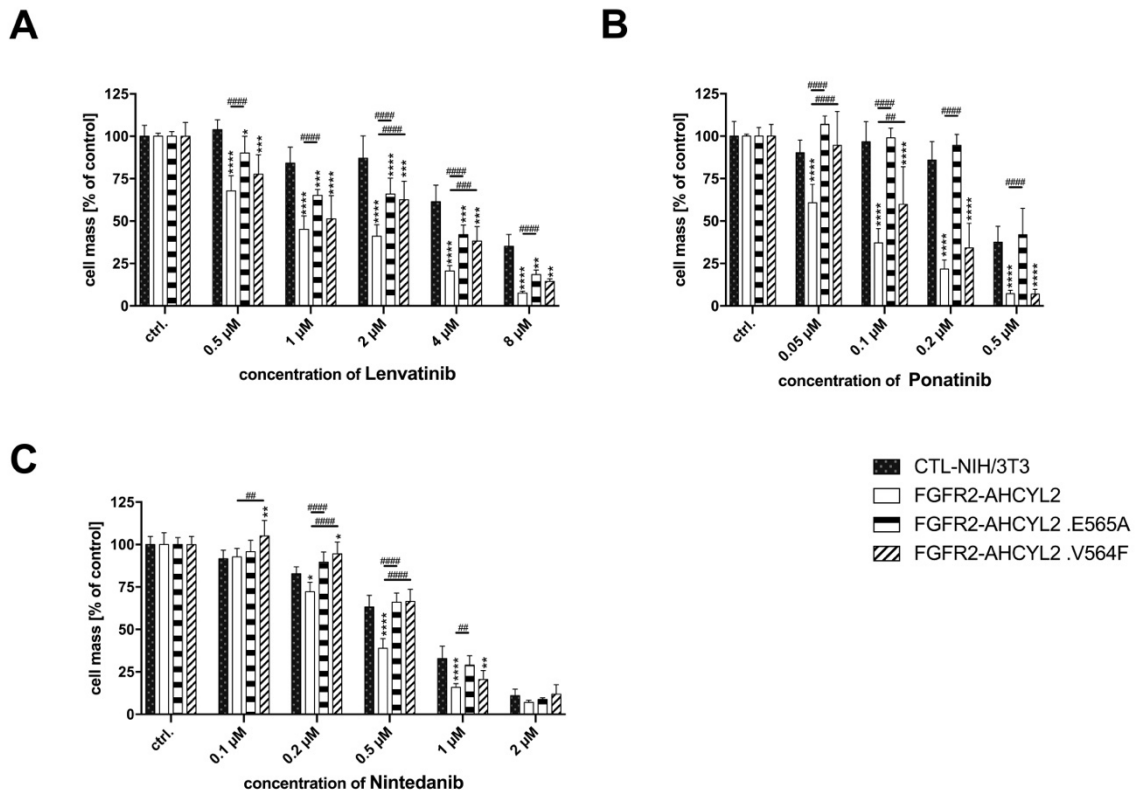

Figure 19: *Efficacy of multikinase inhibitors with FGFR-inhibitory capacity in FGFR2 fusion-expressing cell lines with kinase point mutation p.E565A or p.V564F.* Proliferation analyses using SRB assays after 7 days of treatment with the indicated unselective inhibitors **(A)** lenvatinib, **(B)** ponatinib and **(C)** nintedanib, graphs show mean ± SD, **P* ≤ 0.05, ***P* ≤ 0.01, ****P* ≤ 0.001, *****P* ≤ 0.0001 compared to control-transfected NIH/3T3 cells, #*P* ≤ 0.05, ##*P* ≤ 0.01, ###*P* ≤ 0.001, ####*P* ≤ 0.0001 compared to FGFR2-AHCYL2 wild type-transfected cells, n = 6. Experiments were performed together with FGFR2 fusions with wild type kinase. Data of FGFR2-AHCYL2 wild type fusion-expressing cells correspond to the previously shown (Fig. 10).

Investigation of the multikinase inhibitor cabozantinib without FGFR-inhibitory activity and the chemotherapeutic substance gemcitabine in SRB assays

FGFR2-AHCYL2, ".E565A" and ".V564F" cells were treated with cabozantinib, a multikinase inhibitor with no known FGFR-inhibitory effect, and with gemcitabine, as a classical chemotherapeutic agent for CCA treatment.

First, as already shown, cabozantinib inhibited FGFR2-AHCYL2 wild type cells less than control transfected NIH/3T3 cells (see **Fig. 12**). Interestingly, ".E565A" and ".V564F" cells were in part significantly better restrained in proliferation than the wild type fusion-positive cells, similar to control transfected NIH/3T3 cells (**Fig. 20 A**). Gemcitabine experiments revealed increased responses to the substance for point mutated fusion cells in contrast to the wild type FGFR2-AHCYL2 cells. ".E565A" and ".V564F" cells exposed in part even higher gemcitabine treatment effects than detected for CTL-NIH/3T3 cells (**Fig. 20 B**).

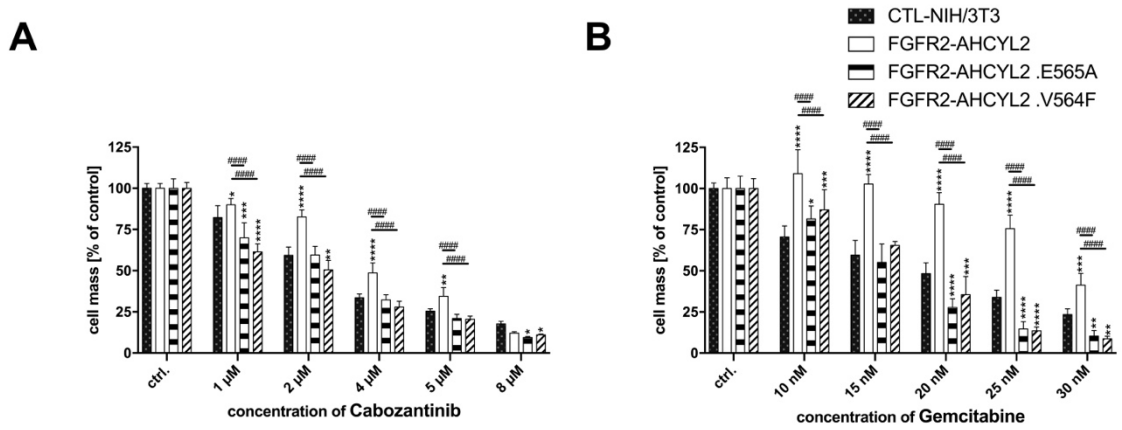

Figure 20: *Efficacy of an unselective tyrosine kinase inhibitor without FGFR inhibition capacity and gemcitabine as one component of standard CCA chemotherapy treatment in FGFR2 fusion-expressing cell lines with kinase point mutation p.E565A or p.V564F.* Proliferation analyses using SRB assays after 7 days of treatment with the indicated not FGFR-inhibiting unselective inhibitor **(A)** cabozantinib and the current standard chemotherapy treatment **(B)** gemcitabine, graphs show mean ± SD, **P* ≤ 0.05, ***P* ≤ 0.01, ****P* ≤ 0.001, *****P* ≤ 0.0001 compared to control-transfected NIH/3T3 cells, ####*P* ≤ 0.0001 compared to FGFR2-AHCYL2 wild type-transfected cells n = 6. Experiments were performed together with FGFR2 fusions with wild type kinase. Data of FGFR2-AHCYL2 wild type fusion-expressing cells correspond to the previously shown (Fig. 12).

Influence of point mutations in FGFR2-AHCYL2 on IC_{50} values of tested drugs

Investigating the influence of point mutations in the FGFR2-AHCYL2 cell model on response behavior of the tested substances, IC_{50} values were compared (**Fig. 21**). IC_{50} values of ".E565A" and ".V564F" cells were calculated as the corresponding multiple of values of wild type FGFR2-AHCYL2 cells. When point mutated cells were treated with FGFR inhibiting TKIs, their sensitivity to the drugs was generally decreased compared to wild type *FGFR2-AHCYL2* gene-harboring cells. Though, the extent of this resistance differed between the selected substances. IC_{50} values for the selective FGFR-inhibitors administered to the ".E565A" and ".V564F" cells ranged from 7.6-28.5 times the IC_{50} values of the wild type FGFR2-AHCYL2 cells. This observed effect was less pronounced for FGFR-inhibiting multikinase inhibitors with the multiple of doses required for point-mutated cells compared with wild type FGFR2-AHCYL2 cells ranging from 1.7-6.6. Looking at cabozantinib without FGFR-inhibitory activity or the chemotherapeutic gemcitabine, the ".E565A" and ".V564F" cells even seemed to have a slightly higher drug sensitivity relative to their wild type FGFR2-AHCYL2 counterpart.

In summary, ".E565A" and ".V564F" cells were resistant to infigratinib and, to a lesser extent, futibatinib, whereas the nonselective FGFR TKIs lenvatinib and ponatinib remained effective.

To better illustrate the respective drug sensitivity for FGFR2 fusion-positive cells with kinase mutation, additional color coding was used in the figure according to the multiple of the IC_{50} value for the FGFR2-AHCYL2 wild type-transfected cells. Different color intensities of green and red were used for relative increased or decreased sensitivity to the drugs (multiple of IC_{50} value for FGFR2-AHCYL2 wild type: < 1-fold: intense green, 1 – 5-fold: green, 5 – 10-fold: bright red, > 10-fold: red). (Spahn et al., 2024)

	selective FGFR inhibitors				unselective FGFR inhibitors									
	Infigratinib		Futibatinib		Lenvatinib		Ponatinib		Nintedanib		Cabozantinib		Gemcitabine	
	IC_{50} in nmol/L	foldD	IC_{50} in nmol/L	foldD	IC_{50} in nmol/L	foldD	IC_{50} in nmol/L	foldD	IC_{50} in nmol/L	foldD	IC_{50} in nmol/L	foldD	IC_{50} in nmol/L	foldD
	SD (n)	(foldD of CTL-NIH/3T3)	SD (n)	(foldD of CTL-NIH/3T3)	SD (n)	(foldD of CTL-NIH/3T3)	SD (n)	(foldD of CTL-NIH/3T3)	SD (n)	(foldD of CTL-NIH/3T3)	SD (n)	(foldD of CTL-NIH/3T3)	SD (n)	(foldD of CTL-NIH/3T3)
CTL-NIH/3T3	**1815**	**13.6**	**2389**	**56.9**	**5456**	**5.3**	**408**	**5.9**	**634**	**1.7**	**2594**	**0.7**	**17.6**	**0.6**
	184 (6)		203 (6)		405 (6)		26 (6)		26 (6)		66 (6)		0,5 (6)	
FGFR2-AHCYL2 wt	**133**	**1.0**	**42**	**1.0**	**1021**	**1.0**	**69**	**1.0**	**376**	**1.0**	**3893**	**1.0**	**28.7**	**1.0**
	19 (6)		14 (6)		69 (6)		4 (6)		13 (6)		84 (6)		0,5 (6)	
FGFR2-AHCYL2 .E565A	**1015**	**7.6**	**1197**	**28.5**	**2735**	**2.7**	**455**	**6.6**	**661**	**1.8**	**2206**	**0.6**	**15.6**	**0.5**
	82 (6)	0.6	279 (6)	0.5	193 (6)	0.5	19 (6)	1.1	20 (6)	1.0	97 (6)	0.9	0,3 (6)	0.9
FGFR2-AHCYL2 .V564F	**1688**	**12.7**	**777**	**18.5**	**1933**	**1.9**	**136**	**2.0**	**639**	**1.7**	**1707**	**0.4**	**17.1**	**0.6**
	237 (6)	0.9	113 (6)	0.3	264 (6)	0.4	12 (6)	0.3	25 (6)	1.0	71 (6)	0.7	0,3 (6)	1.0

Figure 21: *IC_{50} values of selected substances in NIH/3T3 cells harboring FGFR2-AHCYL2 fusion with point mutation p.E565A or p.V564F in the kinase region.* Illustration shows IC_{50} values of different drugs for NIH/3T3 cells expressing the indicated construct in nmol/L ± SD and their respective multiplication of the value for FGFR-AHCYL2 wild type-expressing cells, n = 6. Additional color coding was used for the multiple of IC_{50} value for FGFR2-AHCYL2 wild type: < 1-fold: intense green, 1 – 5-fold: green, 5 – 10-fold: bright red, > 10-fold: red)

Selective and unselective FGFR-inhibitory TKIs in colony formation assays

".V564F" cells were examined in soft agar colony formation assays to verify determined drug effects using another functional assay. Although formation of colonies by infigratinib was also significantly reduced for this cell line, some colonies were still present. Comparing the percentage of colonies remaining after infigratinib treatment with respective DMSO treated cells, about 10 % were left for ".V564F" cells. This was significantly higher than for wild type FGFR2-AHCYL2 cells (**Fig. 22 A**). When ".V564F" cells were exposed to lenvatinib in these soft agar assays, the percentage of colonies developed despite treatment was about 7 % of their DMSO treated control cells. Again, treatment could significantly reduce the number of colonies formed for ".V564F" cells compared to DMSO treated cells. Yet, a difference in formed colonies despite lenvatinib exposure was found between ".V564F" cells and wild type FGFR2-AHCYL2 cells (**Fig. 22 B**).

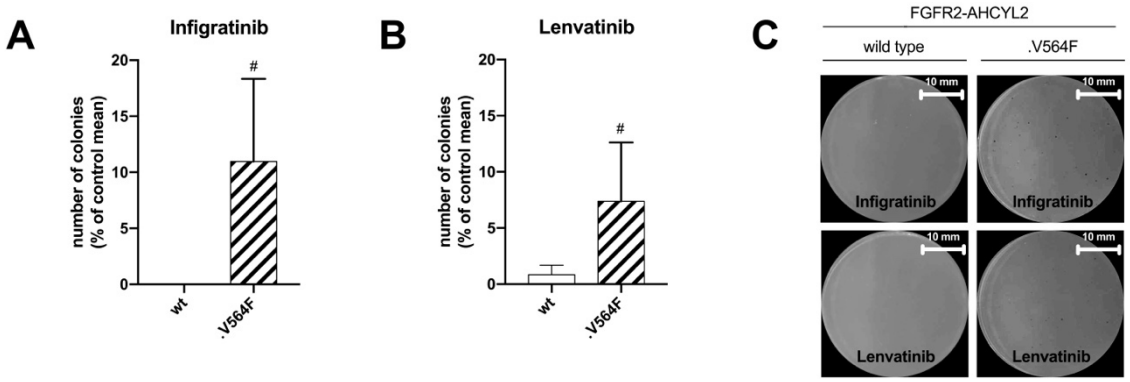

Figure 22: *Comparison of drug inhibitory effects between FGFR2-AHCYL2 wild type and FGFR2-AHCYL2 p.V564F-expressing cell lines in colony formation assays.* Quantification of soft agar colony formation after 21 days of incubation with **(A)** infigratinib (0,5 µM) and **(B)** lenvatinib (0,25 µM), graphs show mean ± SD, *#P* ≤ 0.05 compared to the equally treated FGFR2-AHCYL2 wild type cells, n = 6. **(C)** Representative images of soft agar wells after 21 days of incubation (scale bar = 10 mm). Experiments were performed together with FGFR2 fusions with wild type kinase. Experiments were performed together with FGFR2 fusions with wild type kinase. Data of FGFR2-AHCYL2 wild type fusion-expressing cells correspond to the previously shown (Fig. 14).

3.5.2 Western blot analysis of downstream signals in FGFR2-AHCYL2 p.V564F cells after gemcitabine treatment

Looking at the cell lines with the kinase mutated fusion genes, it was astonishing that the sensitivity to gemcitabine seemed to be increased compared to cells that harbor the wildtype *FGFR2-AHCYL2* fusion gene (see **Fig. 21**). Therefore, a final experiment was performed to investigate FGFR downstream signaling during the treatment with gemcitabine in ".V564F" and FGFR2-AHCYL2 wild type cells (**Fig. 23**).

Whereas for wild type FGFR2-AHCYL2 cells no effects of gemcitabine on pFGFR expression could be identified, densitometric analysis distinguished a weaker pFGFR signal (about 25 %) for ".V564F" cells exposed to gemcitabine as compared with DMSO treatment (**Fig. 23 B and F**). Referring to pMAPK, wild type FGFR2-AHCYL2 cells exhibited a significantly enhanced signal (about 30 %) after treatment with the chemotherapeutic (**Fig. 23 C**). Surprisingly, this enhancement could not be observed after treatment of the point mutated *FGFR2* fusion gene-expressing cells (**Fig. 23 G**). Consistent effects were found for pSTAT3,

with significant signal reduction by gemcitabine for both the wild type FGFR2-AHCYL2 and ".V564F" cells (**Fig. 23 D and H**). Taken together, a different activation pattern of pMAPK was noticed in the presence of one of the investigated FGFR2 kinase mutations.

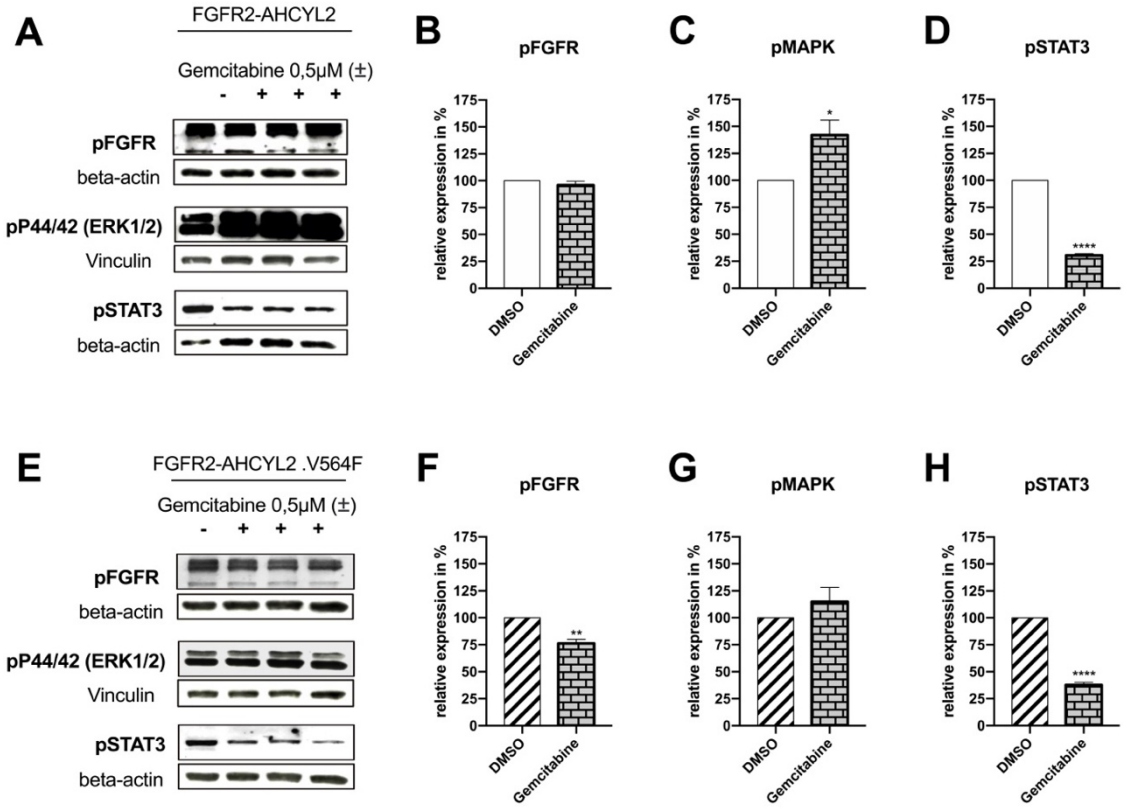

Figure 23: *Western blot analysis of NIH/3T3 cells with either FGFR2-AHCYL2 wild type or additional p.V564F expression after the treatment with gemcitabine.* Western blot analysis of the FGFR2 pathway in **(A)** FGFR2-AHCYL2 wild type and **(C)** FGFR2-AHCYL2 p.V564F NIH/3T3 cells after 24h treatment with gemcitabine. Densitometric analyses of **(B)** pFGFR, **(C)** pMAPK and **(D)** pSTAT3 in FGFR2-AHCYL2 wild type cell line as well as for resistance point mutated p.V564F cells **(F)** pFGFR, **(G)** pMAPK and **(H)** pSTAT3 after treatment with gemcitabine, graphs show mean ± SEM, **P* ≤ 0.05, ***P* ≤ 0.01, *****P* ≤ 0.0001 compared to DMSO treated cells, n = 3.

4. Discussion

4.1 Clinical considerations on FGFR2 fusion-positive CCAs

Due to the recent detection of druggable molecular FGFR aberrations, especially FGFR2 fusions, which occur in up to 16 % of patients, iCCA has become a promising candidate for precision medicine (Valle et al., 2017, Javle et al., 2016, Vogel et al., 2023). However, little is known about whether these tumors have specific clinical features and whether the fusion genes have an impact on the response to classical chemotherapeutics (Jain et al., 2018, Lamarca et al., 2020, Silverman et al., 2020).

First, focusing on two cases, the detailed analysis of patients' disease course revealed some interesting clinical features. Some of the findings were consistent with recent studies highlighting special features for patients with FGFR2 alterations. The age of the patients at diagnosis was 42 (patient #1, *FGFR2-SH3GLB1*) and 35 (patient #2, *FGFR2-AHCYL2*) years, supporting the hypothesis, that CCAs with FGFR aberrations are more common in younger patients (Jain et al., 2018). Both patients were diagnosed at an advanced tumor stadium, although noticing hardly any symptoms. Diagnosis at advanced or unresectable stage with poor symptoms is characteristic for iCCA patients in general, but not specifically for those with FGFR2 alterations (Khan et al., 2012). Patient #2 could undergo surgical treatment after neoadjuvant gemcitabine/cisplatin treatment, yet suffering a relapse 3 months later, which is quite common in CCA patients (Cillo et al., 2019, Bitzer et al., 2022). Among CCA patients, there was preliminary evidence that FGFR2 alterations might be associated with longer median OS, even independent of therapy with FGFR inhibitors (Javle et al., 2016, Jain et al., 2018). While for patients diagnosed with CCA in an advanced stage median OS is about 11.7 months with gemcitabine/cisplatin treatment, patient #1 and patient #2 displayed an OS of 29 and 38 months respectively (Valle et al., 2010). Nevertheless, the long OS in these two patients was most likely influenced by FGFR-targeted TKIs, as discussed later.

Response to first-line palliative chemotherapeutic treatment consisting of gemcitabine/cisplatin was rather poor in both patients (Valle et al., 2010). Although,

patient #2 initially showed a partial response, the tumor already progressed after 4.2 months under therapy. For patient #1, a tumor growth was detected already in the first treatment efficacy assessment after 2.2 months (see **Fig. 3 and 4)**. The median PFS for gemcitabine/cisplatin was only 2.1 months in the entire cohort of patients (n = 6) studied in this trial. In contrast, the usual median PFS which has been observed in the phase III study with gemcitabine/cisplatin combination therapy was 8.0 months for the treatment (Valle et al., 2010). A comparison with this study therefore suggests that CCA patients, whose tumor harbor an FGFR2 alteration, might progress more quickly to the standard therapy, but the patient numbers in the reported cohort are small. In a retrospective assessment of 135 patients harboring CCA and an *FGFR* alteration, the median time to first-line palliative treatment with gemcitabine/cisplatin was also determined to be quite short (6.2 months) (Goyal et al., 2020). Similarly, in a retrospective analysis of data from patients with *FGFR*-altered CCA who received pemigatinib in the FIGHT-202 trial, the median PFS for prior first-line therapy (most commonly gemcitabine/cisplatin) in 102 CCA patients with FGFR2 fusion was only 5.5 months (Bibeau et al., 2022). Even if a tendency can perhaps be identified, further studies are mandatory to investigate the clinical differences in response to current first-line therapy when CCAs are driven by FGFR alterations.

Despite early tumor progression on standard therapy, the OS of patients with FGFR2 alteration in this study was even longer than the median OS of patients with advanced CCA in general under the same standard treatment studied in a previous trial (Valle et al., 2010). This observation highlights the relevance of FGFR-inhibitory therapy and supports that all patients with CCA should undergo elaborated molecular testing. However, the patients' tumors did not respond well to all FGFR-targeted multikinase inhibitors administered.

Based on the clinical observations, two main questions were chosen for a “bed to benchside” approach: First, cellular *in vitro* models were developed to compare known FGFR2-fusions with the newly discovered FGFR2-AHCYL2 fusion, second to study the effects of clinically available drugs in these cell types.

4.2 *in vitro* characteristics of FGFR2 fusions

To characterize FGFR2 fusions detected in patients with iCCA by the MTB Tuebingen *in vitro*, NIH/3T3 cells were stably transfected with patient-analogue *FGFR2* fusion genes as a cellular model. Moreover, the idea was that these models could help select the ideal therapy for each patient based on their individual FGFR2 fusion.

Previously, comparable cellular models based on NIH/3T3 cells were used by several other groups to determine the oncogenic potential of unknown fusion genes in CCA, with slight methodological differences (Wu et al., 2013, Arai et al., 2014, Sia et al., 2015). In all three studies FGFR2 fusion expression led to characteristics that are observed after malignant transformation.
In the newly generated fusion-positive cell lines, the different sized bands for FGFR2 protein in Western blot analyses confirmed that the different fusion genes lead to the formation of the corresponding fusion proteins (see **Fig. 7**). Hence, the investigated *FGFR2* fusion genes seemed to share the ability to produce a functional protein.

In line with previous findings for other fusions, Western blot analyses support the hypothesis that the previously uncharacterized *FGFR2-SH3GLB1* and *FGFR2-AHCYL2* fusion genes activate oncogenic downstream pathways. Without adding FGF ligands, pFGFR expression was enhanced for FGFR2 fusion gene-positive cells, thus indicating a ligand-independent activation (see **Fig. 8**). Moreover, autophosphorylation of the receptor is associated with consequent activation of downstream signals, as it was in all newly generated cell lines (Katoh, 2019). All examined FGFR2 fusion-expressing cells exhibited increased signaling via pFRS2 and pMAPK, whereas pSTAT3 was only enhanced in FGFR2-SH3GLB1 and FGFR2-AHCYL2 cells (see **Fig. 8 A and B**). Previous studies have consistently reported that FGFR2 fusion expression activates the MAPK pathway, as demonstrated by increased pMAPK protein signaling (Arai et al., 2014, Sia et al., 2015, Krook et al., 2019, Li et al., 2020, Goyal et al., 2019). This activation is in accordance with the results of this study, thus highlighting the importance of the

MAPK pathway for FGFR2 signaling. Therefore, combination therapies that both target the MAPK pathway, for example with FGFR inhibitors and MEK inhibitors, such as trametinib, may represent an interesting new option (Li et al., 2020, Kendre et al., 2021). Consistent results, in line with previous findings, were also found in this study for pFRS2, which showed enhanced signaling in all fusion-positive cell lines (Krook et al., 2019, Goyal et al., 2019). Results related to the pSTAT3 signaling pathway were inconsistent across the cell lines studied. Activation of pSTAT3, demonstrated here for FGFR2-SH3GLB1 and FGFR2-AHCYL2 cells, has previously been reported only for the *FGFR2-PPHLN1* fusion gene (Li et al., 2020). While for the *FGFR2-CLIP1* and the *FGFR2-KIAA1598* gene an enhanced pAKT signaling was described in the literature, it was not for the *FGFR2-AHCYL1* and *FGFR2-BICC1* genes (Arai et al., 2014, Krook et al., 2019, Krook et al., 2020). Concerning further downstream signals, several different proteins were investigated in the cited papers, which in turn led to partially inconsistent results. Therefore, it might be possible that different fusion genes activate signaling pathways in a dissimilar manner in general or depending on the fusion protein expressing cell types.

In accordance with other studies that investigated FGFR2 fusions found in iCCA, functional analyses by cell viability assays showed an increased proliferation for cells expressing the FGFR2-SH3GLB1 or FGFR2-AHCYL2 fusion (see **Fig. 9 A**) (Wu et al., 2013, Sia et al., 2015). Moreover, an anchorage-independent growth has been ascertained for both novel fusion cell lines (see **Fig. 9 B**). This has also been presented for other cells transfected with an *FGFR2* fusion gene (Arai et al., 2014, Sia et al., 2015, Li et al., 2020).

Experiments using the already characterized *FGFR2-BICC1* fusion gene were performed as a positive control. In line with data from Arai et al., protein expression of pAKT and pSTAT3 was less clear than for pFGFR and pMAPK in FGFR2-BICC1-expressing NIH/3T3 cells (see **Fig. 8 A and B**) (Arai et al., 2014). Additionally, as previously demonstrated by others, the experiments conducted

verified enhanced proliferation of FGFR2-BICC1 cells in the SRB assay (see **Fig. 9 B**) (Wu et al., 2013).

Taken together, this study revealed results in line with previous investigations that have examined FGFR2 fusions using cellular experiments, particularly for the most often reported *FGFR2-BICC1* fusion. Overall, the detailed *in vitro* characterization defines *FGFR2-SH3GLB1* and *FGFR2-AHCYL2* gene fusions as potential oncogenic drivers in iCCA. Moreover, these results suggest that CCAs are dependent on FGFR2 signaling, highlighting its potential as a therapeutic target.

4.3 TKIs and chemotherapeutics from "bed to benchside"

Recently, numerous translational studies have been published investigating the application of TKIs in iCCA with FGFR alterations. Yet, most of these have focused on selective FGFR inhibitors. To elucidate the effects of different drugs on diverse FGFR2 fusions in iCCA and compare selective and unselective TKIs, various examinations were conducted using the generated cellular *in vitro* model.

Infigratinib is a selective FGFR-targeting TKI, that has been evaluated in detail preclinically and clinically (Kelley et al., 2020). The FGFR inhibitor was shown to inhibit pFGFR and pMAPK signaling in cell lines expressing *FGFR2* fusion genes that were detected in CCA (Arai et al., 2014, Li et al., 2020). Additionally, functional assays revealed an increased sensitivity to infigratinib as well as the ability of the drug to prevent colony formation in FGFR2 fusion-positive cells (Sia et al., 2015, Li et al., 2020). The collected *in vitro* data of this present study fully support these findings. Furthermore, they support the theory that infigratinib is effective for a variety of fusion genes, as its efficacy was demonstrated in proliferation and soft agar colony formation assays for all fusion genes tested, including the previously uncharacterized fusion genes *FGFR2-SH3GLB1* and *FGFR2-AHCYL2* (see **Fig. 11 A and 14**). In addition to inhibition of pFGFR and pMAPK, Western blot experiments in this study also demonstrated reduced pSTAT3 expression by infigratinib, emphasizing its broad effects on intracellular downstream signaling pathways (see **Fig. 15**).

Evaluation of futibatinib, an irreversibly binding selective FGFR inhibitor, similarly showed efficacy in SRB assays that was comparable to infigratinib (see **Fig. 11 B**). Recently, futibatinib was presented to prevent colony formation as well as to reduce pFGFR and pMAPK signaling in a cellular model (Li et al., 2020).
Taken together, these examinations emphasize the efficacy of selective FGFR inhibitors to potently inhibit proliferation in numerous different *FGFR2* fusion gene-positive cells.

Regarding the role of unselective multikinase inhibitors, this study demonstrated noteworthy efficacy of lenvatinib against *FGFR2* fusion gene-harboring cells *in vitro*. Besides an increased sensitivity in SRB assays, its effects were also demonstrated in the soft agar colony formation assay (see **Fig. 10 A and 14**). Western blot studies displayed inhibition of pFGFR in FGFR2 fusion-positive cells after treatment with lenvatinib. Yet, no significant inhibition was found for pMAPK after treatment with a 1µM concentration of the drug, a concentration that led to around 50 % reduced cell viability. However, lenvatinib achieved reduced STAT3 pathway signaling, which may have resulted in proliferation inhibition. Notably, lenvatinib treatment led to a stronger reduction of pSTAT3 signal than treatment with infigratinib (see **Fig. 15**). The additional effect on pSTAT3 signal inhibition could be caused by inhibition of additional other receptor tyrosine kinases, whose pathways overlap with those of the FGFR and influence each other (Capozzi et al., 2019, Schlessinger, 2000). If the *FGFR2* fusion gene-transfected cells were treated with a higher dose of lenvatinib, inhibition of the MAPK pathway might also be seen, as other studies have bared in human HCC xenograft models (Matsuki et al., 2018).

A similar deviation from published observations was noted for ponatinib with respect to the influence of the drug on downstream signaling. Western blot experiments displayed a reduction of pFGFR and pSTAT3 by ponatinib, but not for pMAPK (see **Fig. 15**). This observation is in contrast to the results of Wang et al., who reported a growth inhibition of FGFR2 fusion gene-positive

cholangiocarcinoma xenograft model by ponatinib, presumably attributed by decreased pFGFR, pMAPK and pAKT signals (Wang et al., 2016). Again, administering a higher dose of ponatinib might have led to a reduction of pMAPK as well.

Nevertheless, the concentrations of infigratinib, lenvatinib and ponatinib investigated by Western blotting led to a comparable inhibition of proliferation in SRB assays, thus suggesting different influences on downstream signals leading to comparable inhibitory effects (see **Fig. 11 A and 10 A and B**). Therefore, the results imply that unselective FGFR-inhibitors may provide broader inhibition of downstream signals that is less focused on MAPK signaling. Further proteomic analyses comparing the differential effects of selective FGFR-inhibiting TKIs on downstream signaling pathways with those of multikinase inhibitors with FGFR activity have been obtained, supporting this hypothesis. FGFR-selective TKIs were found to exclusively inhibit members of the MAPK pathway (Spahn et al., 2024). In contrast, additional inhibition of MAPK-unrelated proteins and broader inhibition of MAPK-related proteins were detected only after treatment with a non-selective FGFR-targeting TKI (Spahn et al., 2024).

In contrast to the experiments with lenvatinib and ponatinib, those with nintedanib did not provide clear results regarding proliferation inhibition (see **Fig. 10 C**). To date, little is known about nintedanib effects on FGFR2-altered CCA models. In context to CCA, the substance only was described having inhibiting effects on iCCA aggressiveness via suppression of cytokines extracted from cancer-associated fibroblasts in a cell model (Yamanaka et al., 2020). Nevertheless, it appears that not all TKIs with FGFR-inhibitory function are equally effective in *FGFR2* fusion gene-expressing cells, which might be an important issue for treatment recommendations in molecular tumor boards.

As a further control, the above discussed signaling cascade was also investigated in gemcitabine treated cells. As expected, Western blot analyses of FGFR2 fusion cells after gemcitabine treatment did not disclose an inhibition of pFGFR (see **Fig. 23 A and B**). Moreover, despite the higher proliferation of *FGFR2* fusion

gene-transfected cells, gemcitabine treatment had a less inhibitory influence on these same cells (see **Fig. 12 B**). When FGFR2-AHCYL2 cells were investigated using Western blot after gemcitabine treatment, they showed increased pMAPK signaling (see **Fig. 23 A and C**). A similar pMAPK signal increase after gemcitabine was found in pancreatic cancer cells. This activation could be explained by the fact that gemcitabine leads to increased EGF release, which in turn stimulates the EGFR and the MAPK pathway (Miyabayashi et al., 2013). A corresponding mechanism could explain the poor response to gemcitabine in FGFR2-positive cells through activation of pMAPK and consequent increased proliferation. However, further investigations are mandatory to substantiate this assumption.

Finally, *FGFR2* fusion gene-transfected cells exhibited a worse response than NIH/3T3 control cells regarding cabozantinib, which was used as a control as a TKI without relevant FGFR-inhibitory activity (see **Fig. 12 A**). These results support the hypothesis that the observed inhibitory effects in FGFR2 fusion-expressing cells by FGFR-targeting TKIs are mainly dominated by the influence of the FGFR fusion.

The comparison of the collected *in vitro* effects of TKIs with the patients' clinical courses revealed some exciting similarities that support the clinical observations made previously. However, the cellular experiments do not reflect the complex situation in patients *in vivo* and therefore have limitations that became apparent. The selective TKI infigratinib presented promising results for both newly characterized patient-analogue FGFR2 fusions investigated *in vitro* in agreement with results for other FGFR2 fusions examined (Arai et al., 2014, Sia et al., 2015, Li et al., 2020). Results of the phase II trial of infigratinib showed likewise promising *in vivo* data for patients with FGFR2 fusion-positive CCA (Javle et al., 2018, Javle et al., 2021). In accordance, patient #2 (*FGFR2-AHCYL2*) initially showed a similarly good response to infigratinib. Unfortunately, after a persistent partial response, she was removed from the study due to therapy interruptions caused by recurrent cholangitis (see **Fig. 4**). Despite this short therapy duration infigratinib resulted in a PFS of 5.5 months. Of note, the selective TKI did not lead to a

response in all tumor lesions of patient #1 (*FGFR2-SH3GLB1*) (see **Fig. 3**). Whereas most of the tumor lesions were stable during the treatment with infigratinib, bone metastasis showed a progressive disease which might reflect a role of the microenvironment that negatively influenced the bone lesions in this patient. Overall, the *in vitro* data were partially consistent with the *in vivo* data for infigratinib. However, patient-specific factors or the *in vivo* emergence of resistance mechanisms that may be responsible for a poorer drug response cannot be reflected in these investigations.

Interestingly, lenvatinib also was assessed having good efficacy in the studied cell model with patient-analogue *FGFR2* fusion genes. These results compare favorably with those seen for patient #1 and #2, who exhibited a PFS of 10.4 and 9.0 months, respectively (see **Fig. 5 A**). All seven patient histories summarized, median PFS was 7.0 months (see **Fig. 5 C**). A recently published study by Ueno et al. tested lenvatinib as second-line treatment for 26 patients with BTC. In this study lenvatinib achieved a median PFS of only 3.19 months (Ueno et al., 2020). However, they did not consider whether the patients had an FGFR2 alteration or not. In contrast to that, the seven patients included in this study all had confirmed FGFR2 alterations. Even though including only a small number of patients, the median PFS under lenvatinib was remarkable. The calculated median PFS of 7.0 months under lenvatinib therapy is roughly comparable to the reports for pemigatinib (6.9 months), infigratinib (7.3 months) and futibatinib (9.0 months) (Abou-Alfa et al., 2020, Javle et al., 2021, Goyal et al., 2023). In addition to the small number of patients treated in this investigation, individual differences in the properties of the patients included in the studies should be taken into account. Nevertheless, the combination of promising *in vivo* data with observations from the cell model suggest, that lenvatinib may be a therapeutic option for iCCA with FGFR2 alterations. Considered together with the study by Ueno et al., in which the median PFS was significantly worse without a proven FGFR2 change, the data suggest that lenvatinib seems to be only a good choice for CCA if the tumor cells harbor an FGFR2 alteration (Ueno et al., 2020). However further clinical trials are needed to confirm these findings.

Such a clear concordance could not be achieved for other multikinase inhibitors tested. Patient #2 was administered nintedanib and ponatinib, neither of which provided any benefit. Indeed, nintedanib did not deliver clearly good results in the *in vitro* drug assays. However, ponatinib *in vitro* data suggested that the substance has an effect on *FGFR2* fusion genes. This deviation from the patients' courses outlines again the limitations of the cell experiments representing only a basic model. The lack of *in vivo* efficacy might be due to pharmacologic distribution differences to the tumor, tumor microenvironment or other genetic and epigenetic alterations that have an impact on the response to TKI treatment (Banales et al., 2016).

Still, another interesting finding of the "bed to benchside" approach was discovered for gemcitabine treatment. In addition to the previously described poor patient response to gemcitabine/cisplatin, which resulted in a median PFS of only 2.1 months, cells containing the *FGFR2-SH3GLB1* or *FGFR2-AHCYL2* fusion gene were shown to have lower sensitivity to single gemcitabine treatment than CTL-NIH/3T3 cells (Valle et al., 2010). Based on the concordant *in vitro* and *in vivo* results, it might be interesting to investigate whether patients with iCCA harboring FGFR2 fusions benefit less from chemotherapy with gemcitabine. In this regard, further studies are necessary to possibly change the therapy strategy for patients with FGFR2 alterations. Currently, the substances pemigatinib, infigratinib and futibatinib are being investigated in phase III trials as first-line therapy after being approved in the chemorefractory setting (Vogel et al., 2023).

Taken together, despite the lack of many factors, such as tumor microenvironment, many clinical observations were similar in *in vitro* experiments and, in turn, may provide indications of a potential response to therapy with different TKIs in a clinical setting. Fundamentally, this study highlights the impact that tumor sequencing and subsequent personalized treatment with TKIs matched to tumor genetics may have on patient survival.

4.4 Secondary FGFR2 kinase mutations leading to resistance to TKIs

Although FGFR-inhibiting TKIs demonstrated clinical efficacy, durable responses are rare due to the development of acquired resistance (Goyal et al., 2017, Goyal et al., 2019, Krook et al., 2019, Krook et al., 2020). Goyal et al. were the first to find an explanation for this phenomenon, describing 3 patients (Goyal et al., 2017).

By performing liquid biopsies for cfDNA and tumor biopsies for DNA sequencing, they discovered several secondary point mutations within the FGFR2 kinase domain that confer acquired resistance to selective FGFR inhibitors (Goyal et al., 2017). Specifically, these point mutations could not be identified in either cfDNA or tumor DNA analyses prior to infigratinib treatment. However, after progress on therapy, several point mutations were found that could explain the resistance of tumors to the selected treatment, including p.N549H and p.E565A, found in 2 of 3 patients cfDNA, as well as p.V564F, seen in 3 of 3 patients cfDNA and also detectable in 1 tumor biopsy (Goyal et al., 2017).

For the patients observed in this study, TKIs exhibited a limited duration of action as well. Under suspicion that these short-lasting efficacies could likewise be based on resistance mechanisms, the last aim of this study was to investigate the upcoming problem of acquired resistance to TKIs. For this purpose, extended cell model studies as well as tumor biopsies and cfDNA sequencing of the patients were performed. Based on previously discovered point mutations that have been described as desensitizing to TKIs and were also found in patient #2, the focus was on finding ways to overcome the resistance using the point mutations p.E565A and p.V564F as examples (Goyal et al., 2017, Goyal et al., 2019).

To investigate these resistance mechanisms, two additional plasmids were constructed containing the *FGFR2-AHCYL2* gene fusion modified with one of these point mutations and then were stably transfected into NIH/3T3 cells. Thus, cells harboring the *FGFR2-AHCYL2* wild type as well as point-mutated *FGFR2-*

AHCYL2 p.E565A („.E565A”) and *FGFR2-AHCYL2* p.V564F („.V564F”) genes were analyzed for comparative studies.

First, a basic characterization showed, that “.E565A”- and “.V564F”-positive cells have similar cell characteristics and functional features as their wild type. Noticeably, the FGFR2 protein-representing bands related to ".E565A" and ".V564F"-bearing cells were of the same size as those of the FGFR2-AHCYL2 wild type ones (see **Fig. 16 B** and **Fig. 7 C**). Likewise, the „.E565A“ and „.V564F“-expressing cells FGFR downstream signaling was enhanced (see **Fig. 16 C** and **Fig. 8**). What was striking, however, was that „.E565A”-transfected cells demonstrated a weaker signal for pFRS2 and pMAPK. This observation is in line with the results of Goyal et al. who evaluated the same point mutation in a similar cell model examining *FGFR2* fusion genes (Goyal et al., 2019). This brings to mind that an amino acid change could have different influences on downstream signaling, for example due to steric changes. Supported by the fact that equivalent mutations of *FGFR2* have been reported as drivers in many types of cancer, further detailed investigation of these distinct point mutations may be valuable (Patani et al., 2016).

Apart from this slight deviation regarding the downstream signals, the cellular characteristics of „.E565A“ and „.V564F“-expressing cells were similar compared to FGFR2-AHCYL2 wild type-harboring cells. This is in accordance to previous publications investigating signaling differences between FGFR fusion gene wild types and point mutant variants (Goyal et al., 2019, Krook et al., 2019, Krook et al., 2020, Li et al., 2020). As both point mutation carrying fusion gene-transfected cell lines exhibited increased proliferation compared to CTL-NIH/3T3 cells and „.V564F“-transfected cells formed colonies in the soft agar assay, their oncogenic potential was likewise demonstrated (see **Fig. 17**).

The mechanisms leading to the acquisition of resistance differ slightly between the different secondary point mutations. However, they are all the result of drug-induced selection of subclones carrying corresponding point mutations (Goyal et

al., 2017). Point mutations p.N549H and p.E565A lead to a shift stabilizing active conformation with constitutive FGFR kinase activation (Chen et al., 2007, Goyal et al., 2019). By contrast, p.V564F is a gatekeeper mutation causing a steric clash preventing infigratinib from binding into the ATP pocket (Goyal et al., 2019, Babina and Turner, 2017). These differences are particularly significant for the degree of resistance to TKIs, which also varies.

In vitro studies using drug assays and Western blotting displayed that mutation p.V564F is causing the greatest level of resistance to infigratinib (Goyal et al., 2019). The point mutations were shown to confer the described resistance to infigratinib also in the cell model used in this study, as discussed in the following section (see **Fig. 16 A and 20 A and C**). Furthermore, cell based studies revealed the detected mutations to cause resistance to other inhibitors as well. Additionally, point-mutated fusion genes were observed having lower sensitivity compared to their wild type fusion gene carrying cells for selective inhibitors AZD-4547, Debio-1347, FIIN-2, pemigatinib and erdafitinib (Goyal et al., 2017, Krook et al., 2019, Krook et al., 2020). The fact that these point mutations confer resistance to a variety of selective TKIs again emphasizes the importance of finding mechanisms to overcome them.

4.5 Overcoming the increasing problem of acquired resistance to TKIs

To carry out further investigations on overcoming the resistance to selective FGFR-inhibitors caused by secondary *FGFR2* kinase point mutations, it was first demonstrated that the mutations also confer resistance to infigratinib in the cell model tested. Using SRB assays and soft agar colony formation assays, both variants, „.E565A”- and „.V564F”-expressing cells, bared significantly lower sensitivity to infigratinib than their FGFR2-AHCYL2 wild type equivalent. In accordance with Goyal et al. cells harboring the „.V564F” fusion gene showed the strongest resistance to infigratinib (see **Fig. 18 A and 21**).

Various other TKIs with FGFR-inhibitory effect were then assayed using this cell model, including the covalent binding selective FGFR inhibitor futibatinib, which was shown to be able to overcome infigratinib resistance *in vitro* and *in vivo* in the presence of certain kinase mutations (Tan et al., 2014, Goyal et al., 2019).
Although some inhibitory effect of futibatinib was shown for „.E565A" and „.V564F"-bearing cells, both kinase mutations resulted in a certain degree of resistance to the substance (see **Fig. 18 B**). While previous studies indicated FGFR2 fusion kinases harboring the p.E565A point mutation to be still sensitive to futibatinib, this could not be confirmed by the methods applied here (see **Fig. 21**) (Goyal et al., 2019, Krook et al., 2019). Similar deviations from previous results were noted by Li et al., who showed that futibatinib was ineffective in the p.N550K kinase mutation in another *FGFR2* fusion gene cell model (Li et al., 2020). While there is some evidence that futibatinib may be effective in the presence of a kinase mutation, the results of these and other studies are inconclusive. Since hardly any *in vivo* data are available, no definitive evaluation can be made.
Remarkably, for the tested multikinase inhibitors with FGFR activity ponatinib an lenvatinib, the degree of drug resistance was considerably lower, when cells harboring the FGFR2-AHCYL2 fusion with an additional kinase mutation were assayed.
Consistently, ponatinib has also been described in previous studies as being able to overcome resistance, yet with a difference in detail. Ponatinib showed good results regarding the p.E565A kinase mutation, while the p.V564F mutation was the one that produced the greatest resistance to the drug (Goyal et al., 2017, Krook et al., 2020).
The experiments of this study displayed that „.V564F"-positive cells were even sensitive to this substance, whereas ".E565A"-bearing cells were not, yet also at a lower level of resistance than that observed for selective TKIs (see **Fig. 19 B** and **Fig. 21**). Unfortunately, there is no clinical case report to date demonstrating that the drug is able to overcome secondary acquired resistance to selective FGFR-inhibiting TKIs due to an FGFR2 kinase mutation.

Strikingly good results were uniformly obtained for lenvatinib treatment in kinase-mutated FGFR2 fusion-positive cell lines, which combined with the clinical data from this study led to very interesting aspects. *FGFR2-AHCYL2* fusion gene-expressing cells carrying resistance point mutations p.V564F or p.E565A were both sensitive to the multikinase inhibitor lenvatinib, even at low doses (see **Fig. 19 A**, **Fig. 21** and **Fig. 22**). Consistent with the previously discussed broader effects of lenvatinib on downstream signaling in FGFR2 wild type kinase, these effects were also demonstrated in cells harboring FGFR2 fusions with kinase mutation. When proteomic analyses were performed on NIH/3T3 cells containing the FGFR2-AHCYL2 fusion with p.V564F kinase mutation after lenvatinib treatment, the drug reduced the phosphorylation of FGFR2 as well as non-MAPK signaling proteins mainly involved in PI3K/AKT signaling, which was not the case after infigratinib treatment (Spahn et al., 2024). Furthermore, in this cell line, the effects on inhibition of phosphorylation of selected MAPK proteins were stronger for lenvatinib than for infigratinib (Spahn et al., 2024). In-silico modeling further suggested that lenvatinib may adapt better to FGFR2 with the p.V564F, p.E565A and p.N549K kinase mutations than infigratinib or pemigatinib (Spahn et al., 2024).

Reconsidering the clinical course of patients treated with lenvatinib, the drug induced a promising long median PFS, as previously highlighted. Furthermore, other than for infigratinib, after lenvatinib treatment, no kinase mutation was found (see **Fig. 3** and **Fig. 4**). Moreover, lenvatinib was even able to achieve partial response and sustained PFS in a patient with FGFR2-BICC1 fusion-positive iCCA with acquired p.N549K kinase mutation after disease progression during treatment with pemigatinib (Spahn et al., 2024).

Taken together this leads to the assumption that the unselective TKI lenvatinib causes less resistance, which might originate from the additional inhibition of other tyrosine kinases and the corresponding different influence on downstream signaling. Further, it is reasonable to assume that the development of resistance-causing point mutations in the *FGFR2* kinase region may be a predominant phenomenon of selective FGFR inhibitors and that the non-selective FGFR inhibitor

lenvatinib can be used to overcome secondary resistance in FGFR2 fusion-positive iCCA. Since lenvatinib appears to cause less resistance while potentially overcoming previously acquired ones, its role in the therapy of iCCA with FGFR2 alterations should be reevaluated. These observations might be the most relevant finding of this study in respect to a clinical relevance for FGFR2-driven cholangiocarcinomas.

There are other different approaches to overcome kinase mutation-acquired resistance, but these have hardly been investigated so far.
One of them is the application of combination therapies. The idea is that in addition to FGFR inhibition, subsequent upregulated downstream signaling pathways can be blocked. Using cells expressing an *FGFR2* fusion gene with the resistance mutation p.E565A, Krook et al. demonstrated that treatment with the mTOR inhibitor INK128 restores a response to FGFR inhibition in resistant cells (Krook et al., 2020). Further, a synergistic effect of trametinib, a MEK inhibitor, was bared for infigratinib and futibatinib in a cell model that examined the effects of the p.N550K point mutation in an *FGFR2* fusion gene (Li et al., 2020).

As amplifications of the FRS2 adapter protein were noticed quite often by tumor panel sequencing of iCCA patients by the MTB and an enhanced pFRS2 signal was detected in *FGFR2* fusion gene-positive cells, the hypothesis emerged whether this protein could also serve as a target. Various studies have already presented hopeful *in vitro* results via FRS2 inhibition in relation to other types of cancer (Li et al., 2018, Li and Luo, 2020). Since FRS2 is at the beginning of the FGFR signaling pathway and RAS/MAPK and PI3K/AKT signaling are dependent on it, inhibiting this protein could be even more successful than targeting MAPK or AKT alone (Ornitz and Itoh, 2015).

Surprisingly, when „.E565A”- and „.V564F”-expressing cells were treated with gemcitabine, they bared a noticeable higher sensitivity to the chemotherapeutic than their FGFR2-AHCYL2 wild type equivalent (see **Fig. 20 B**). Following, Western blot experiments showed that in FGFR2-AHCYL2-positive cells, pFGFR was

not affected, while pMAPK signaling increased, after treatment with gemcitabine, as discussed previously. Furthermore, when „.E565A" and „.V564F" cells were treated with cabozantinib, a TKI with no known FGFR-inhibitory activity, they exposed a significantly better inhibition compared to the FGFR2-AHCYL2 cells with wild type kinase, and even compared to the empty vector-transfected cells (see **Fig. 20 A)**. The enhanced proliferation inhibitory effect of gemcitabine and cabozantinib could possibly be attributed to conformational changes through the point mutations of the FGFR2 ATP-binding pocket, leading to altered accessibility of the respective ligands. Although these hypotheses are highly speculative and need further investigation, the results nevertheless reinforce the importance of evaluating such resistance-causing point mutations in detail.

4.6 Conclusions and future perspectives

This study was initially driven by the detailed analysis of the clinical course of two exceptional patients with iCCA and intratumoral *FGFR2* fusion genes, namely *FGFR2-SH3GLB1* and *FGFR2-AHCYL2*. Both patients showed an impressive clinical benefit during the treatment with lenvatinib, which was recommended by the MTB of Tuebingen University Hospital. These two case studies stimulated a "bed to benchside" approach for an *in vitro* cellular model and a further characterization of several additional patients with FGFR2-driven CCA.

The newly generated and characterized cell lines demonstrated that *FGFR2-SH3GLB1* and *FGFR2-AHCYL2* are fusion genes with oncogenic potential, comparable to previously reported results for other fusion genes in iCCA. With the cell lines exhibiting enhanced proliferation and anchorage-independent growth likely caused by activation of downstream FGFR signaling, the experiments underscore that *FGFR2* fusion genes with diverse fusion partners have malignant potential and trigger FGFR signaling. Since the results for the already well-studied *FGFR2-BICC1* fusion gene agree with previous findings, the methods used in this study seem to be suitable to investigate further different fusion genes.
One interesting finding from the clinically analyzed patient histories was that FGFR2-altered iCCAs might benefit less from standard first-line chemotherapy

with gemcitabine/cisplatin. Certainly, further studies, especially with larger number of clinical cases, are needed to support this assumption.

Starting with the initial finding in the patient cohort that lenvatinib can induce meaningful responses in FGFR2 fusion-driven iCCAs, *in vitro* studies showed comparable efficacies for the multikinase inhibitor lenvatinib and for selective TKIs such as infigratinib or futibatinib. Therefore, lenvatinib might be an effective alternative treatment option in FGFR2 fusion-positive iCCAs, which might be especially interesting for patients with characteristic adverse events during the treatment with the more specific drugs.

One of the main findings of this study was the observation that when *FGFR2-AHCYL2*-harboring cells with an additional resistance causing point mutation of the kinase region were treated with unselective TKIs such as lenvatinib or ponatinib, these drugs still induced proliferation inhibiting effects. One explanation for this persistent efficacy of unselective TKIs despite resistance mutations was found to be altered downstream signal inhibition compared to selective ones. Further investigations on this subject are currently ongoing. Interestingly, a clinical case that has not been included in this study and is part of a separate report, underscores the importance of this study: this patient showed a response to lenvatinib despite the development of resistance mutations during the treatment with pemigatinib (Spahn et al., 2024). In summary, the work of this study and further observations suggest that the role of multikinase inhibitors with FGFR-inhibiting activities, such as lenvatinib, should be further explored in clinical studies.

5.a Summary

There are currently limited treatment options for intrahepatic cholangiocarcinoma (iCCA), a lethal tumor with increasing incidence. However, studies have identified *FGFR2* fusion genes, present in up to 16 % of iCCA patients, as a promising new therapeutic target.

Three selective FGFR-targeting tyrosine kinase inhibitors (TKIs) (pemigatinib, infigratinib, and futibatinib) have already been approved in patients with iCCA and FGFR2 alteration. However, durable responses are rarely observed due to the development of resistance to these TKIs.

FGFR2 fusion genes, including the previously unknown *FGFR2-AHCYL2* fusion gene, were also identified in patients of the Molecular Tumor Board (MTB) of Tuebingen University Hospital. These were subsequently treated among others with different FGFR-targeting TKIs.

The initial aim of this study was to analyze the clinical course of a cohort of patients from the MTB with FGFR2-driven iCCA. To gain further knowledge about the malignant potential of the detected *FGFR2* fusion genes, especially a newly detected *FGFR2-AHCYL2* fusion, and efficacy of different FGFR-attacking TKIs, a cell model containing the patient-specific FGFR2 fusions was generated and investigated using NIH/3T3 cells.

Furthermore, *FGFR2* fusion gene-expressing cell lines were generated that additionally contain point mutations of the FGFR2 kinase region, which according to current studies lead to resistance to FGFR-selective TKIs.

The analysis of the clinical courses of the patients showed a rather poor response to standard chemotherapy with gemcitabine/cisplatin. Furthermore, not all TKIs with FGFR activity were found to be effective. However, therapy with the non-selective TKI lenvatinib led to meaningful clinical responses in the investigated patient cohort.

Cell lines stably expressing the patient-specific fusion genes *FGFR2-SH3GLB1*, *FGFR2-AHCYL2* and the most common fusion gene *FGFR2-BICC1* were successfully generated. Subsequent assays demonstrated increased phosphorylation of downstream FGFR signaling proteins, increased proliferation and

anchorage-independent growth for these cell lines. In cell-based studies on the effect of TKIs, both the FGFR-selective TKIs infigratinib and futibatinib and the multikinase inhibitors with FGFR activity ponatinib and lenvatinib showed good efficacy in terms of proliferation inhibition. However, the chemotherapeutic agent gemcitabine remained ineffective in these experiments. Western blot analyses were performed that indicate differential influence on FGFR downstream signaling pathways of selective and nonselective TKIs. The presence of an additional point mutation p.V564F or p.E565A in the kinase region of *FGFR2-AHCYL2*-bearing cell lines significantly attenuated the efficacy of infigratinib and to a lower degree of futibatinib, whereas the efficacy of the nonselective TKIs ponatinib and lenvatinib remained effective. This observation might be important for patients that develop resistance mutations during the therapy with FGFR-selective TKIs.

Taken together, the results of this study show that the newly found fusion gene *FGFR2-AHCYL2* has comparable oncogenic properties in our *in vitro* model than previously described fusions. Moreover, the non-selective TKI lenvatinib showed *in vitro* and in patients meaningful antitumor responses, in the established cellular model even in the presence of resistance mediating point mutations. This work suggests further clinical studies to get more insight into the role of FGFR selective and non-selective TKIs in FGFR-driven iCCA.

5.b Zusammenfassung

Für das intrahepatische Cholangiokarzinom (iCCA), einen tödlichen Tumor mit steigender Inzidenz, bestehen derzeit nur begrenzte Behandlungsmöglichkeiten. In Studien wurden jedoch *FGFR2* Fusionsgene, die bei bis zu 16 % der iCCA Patient*innen vorkommen, als ein vielversprechendes neues therapeutisches Ziel identifiziert. Drei selektiv am FGFR-angreifende Tyrosinkinaseinhibitoren (TKIs) (Pemigatinib, Infigratinib und Futibatinib) sind bei Patient*innen mit iCCA und FGFR2 Veränderung bereits zugelassen worden. Aufgrund der Entwicklung von Resistenzen gegen diese TKIs ist ein dauerhaftes Ansprechen jedoch nur selten zu beobachten.

Derartige *FGFR2* Fusionsgene, darunter das bisher unbekannte *FGFR2-AHCYL2* Fusionsgen, wurden auch bei Patient*innen des Molekularen Tumorboards (MTB) des Universitätsklinikums Tübingen identifiziert. Diese wurden daraufhin unter anderem mit verschiedenen FGFR-wirksamen TKIs behandelt.

Das anfängliche Ziel dieser Studie war die Analyse des klinischen Verlaufs einer Kohorte von Patient*innen des MTB mit FGFR2-bedingtem iCCA.

Um weitere Erkenntnisse über das maligne Potenzial der entdeckten *FGFR2* Fusionsgene, insbesondere der neu entdeckten *FGFR2-AHCYL2* Fusion, und die Wirksamkeit verschiedener am FGFR-angreifenden TKIs zu gewinnen, wurde mithilfe von NIH/3T3 Zellen ein Zellmodell erzeugt und untersucht, das die patient*innenspezifischen *FGFR2* Fusionen enthält. Weiterhin wurden *FGFR2* Fusionsgen-exprimierende Zelllinien generiert, die zusätzlich Punktmutationen der Kinase Region des FGFR2 enthalten, welche aktuellen Studien zufolge zu einer Resistenz gegenüber FGFR selektiven TKIs führt.

Die Analyse der klinischen Verläufe der Patient*innen zeigte ein geringes Ansprechen auf die Standardchemotherapie mit Gemcitabine/Cisplatin. Weiterhin erwiesen sich nicht alle TKIs mit FGFR-Aktivität als wirksam. Die Therapie mit dem unselektiven TKI Lenvatinib führte jedoch zu bedeutsamen klinischen Wirkungen in der untersuchten Patient*innenkohorte.

Es konnten erfolgreich Zelllinien generiert werden, die die patient*innenanalogen Fusionsgene *FGFR2-SH3GLB1*, *FGFR2-AHCYL2* und das am häufigsten

vorkommende Fusionsgen *FGFR2-BICC1* stabil exprimieren. In nachfolgenden Assays konnte für diese Zelllinien eine vermehrte Phosphorylierung der nachgeschalteten FGFR-Signalproteine, eine vermehrte Proliferation und ein verankerungsunabhängiges Wachstum nachgewiesen werden. In zellbasierten Untersuchungen zur Wirkung der TKIs, zeigten sowohl die selektiven TKIs Infigratinib und Futibatinib als auch die Multikinase Inhibitoren mit FGFR Aktivität Ponatinib und Lenvatinib eine gute Wirksamkeit bezüglich der Proliferationshemmung. Hingegen blieb das Chemotherapeutikum Gemcitabine in diesen Versuchen unwirksam. Die durchgeführten Western Blot Analysen wiesen auf eine unterschiedliche Beeinflussung nachgeschalteter FGFR-Signalwege zwischen selektiven und unselektiven TKIs hin. Das Vorliegen einer zusätzlichen Punktmutation p.V564F oder p.E565A in der Kinase Region von *FGFR2-AHCYL2*-tragenden Zelllinien führte zu einer deutlichen Wirkabschwächung von Infigratinib und in geringerem Maße von Futibatinib, während die Wirksamkeit der nicht-selektiven TKIs Ponatinib und Lenvatinib erhalten blieb. Diese Beobachtung könnte für Patient*innen wichtig sein, die während der Therapie mit FGFR-selektiven TKIs Resistenzmutationen entwickeln.

Insgesamt zeigen die Ergebnisse dieser Studie, dass das neu entdeckte Fusionsgen *FGFR2-AHCYL2* in unserem *in vitro* Modell vergleichbare onkogene Eigenschaften aufweist wie zuvor beschriebene Fusionen. Darüber hinaus zeigte der nicht-selektive TKI Lenvatinib *in vitro* und bei Patient*innen eine bedeutsame antitumorale Wirksamkeit, im entwickelten Zellmodell sogar bei Vorliegen einer resistenzvermittelnden Punktmutation. Auf Grundlage dieser Arbeit sollten weiterführende klinische Studien durchgeführt werden, um tiefere Erkenntnisse bezüglich der Rolle von FGFR selektiven und nicht-selektiven TKIs bei FGFR-bedingtem iCCA zu bekommen.

6. Bibliography

Abou-Alfa, G. K., Sahai, V., Hollebecque, A., Vaccaro, G., Melisi, D., Al-Rajabi, R., Paulson, A. S., Borad, M. J., Gallinson, D., Murphy, A. G., Oh, D. Y., Dotan, E., Catenacci, D. V., Van Cutsem, E., Ji, T., Lihou, C. F., Zhen, H., Feliz, L. & Vogel, A. 2020. Pemigatinib for previously treated, locally advanced or metastatic cholangiocarcinoma: a multicentre, open-label, phase 2 study. *Lancet Oncol,* 21**,** 671-684.

Ahmad, I., Iwata, T. & Leung, H. Y. 2012. Mechanisms of FGFR-mediated carcinogenesis. *Biochim Biophys Acta,* 1823**,** 850-60.

Alvaro, D., Bragazzi, M. C., Benedetti, A., Fabris, L., Fava, G., Invernizzi, P., Marzioni, M., Nuzzo, G., Strazzabosco, M., Stroffolini, T. & committee, A. C. 2011. Cholangiocarcinoma in Italy: A national survey on clinical characteristics, diagnostic modalities and treatment. Results from the "Cholangiocarcinoma" committee of the Italian Association for the Study of Liver disease. *Dig Liver Dis,* 43**,** 60-5.

Arai, Y., Totoki, Y., Hosoda, F., Shirota, T., Hama, N., Nakamura, H., Ojima, H., Furuta, K., Shimada, K., Okusaka, T., Kosuge, T. & Shibata, T. 2014. Fibroblast growth factor receptor 2 tyrosine kinase fusions define a unique molecular subtype of cholangiocarcinoma. *Hepatology,* 59**,** 1427-34.

Babina, I. S. & Turner, N. C. 2017. Advances and challenges in targeting FGFR signalling in cancer. *Nat Rev Cancer,* 17**,** 318-332.

Banales, J. M., Cardinale, V., Carpino, G., Marzioni, M., Andersen, J. B., Invernizzi, P., Lind, G. E., Folseraas, T., Forbes, S. J., Fouassier, L., Geier, A., Calvisi, D. F., Mertens, J. C., Trauner, M., Benedetti, A., Maroni, L., Vaquero, J., Macias, R. I., Raggi, C., Perugorria, M. J., Gaudio, E., Boberg, K. M., Marin, J. J. & Alvaro, D. 2016. Expert consensus document: Cholangiocarcinoma: current knowledge and future perspectives consensus statement from the European Network for the Study of Cholangiocarcinoma (ENS-CCA). *Nat Rev Gastroenterol Hepatol,* 13**,** 261-80.

Belfiore, M. P., Reginelli, A., Maggialetti, N., Carbone, M., Giovine, S., Laporta, A., Urraro, F., Nardone, V., Grassi, R., Cappabianca, S. & Brunese, L. 2020. Preliminary results in unresectable cholangiocarcinoma treated by CT percutaneous irreversible electroporation: feasibility, safety and efficacy. *Med Oncol,* 37**,** 45.

Bibeau, K., Feliz, L., Lihou, C. F., Ren, H. & Abou-Alfa, G. K. 2022. Progression-Free Survival in Patients With Cholangiocarcinoma With or Without FGF/FGFR Alterations: A FIGHT-202 Post Hoc Analysis of Prior Systemic Therapy Response. *JCO Precis Oncol,* 6**,** e2100414.

Bitzer, M., Ostermann, L., Horger, M., Biskup, S., Schulze, M., Ruhm, K., Hilke, F., Oner, O., Nikolaou, K., Schroeder, C., Riess, O., Fend, F., Zips, D., Hinterleitner, M., Zender, L., Tabatabai, G., Beha, J. & Malek, N. P. 2020. Next-Generation Sequencing of Advanced GI Tumors Reveals Individual Treatment Options. *JCO Precis Oncol,* 4.

Bitzer, M., Spahn, S., Babaei, S., Horger, M., Singer, S., Schulze-Osthoff, K., Missios, P., Gatidis, S., Nann, D., Mattern, S., Scheble, V., Nikolaou, K., Armeanu-Ebinger, S., Schulze, M., Schroeder, C., Biskup, S., Beha, J., Claassen, M., Ruhm, K., Poso, A. & Malek, N. P. 2021. Targeting extracellular and juxtamembrane FGFR2 mutations in chemotherapy-refractory cholangiocarcinoma. *npj Precision Oncology,* 5**,** 80.

Bitzer, M., Voesch, S., Albert, J., Bartenstein, P., Bechstein, W., Blödt, S., Brunner, T., Dombrowski, F., Evert, M., Follmann, M., La Fougère, C., Freudenberger, P., Geier, A., Gkika, E., Götz, M., Hammes, E., Helmberger, T., Hoffmann, R. T., Hofmann, W. P., Huppert, P., Kautz, A., Knötgen, G., Körber, J., Krug, D., Lammert, F., Lang, H., Langer, T., Lenz, P., Mahnken, A., Meining, A., Micke, O., Nadalin, S., Nguyen, H. P., Ockenga, J., Oldhafer, K., Paprottka, P., Paradies, K., Pereira, P., Persigehl, T., Plauth, M., Plentz, R., Pohl, J., Riemer, J., Reimer, P., Ringwald, J., Ritterbusch, U., Roeb, E., Schellhaas, B., Schirmacher, P., Schmid, I., Schuler, A., von Schweinitz, D., Seehofer, D., Sinn, M., Stein, A., Stengel, A., Steubesand, N., Stoll, C., Tannapfel, A., Taubert, A., Trojan, J., van Thiel, I., Tholen, R., Vogel, A., Vogl, T., Vorwerk, H., Wacker, F., Waidmann, O., Wedemeyer, H., Wege, H., Wildner, D., Wittekind, C., Wörns, M. A., Galle, P. & Malek, N. 2022. S3-Leitlinie: Diagnostik und Therapie biliärer Karzinome. *Z Gastroenterol,* 60**,** 219-238.

Borad, M. J., Champion, M. D., Egan, J. B., Liang, W. S., Fonseca, R., Bryce, A. H., McCullough, A. E., Barrett, M. T., Hunt, K., Patel, M. D., Young, S. W., Collins, J. M., Silva, A. C., Condjella, R. M., Block, M., McWilliams, R. R., Lazaridis, K. N., Klee, E. W., Bible, K. C., Harris, P., Oliver, G. R., Bhavsar, J. D., Nair, A. A., Middha, S., Asmann, Y., Kocher, J. P., Schahl, K., Kipp, B. R., Barr Fritcher, E. G., Baker, A., Aldrich, J., Kurdoglu, A., Izatt, T., Christoforides, A., Cherni, I., Nasser, S., Reiman, R., Phillips, L., McDonald, J., Adkins, J., Mastrian, S. D., Placek, P., Watanabe, A. T., Lobello, J., Han, H., Von Hoff, D., Craig, D. W., Stewart, A. K. & Carpten, J. D. 2014. Integrated genomic characterization reveals novel, therapeutically relevant drug targets in FGFR and EGFR pathways in sporadic intrahepatic cholangiocarcinoma. *PLoS Genet,* 10**,** e1004135.

Borowicz, S., Van Scoyk, M., Avasarala, S., Karuppusamy Rathinam, M. K., Tauler, J., Bikkavilli, R. K. & Winn, R. A. 2014. The soft agar colony formation assay. *J Vis Exp***,** e51998.

Burnette, W. N. 1981. "Western blotting": electrophoretic transfer of proteins from sodium dodecyl sulfate--polyacrylamide gels to unmodified nitrocellulose

and radiographic detection with antibody and radioiodinated protein A. *Anal Biochem,* 112**,** 195-203.

Byron, S. A., Chen, H., Wortmann, A., Loch, D., Gartside, M. G., Dehkhoda, F., Blais, S. P., Neubert, T. A., Mohammadi, M. & Pollock, P. M. 2013. The N550K/H mutations in FGFR2 confer differential resistance to PD173074, dovitinib, and ponatinib ATP-competitive inhibitors. *Neoplasia,* 15**,** 975-88.

Capozzi, M., De Divitiis, C., Ottaiano, A., von Arx, C., Scala, S., Tatangelo, F., Delrio, P. & Tafuto, S. 2019. Lenvatinib, a molecule with versatile application: from preclinical evidence to future development in anti-cancer treatment. *Cancer Manag Res,* 11**,** 3847-3860.

Chae, Y. K., Ranganath, K., Hammerman, P. S., Vaklavas, C., Mohindra, N., Kalyan, A., Matsangou, M., Costa, R., Carneiro, B., Villaflor, V. M., Cristofanilli, M. & Giles, F. J. 2017. Inhibition of the fibroblast growth factor receptor (FGFR) pathway: the current landscape and barriers to clinical application. *Oncotarget,* 8**,** 16052-16074.

Chen, H., Ma, J., Li, W., Eliseenkova, A. V., Xu, C., Neubert, T. A., Miller, W. T. & Mohammadi, M. 2007. A molecular brake in the kinase hinge region regulates the activity of receptor tyrosine kinases. *Mol Cell,* 27**,** 717-30.

Chmiel, P., Geca, K., Rawicz-Pruszynski, K., Polkowski, W. P. & Skorzewska, M. 2022. FGFR Inhibitors in Cholangiocarcinoma-A Novel Yet Primary Approach: Where Do We Stand Now and Where to Head Next in Targeting This Axis? *Cells,* 11.

Cillo, U., Fondevila, C., Donadon, M., Gringeri, E., Mocchegiani, F., Schlitt, H. J., Ijzermans, J. N. M., Vivarelli, M., Zieniewicz, K., Olde Damink, S. W. M. & Groot Koerkamp, B. 2019. Surgery for cholangiocarcinoma. *Liver Int,* 39 Suppl 1**,** 143-155.

Coughlin, S. R., Barr, P. J., Cousens, L. S., Fretto, L. J. & Williams, L. T. 1988. Acidic and basic fibroblast growth factors stimulate tyrosine kinase activity in vivo. *J Biol Chem,* 263**,** 988-93.

Dai, S., Zhou, Z., Chen, Z., Xu, G. & Chen, Y. 2019. Fibroblast Growth Factor Receptors (FGFRs): Structures and Small Molecule Inhibitors. *Cells,* 8.

Dienstmann, R., Rodon, J., Prat, A., Perez-Garcia, J., Adamo, B., Felip, E., Cortes, J., Iafrate, A. J., Nuciforo, P. & Tabernero, J. 2014. Genomic aberrations in the FGFR pathway: opportunities for targeted therapies in solid tumors. *Ann Oncol,* 25**,** 552-63.

Eisenhauer, E. A., Therasse, P., Bogaerts, J., Schwartz, L. H., Sargent, D., Ford, R., Dancey, J., Arbuck, S., Gwyther, S., Mooney, M., Rubinstein, L., Shankar, L., Dodd, L., Kaplan, R., Lacombe, D. & Verweij, J. 2009. New

response evaluation criteria in solid tumours: revised RECIST guideline (version 1.1). *Eur J Cancer,* 45**,** 228-47.

Esnaola, N. F., Meyer, J. E., Karachristos, A., Maranki, J. L., Camp, E. R. & Denlinger, C. S. 2016. Evaluation and management of intrahepatic and extrahepatic cholangiocarcinoma. *Cancer,* 122**,** 1349-69.

Eswarakumar, V. P., Lax, I. & Schlessinger, J. 2005. Cellular signaling by fibroblast growth factor receptors. *Cytokine Growth Factor Rev,* 16**,** 139-49.

European Medicines Agency. 2021. *Pemazyre (Pemigatinib) - an overview of Pemazyre and why it is authorised in the EU* [Online]. Available: https://www.ema.europa.eu/en/documents/overview/pemazyre-epar-medicine-overview_en.pdf [Accessed 21.02.2023].

Facchinetti, F., Hollebecque, A., Bahleda, R., Loriot, Y., Olaussen, K. A., Massard, C. & Friboulet, L. 2019. Facts and new hopes on selective FGFR inhibitors in solid tumors. *Clin Cancer Res*.

Frazier-Wood, A. C., Aslibekyan, S., Borecki, I. B., Hopkins, P. N., Lai, C. Q., Ordovas, J. M., Straka, R. J., Tiwari, H. K. & Arnett, D. K. 2012. Genome-wide association study indicates variants associated with insulin signaling and inflammation mediate lipoprotein responses to fenofibrate. *Pharmacogenet Genomics,* 22**,** 750-7.

Frisch, S. M. & Francis, H. 1994. Disruption of epithelial cell-matrix interactions induces apoptosis. *J Cell Biol,* 124**,** 619-26.

Goyal, L., Kongpetch, S., Crolley, V. E. & Bridgewater, J. 2021. Targeting FGFR inhibition in cholangiocarcinoma. *Cancer Treat Rev,* 95**,** 102170.

Goyal, L., Lamarca, A., Strickler, J. H., Cecchini, M., Ahn, D. H., Baiev, I., Boileve, A., Tazdait, M., Hannan, L. M., Jia, J., Marble, H. D., Barzi, A., Sahai, V., Lennerz, J. K., Kelley, R. K., Bekaii-Saab, T. S., Javle, M. M., Uboha, N. V., Harris, W. P. & Hollebecque, A. 2020. The natural history of fibroblast growth factor receptor (FGFR)-altered cholangiocarcinoma (CCA). *Journal of Clinical Oncology,* 38**,** e16686-e16686.

Goyal, L., Meric-Bernstam, F., Hollebecque, A., Morizane, C., Valle, J. W., Karasic, T. B., Abrams, T. A., Kelley, R. K., Cassier, P. A., Furuse, J., Klümpen, H.-J., Chang, H.-M., Chen, L.-T., Komatsu, Y., Masuda, K., Ahn, D. H., Li, K., Benhadji, K. A., Wacheck, V. & Bridgewater, J. A. 2022. Updated results of the FOENIX-CCA2 trial: Efficacy and safety of futibatinib in intrahepatic cholangiocarcinoma (iCCA) harboring FGFR2 fusions/rearrangements. *Journal of Clinical Oncology,* 40**,** 4009-4009.

Goyal, L., Meric-Bernstam, F., Hollebecque, A., Valle, J. W., Morizane, C., Karasic, T. B., Abrams, T. A., Furuse, J., Kelley, R. K., Cassier, P. A.,

Klumpen, H. J., Chang, H. M., Chen, L. T., Tabernero, J., Oh, D. Y., Mahipal, A., Moehler, M., Mitchell, E. P., Komatsu, Y., Masuda, K., Ahn, D., Epstein, R. S., Halim, A. B., Fu, Y., Salimi, T., Wacheck, V., He, Y., Liu, M., Benhadji, K. A., Bridgewater, J. A. & Investigators, F.-C. S. 2023. Futibatinib for FGFR2-Rearranged Intrahepatic Cholangiocarcinoma. *N Engl J Med,* 388**,** 228-239.

Goyal, L., Saha, S. K., Liu, L. Y., Siravegna, G., Leshchiner, I., Ahronian, L. G., Lennerz, J. K., Vu, P., Deshpande, V., Kambadakone, A., Mussolin, B., Reyes, S., Henderson, L., Sun, J. E., Van Seventer, E. E., Gurski, J. M., Jr., Baltschukat, S., Schacher-Engstler, B., Barys, L., Stamm, C., Furet, P., Ryan, D. P., Stone, J. R., Iafrate, A. J., Getz, G., Porta, D. G., Tiedt, R., Bardelli, A., Juric, D., Corcoran, R. B., Bardeesy, N. & Zhu, A. X. 2017. Polyclonal Secondary FGFR2 Mutations Drive Acquired Resistance to FGFR Inhibition in Patients with FGFR2 Fusion-Positive Cholangiocarcinoma. *Cancer Discov,* 7**,** 252-263.

Goyal, L., Shi, L., Liu, L. Y., Fece de la Cruz, F., Lennerz, J. K., Raghavan, S., Leschiner, I., Elagina, L., Siravegna, G., Ng, R. W. S., Vu, P., Patra, K. C., Saha, S. K., Uppot, R. N., Arellano, R., Reyes, S., Sagara, T., Otsuki, S., Nadres, B., Shahzade, H. A., Dey-Guha, I., Fetter, I. J., Baiev, I., Van Seventer, E. E., Murphy, J. E., Ferrone, C. R., Tanabe, K. K., Deshpande, V., Harding, J. J., Yaeger, R., Kelley, R. K., Bardelli, A., Iafrate, A. J., Hahn, W. C., Benes, C. H., Ting, D. T., Hirai, H., Getz, G., Juric, D., Zhu, A. X., Corcoran, R. B. & Bardeesy, N. 2019. TAS-120 Overcomes Resistance to ATP-Competitive FGFR Inhibitors in Patients with FGFR2 Fusion-Positive Intrahepatic Cholangiocarcinoma. *Cancer Discov,* 9**,** 1064-1079.

Graham, R. P., Barr Fritcher, E. G., Pestova, E., Schulz, J., Sitailo, L. A., Vasmatzis, G., Murphy, S. J., McWilliams, R. R., Hart, S. N., Halling, K. C., Roberts, L. R., Gores, G. J., Couch, F. J., Zhang, L., Borad, M. J. & Kipp, B. R. 2014. Fibroblast growth factor receptor 2 translocations in intrahepatic cholangiocarcinoma. *Hum Pathol,* 45**,** 1630-8.

Greenman, C., Stephens, P., Smith, R., Dalgliesh, G. L., Hunter, C., Bignell, G., Davies, H., Teague, J., Butler, A., Stevens, C., Edkins, S., O'Meara, S., Vastrik, I., Schmidt, E. E., Avis, T., Barthorpe, S., Bhamra, G., Buck, G., Choudhury, B., Clements, J., Cole, J., Dicks, E., Forbes, S., Gray, K., Halliday, K., Harrison, R., Hills, K., Hinton, J., Jenkinson, A., Jones, D., Menzies, A., Mironenko, T., Perry, J., Raine, K., Richardson, D., Shepherd, R., Small, A., Tofts, C., Varian, J., Webb, T., West, S., Widaa, S., Yates, A., Cahill, D. P., Louis, D. N., Goldstraw, P., Nicholson, A. G., Brasseur, F., Looijenga, L., Weber, B. L., Chiew, Y. E., DeFazio, A., Greaves, M. F., Green, A. R., Campbell, P., Birney, E., Easton, D. F., Chenevix-Trench, G., Tan, M. H., Khoo, S. K., Teh, B. T., Yuen, S. T., Leung, S. Y., Wooster, R., Futreal, P. A. & Stratton, M. R. 2007. Patterns of somatic mutation in human cancer genomes. *Nature,* 446**,** 153-8.

Heining, C., Horak, P., Uhrig, S., Codo, P. L., Klink, B., Hutter, B., Frohlich, M., Bonekamp, D., Richter, D., Steiger, K., Penzel, R., Endris, V., Ehrenberg, K. R., Frank, S., Kleinheinz, K., Toprak, U. H., Schlesner, M., Mandal, R., Schulz, L., Lambertz, H., Fetscher, S., Bitzer, M., Malek, N. P., Horger, M., Giese, N. A., Strobel, O., Hackert, T., Springfeld, C., Feuerbach, L., Bergmann, F., Schrock, E., von Kalle, C., Weichert, W., Scholl, C., Ball, C. R., Stenzinger, A., Brors, B., Frohling, S. & Glimm, H. 2018. NRG1 Fusions in KRAS Wild-Type Pancreatic Cancer. *Cancer Discov,* 8**,** 1087-1095.

Hoff, D. D. V., Jr, J. J. S., Rosen, P., Loesch, D. M., Borad, M. J., Anthony, S., Jameson, G., Brown, S., Cantafio, N., Richards, D. A., Fitch, T. R., Wasserman, E., Fernandez, C., Green, S., Sutherland, W., Bittner, M., Alarcon, A., Mallery, D. & Penny, R. 2010. Pilot Study Using Molecular Profiling of Patients' Tumors to Find Potential Targets and Select Treatments for Their Refractory Cancers. *Journal of Clinical Oncology,* 28**,** 4877-4883.

Hoy, S. M. 2020. Pemigatinib: First Approval. *Drugs,* 80**,** 923-929.

Jain, A., Borad, M. J., Kelley, R. K., Wang, Y., Abdel-Wahab, R., Meric-Bernstam, F., Baggerly, K. A., Kaseb, A. O., Al-shamsi, H. O., Ahn, D. H., DeLeon, T., Bocobo, A. G., Bekaii-Saab, T., Shroff, R. T. & Javle, M. 2018. Cholangiocarcinoma With FGFR Genetic Aberrations: A Unique Clinical Phenotype. *JCO Precision Oncology***,** 1-12.

Javle, M., Bekaii-Saab, T., Jain, A., Wang, Y., Kelley, R. K., Wang, K., Kang, H. C., Catenacci, D., Ali, S., Krishnan, S., Ahn, D., Bocobo, A. G., Zuo, M., Kaseb, A., Miller, V., Stephens, P. J., Meric-Bernstam, F., Shroff, R. & Ross, J. 2016. Biliary cancer: Utility of next-generation sequencing for clinical management. *Cancer,* 122**,** 3838-3847.

Javle, M., Lowery, M., Shroff, R. T., Weiss, K. H., Springfeld, C., Borad, M. J., Ramanathan, R. K., Goyal, L., Sadeghi, S., Macarulla, T., El-Khoueiry, A., Kelley, R. K., Borbath, I., Choo, S. P., Oh, D. Y., Philip, P. A., Chen, L. T., Reungwetwattana, T., Van Cutsem, E., Yeh, K. H., Ciombor, K., Finn, R. S., Patel, A., Sen, S., Porter, D., Isaacs, R., Zhu, A. X., Abou-Alfa, G. K. & Bekaii-Saab, T. 2018. Phase II Study of BGJ398 in Patients With FGFR-Altered Advanced Cholangiocarcinoma. *J Clin Oncol,* 36**,** 276-282.

Javle, M., Roychowdhury, S., Kelley, R. K., Sadeghi, S., Macarulla, T., Weiss, K. H., Waldschmidt, D. T., Goyal, L., Borbath, I., El-Khoueiry, A., Borad, M. J., Yong, W. P., Philip, P. A., Bitzer, M., Tanasanvimon, S., Li, A., Pande, A., Soifer, H. S., Shepherd, S. P., Moran, S., Zhu, A. X., Bekaii-Saab, T. S. & Abou-Alfa, G. K. 2021. Infigratinib (BGJ398) in previously treated patients with advanced or metastatic cholangiocarcinoma with FGFR2 fusions or rearrangements: mature results from a multicentre, open-label, single-arm, phase 2 study. *Lancet Gastroenterol Hepatol,* 6**,** 803-815.

Juntermanns, B., Kaiser, G. M., Itani Gutierrez, S., Heuer, M., Buechter, M., Kahraman, A., Reis, H., Kasper, S., Paul, A. & Fingas, C. D. 2018. [CA19-9 in intrahepatic cholangiocarcinoma : A diagnostic and prognostic armamentarium?]. *Chirurg,* 89**,** 466-471.

Kang, C. 2021. Infigratinib: First Approval. *Drugs,* 81**,** 1355-1360.

Katoh, M. 2016. Therapeutics Targeting FGF Signaling Network in Human Diseases. *Trends Pharmacol Sci,* 37**,** 1081-1096.

Katoh, M. 2019. Fibroblast growth factor receptors as treatment targets in clinical oncology. *Nat Rev Clin Oncol,* 16**,** 105-122.

Kelley, R. K., Bridgewater, J., Gores, G. J. & Zhu, A. X. 2020. Systemic therapies for intrahepatic cholangiocarcinoma. *J Hepatol,* 72**,** 353-363.

Kendre, G., Marhenke, S., Lorz, G., Becker, D., Reineke-Plaass, T., Poth, T., Murugesan, K., Kuhnel, F., Woller, N., Wirtz, R. M., Pich, A., Marquardt, J. U., Saborowski, M., Vogel, A. & Saborowski, A. 2021. The co-mutational spectrum determines the therapeutic response in murine FGFR2 fusion - driven cholangiocarcinoma. *Hepatology*.

Khan, S. A., Davidson, B. R., Goldin, R. D., Heaton, N., Karani, J., Pereira, S. P., Rosenberg, W. M., Tait, P., Taylor-Robinson, S. D., Thillainayagam, A. V., Thomas, H. C., Wasan, H. & British Society of, G. 2012. Guidelines for the diagnosis and treatment of cholangiocarcinoma: an update. *Gut,* 61**,** 1657-69.

King, G. & Javle, M. 2021. FGFR Inhibitors: Clinical Activity and Development in the Treatment of Cholangiocarcinoma. *Curr Oncol Rep,* 23**,** 108.

Kirstein, M. M. & Vogel, A. 2016. Epidemiology and Risk Factors of Cholangiocarcinoma. *Visc Med,* 32**,** 395-400.

Krook, M. A., Bonneville, R., Chen, H. Z., Reeser, J. W., Wing, M. R., Martin, D. M., Smith, A. M., Dao, T., Samorodnitsky, E., Paruchuri, A., Miya, J., Baker, K. R., Yu, L., Timmers, C., Dittmar, K., Freud, A. G., Allenby, P. & Roychowdhury, S. 2019. Tumor heterogeneity and acquired drug resistance in FGFR2-fusion-positive cholangiocarcinoma through rapid research autopsy. *Cold Spring Harb Mol Case Stud,* 5.

Krook, M. A., Lenyo, A., Wilberding, M., Barker, H., Dantuono, M., Bailey, K. M., Chen, H. Z., Reeser, J. W., Wing, M. R., Miya, J., Samorodnitsky, E., Smith, A. M., Dao, T., Martin, D. M., Ciombor, K. K., Hays, J., Freud, A. G. & Roychowdhury, S. 2020. Efficacy of FGFR Inhibitors and Combination Therapies for Acquired Resistance in FGFR2-Fusion Cholangiocarcinoma. *Mol Cancer Ther,* 19**,** 847-857.

Lamarca, A., Barriuso, J., McNamara, M. G. & Valle, J. W. 2020. Molecular targeted therapies: Ready for "prime time" in biliary tract cancer. *J Hepatol,* 73**,** 170-185.

Li, F., Meyer, A. N., Peiris, M. N., Nelson, K. N. & Donoghue, D. J. 2020. Oncogenic fusion protein FGFR2-PPHLN1: Requirements for biological activation, and efficacy of inhibitors. *Transl Oncol,* 13**,** 100853.

Li, F., Peiris, M. N. & Donoghue, D. J. 2019. Functions of FGFR2 corrupted by translocations in intrahepatic cholangiocarcinoma. *Cytokine Growth Factor Rev*.

Li, J. L. & Luo, P. 2020. MiR-140-5p and miR-92a-3p suppress the cell proliferation, migration and invasion and promoted apoptosis in Wilms' tumor by targeting FRS2. *Eur Rev Med Pharmacol Sci,* 24**,** 97-108.

Li, Q., Alsaidan, O. A., Ma, Y., Kim, S., Liu, J., Albers, T., Liu, K., Beharry, Z., Zhao, S., Wang, F., Lebedyeva, I. & Cai, H. 2018. Pharmacologically targeting the myristoylation of the scaffold protein FRS2alpha inhibits FGF/FGFR-mediated oncogenic signaling and tumor progression. *J Biol Chem,* 293**,** 6434-6448.

Lin, J., Shi, J., Guo, H., Yang, X., Jiang, Y., Long, J., Bai, Y., Wang, D., Yang, X., Wan, X., Zhang, L., Pan, J., Hu, K., Guan, M., Huo, L., Sang, X., Wang, K. & Zhao, H. 2019. Alterations in DNA Damage Repair Genes in Primary Liver Cancer. *Clin Cancer Res,* 25**,** 4701-4711.

Liu, Z., Chen, O., Wall, J. B. J., Zheng, M., Zhou, Y., Wang, L., Vaseghi, H. R., Qian, L. & Liu, J. 2017. Systematic comparison of 2A peptides for cloning multi-genes in a polycistronic vector. *Sci Rep,* 7**,** 2193.

Mahipal, A., Tella, S. H., Kommalapati, A., Anaya, D. & Kim, R. 2019. FGFR2 genomic aberrations: Achilles heel in the management of advanced cholangiocarcinoma. *Cancer Treat Rev,* 78**,** 1-7.

Mahipal, A., Tella, S. H., Kommalapati, A., Yu, J. & Kim, R. 2020. Prevention and treatment of FGFR inhibitor-associated toxicities. *Crit Rev Oncol Hematol,* 155**,** 103091.

Mahmood, T. & Yang, P. C. 2012. Western blot: technique, theory, and trouble shooting. *N Am J Med Sci,* 4**,** 429-34.

Matsuki, M., Hoshi, T., Yamamoto, Y., Ikemori-Kawada, M., Minoshima, Y., Funahashi, Y. & Matsui, J. 2018. Lenvatinib inhibits angiogenesis and tumor fibroblast growth factor signaling pathways in human hepatocellular carcinoma models. *Cancer Med,* 7**,** 2641-2653.

Miyabayashi, K., Ijichi, H., Mohri, D., Tada, M., Yamamoto, K., Asaoka, Y., Ikenoue, T., Tateishi, K., Nakai, Y., Isayama, H., Morishita, Y., Omata, M., Moses, H. L. & Koike, K. 2013. Erlotinib prolongs survival in pancreatic

cancer by blocking gemcitabine-induced MAPK signals. *Cancer Res,* 73**,** 2221-34.

Nakamura, H., Arai, Y., Totoki, Y., Shirota, T., Elzawahry, A., Kato, M., Hama, N., Hosoda, F., Urushidate, T., Ohashi, S., Hiraoka, N., Ojima, H., Shimada, K., Okusaka, T., Kosuge, T., Miyagawa, S. & Shibata, T. 2015. Genomic spectra of biliary tract cancer. *Nat Genet,* 47**,** 1003-10.

Nguyen, D. X., Bos, P. D. & Massague, J. 2009. Metastasis: from dissemination to organ-specific colonization. *Nat Rev Cancer,* 9**,** 274-84.

Oh, D.-Y., He, A. R., Qin, S., Chen, L.-T., Okusaka, T., Vogel, A., Kim, J. W., Suksomboon charoen, T., Lee, M. A., Kitano, M., Burris, H., Bouattour, M., Tanasanvimon, S., McNamara, M. G., Zaucha, R., Avallone, A., Tan, B., Cundom, J., Lee, C.-k., Takahashi, H., Ikeda, M., Chen, J.-S., Wang, J., Makowsky, M., Rokutanda, N., He, P., Kurland, J. F., Cohen, G. & Valle, J. W. 2022. Durvalumab plus Gemcitabine and Cisplatin in Advanced Biliary Tract Cancer. *NEJM Evidence,* 1**,** EVIDoa2200015.

Ornitz, D. M. & Itoh, N. 2015. The Fibroblast Growth Factor signaling pathway. *Wiley Interdiscip Rev Dev Biol,* 4**,** 215-66.

Patani, H., Bunney, T. D., Thiyagarajan, N., Norman, R. A., Ogg, D., Breed, J., Ashford, P., Potterton, A., Edwards, M., Williams, S. V., Thomson, G. S., Pang, C. S., Knowles, M. A., Breeze, A. L., Orengo, C., Phillips, C. & Katan, M. 2016. Landscape of activating cancer mutations in FGFR kinases and their differential responses to inhibitors in clinical use. *Oncotarget,* 7**,** 24252-68.

Pierrat, B., Simonen, M., Cueto, M., Mestan, J., Ferrigno, P. & Heim, J. 2001. SH3GLB, a new endophilin-related protein family featuring an SH3 domain. *Genomics,* 71**,** 222-34.

Plotnikov, A. N., Hubbard, S. R., Schlessinger, J. & Mohammadi, M. 2000. Crystal structures of two FGF-FGFR complexes reveal the determinants of ligand-receptor specificity. *Cell,* 101**,** 413-24.

Primrose, J. N., Fox, R. P., Palmer, D. H., Malik, H. Z., Prasad, R., Mirza, D., Anthony, A., Corrie, P., Falk, S., Finch-Jones, M., Wasan, H., Ross, P., Wall, L., Wadsley, J., Evans, J. T. R., Stocken, D., Praseedom, R., Ma, Y. T., Davidson, B., Neoptolemos, J. P., Iveson, T., Raftery, J., Zhu, S., Cunningham, D., Garden, O. J., Stubbs, C., Valle, J. W., Bridgewater, J. & group, B. s. 2019. Capecitabine compared with observation in resected biliary tract cancer (BILCAP): a randomised, controlled, multicentre, phase 3 study. *Lancet Oncol,* 20**,** 663-673.

Rizvi, S. & Gores, G. J. 2013. Pathogenesis, diagnosis, and management of cholangiocarcinoma. *Gastroenterology,* 145**,** 1215-29.

Rizvi, S., Khan, S. A., Hallemeier, C. L., Kelley, R. K. & Gores, G. J. 2018. Cholangiocarcinoma - evolving concepts and therapeutic strategies. *Nat Rev Clin Oncol,* 15**,** 95-111.

Rodon, J., Soria, J. C., Berger, R., Miller, W. H., Rubin, E., Kugel, A., Tsimberidou, A., Saintigny, P., Ackerstein, A., Brana, I., Loriot, Y., Afshar, M., Miller, V., Wunder, F., Bresson, C., Martini, J. F., Raynaud, J., Mendelsohn, J., Batist, G., Onn, A., Tabernero, J., Schilsky, R. L., Lazar, V., Lee, J. J. & Kurzrock, R. 2019. Genomic and transcriptomic profiling expands precision cancer medicine: the WINTHER trial. *Nat Med,* 25**,** 751-758.

Roskoski, R., Jr. 2020. The role of fibroblast growth factor receptor (FGFR) protein-tyrosine kinase inhibitors in the treatment of cancers including those of the urinary bladder. *Pharmacol Res,* 151**,** 104567.

Schlessinger, J. 2000. Cell signaling by receptor tyrosine kinases. *Cell,* 103**,** 211-25.

Sia, D., Losic, B., Moeini, A., Cabellos, L., Hao, K., Revill, K., Bonal, D., Miltiadous, O., Zhang, Z., Hoshida, Y., Cornella, H., Castillo-Martin, M., Pinyol, R., Kasai, Y., Roayaie, S., Thung, S. N., Fuster, J., Schwartz, M. E., Waxman, S., Cordon-Cardo, C., Schadt, E., Mazzaferro, V. & Llovet, J. M. 2015. Massive parallel sequencing uncovers actionable FGFR2-PPHLN1 fusion and ARAF mutations in intrahepatic cholangiocarcinoma. *Nat Commun,* 6**,** 6087.

Silverman, I. M., Hollebecque, A., Friboulet, L., Owens, S., Newton, R. C., Zhen, H., Feliz, L., Zecchetto, C., Melisi, D. & Burn, T. C. 2020. Clinicogenomic analysis of FGFR2-rearranged cholangiocarcinoma identifies correlates of response and mechanisms of resistance to pemigatinib. *Cancer Discov*.

Skehan, P., Storeng, R., Scudiero, D., Monks, A., McMahon, J., Vistica, D., Warren, J. T., Bokesch, H., Kenney, S. & Boyd, M. R. 1990. New colorimetric cytotoxicity assay for anticancer-drug screening. *J Natl Cancer Inst,* 82**,** 1107-12.

Spahn, S., Kleinhenz, F., Shevchenko, E., Stahl, A., Rasen, Y., Geisler, C., Ruhm, K., Klaumuenzer, M., Kronenberger, T., Laufer, S. A., Sundberg-Malek, H., Bui, K. C., Horger, M., Biskup, S., Schulze-Osthoff, K., Templin, M., Malek, N. P., Poso, A. & Bitzer, M. 2024. The molecular interaction pattern of lenvatinib enables inhibition of wild-type or kinase-mutated FGFR2-driven cholangiocarcinoma. *Nat Commun,* 15**,** 1287.

Szymczak, A. L. & Vignali, D. A. 2005. Development of 2A peptide-based strategies in the design of multicistronic vectors. *Expert Opin Biol Ther,* 5**,** 627-38.

Tan, F. H., Putoczki, T. L., Stylli, S. S. & Luwor, R. B. 2019. Ponatinib: a novel multi-tyrosine kinase inhibitor against human malignancies. *Onco Targets Ther,* 12**,** 635-645.

Tan, L., Wang, J., Tanizaki, J., Huang, Z., Aref, A. R., Rusan, M., Zhu, S. J., Zhang, Y., Ercan, D., Liao, R. G., Capelletti, M., Zhou, W., Hur, W., Kim, N., Sim, T., Gaudet, S., Barbie, D. A., Yeh, J. R., Yun, C. H., Hammerman, P. S., Mohammadi, M., Janne, P. A. & Gray, N. S. 2014. Development of covalent inhibitors that can overcome resistance to first-generation FGFR kinase inhibitors. *Proc Natl Acad Sci U S A,* 111**,** E4869-77.

Tariq, N. U., McNamara, M. G. & Valle, J. W. 2019. Biliary tract cancers: current knowledge, clinical candidates and future challenges. *Cancer Manag Res,* 11**,** 2623-2642.

Tolcher, A. W., Papadopoulos, K. P., Patnaik, A., Wilson, K., Thayer, S., Zanghi, J., Gemo, A. T., Kavanaugh, W. M., Keer, H. N. & LoRusso, P. M. 2016. A phase I, first in human study of FP-1039 (GSK3052230), a novel FGF ligand trap, in patients with advanced solid tumors. *Ann Oncol,* 27**,** 526-32.

Touat, M., Ileana, E., Postel-Vinay, S., Andre, F. & Soria, J. C. 2015. Targeting FGFR Signaling in Cancer. *Clin Cancer Res,* 21**,** 2684-94.

Towbin, H., Staehelin, T. & Gordon, J. 1979. Electrophoretic transfer of proteins from polyacrylamide gels to nitrocellulose sheets: procedure and some applications. *Proc Natl Acad Sci U S A,* 76**,** 4350-4.

Turner, N. & Grose, R. 2010. Fibroblast growth factor signalling: from development to cancer. *Nat Rev Cancer,* 10**,** 116-29.

Tyson, G. L. & El-Serag, H. B. 2011. Risk factors for cholangiocarcinoma. *Hepatology,* 54**,** 173-84.

U.S. Food and Drug Administration. 2019. *FDA approves first targeted therapy for metastatic bladder cancer* [Online]. Available: https://www.fda.gov/news-events/press-announcements/fda-approves-first-targeted-therapy-metastatic-bladder-cancer [Accessed 21.02.2023].

U.S. Food and Drug Administration. 2020. *FDA grants accelerated approval to Pemigatinib for cholangiocarcinoma with an FGFR2 rearrangement or fusion* [Online]. Available: https://www.fda.gov/drugs/resources-information-approved-drugs/fda-grants-accelerated-approval-pemigatinib-cholangiocarcinoma-fgfr2-rearrangement-or-fusion [Accessed 21.02.2023].

U.S. Food and Drug Administration. 2021. *FDA grants accelerated approval to infigratinib for metastatic cholangiocarcinoma* [Online]. Available: https://www.fda.gov/drugs/resources-information-approved-drugs/fda-

grants-accelerated-approval-infigratinib-metastatic-cholangiocarcinoma [Accessed 21.02.2023].

U.S. Food and Drug Administration. 2022. *FDA grants accelerated approval to futibatinib for cholangiocarcinoma* [Online]. Available: https://www.fda.gov/drugs/resources-information-approved-drugs/fda-grants-accelerated-approval-futibatinib-cholangiocarcinoma [Accessed 21.02.2023].

Ueno, M., Ikeda, M., Sasaki, T., Nagashima, F., Mizuno, N., Shimizu, S., Ikezawa, H., Hayata, N., Nakajima, R. & Morizane, C. 2020. Phase 2 study of lenvatinib monotherapy as second-line treatment in unresectable biliary tract cancer: primary analysis results. *BMC Cancer,* 20**,** 1105.

Valencia, T., Joseph, A., Kachroo, N., Darby, S., Meakin, S. & Gnanapragasam, V. J. 2011. Role and expression of FRS2 and FRS3 in prostate cancer. *BMC Cancer,* 11**,** 484.

Valle, J., Wasan, H., Palmer, D. H., Cunningham, D., Anthoney, A., Maraveyas, A., Madhusudan, S., Iveson, T., Hughes, S., Pereira, S. P., Roughton, M., Bridgewater, J. & Investigators, A. B. C. T. 2010. Cisplatin plus gemcitabine versus gemcitabine for biliary tract cancer. *N Engl J Med,* 362**,** 1273-81.

Valle, J. W., Borbath, I., Khan, S. A., Huguet, F., Gruenberger, T., Arnold, D. & Committee, E. G. 2016. Biliary cancer: ESMO Clinical Practice Guidelines for diagnosis, treatment and follow-up. *Ann Oncol,* 27**,** v28-v37.

Valle, J. W., Kelley, R. K., Nervi, B., Oh, D. Y. & Zhu, A. X. 2021. Biliary tract cancer. *Lancet,* 397**,** 428-444.

Valle, J. W., Lamarca, A., Goyal, L., Barriuso, J. & Zhu, A. X. 2017. New Horizons for Precision Medicine in Biliary Tract Cancers. *Cancer Discov,* 7**,** 943-962.

van Brummelen, E. M. J., Levchenko, E., Domine, M., Fennell, D. A., Kindler, H. L., Viteri, S., Gadgeel, S., Lopez, P. G., Kostorov, V., Morgensztern, D., Orlov, S., Zauderer, M. G., Vansteenkiste, J. F., Baker-Neblett, K., Vasquez, J., Wang, X., Bellovin, D. I., Schellens, J. H. M., Yan, L., Mitrica, I., DeYoung, M. P. & Trigo, J. 2020. A phase Ib study of GSK3052230, an FGF ligand trap in combination with pemetrexed and cisplatin in patients with malignant pleural mesothelioma. *Invest New Drugs,* 38**,** 457-467.

Vogel, A., Segatto, O., Stenzinger, A. & Saborowski, A. 2023. FGFR2 Inhibition in Cholangiocarcinoma. *Annu Rev Med,* 74**,** 293-306.

Von Hoff, D. D. 1998. There are no bad anticancer agents, only bad clinical trial designs--twenty-first Richard and Hinda Rosenthal Foundation Award Lecture. *Clinical Cancer Research,* 4**,** 1079-1086.

Wainberg, Z. A., Enzinger, P. C., Kang, Y.-K., Yamaguchi, K., Qin, S., Lee, K.-W., Oh, S. C., Li, J., Turk, H. M., Teixeira, A. C., Cardellino, G. G., Guardeño, R., Mitra, S., Yang, Y., Collins, H. & Catenacci, D. V. T. 2021. Randomized double-blind placebo-controlled phase 2 study of bemarituzumab combined with modified FOLFOX6 (mFOLFOX6) in first-line (1L) treatment of advanced gastric/gastroesophageal junction adenocarcinoma (FIGHT). *Journal of Clinical Oncology,* 39**,** 160-160.

Wang, Y., Ding, X., Wang, S., Moser, C. D., Shaleh, H. M., Mohamed, E. A., Chaiteerakij, R., Allotey, L. K., Chen, G., Miyabe, K., McNulty, M. S., Ndzengue, A., Barr Fritcher, E. G., Knudson, R. A., Greipp, P. T., Clark, K. J., Torbenson, M. S., Kipp, B. R., Zhou, J., Barrett, M. T., Gustafson, M. P., Alberts, S. R., Borad, M. J. & Roberts, L. R. 2016. Antitumor effect of FGFR inhibitors on a novel cholangiocarcinoma patient derived xenograft mouse model endogenously expressing an FGFR2-CCDC6 fusion protein. *Cancer Lett,* 380**,** 163-73.

Weaver, A. & Bossaer, J. B. 2021. Fibroblast growth factor receptor (FGFR) inhibitors: A review of a novel therapeutic class. *Journal of Oncology Pharmacy Practice,* 27**,** 702-710.

Wu, Y. M., Su, F., Kalyana-Sundaram, S., Khazanov, N., Ateeq, B., Cao, X., Lonigro, R. J., Vats, P., Wang, R., Lin, S. F., Cheng, A. J., Kunju, L. P., Siddiqui, J., Tomlins, S. A., Wyngaard, P., Sadis, S., Roychowdhury, S., Hussain, M. H., Feng, F. Y., Zalupski, M. M., Talpaz, M., Pienta, K. J., Rhodes, D. R., Robinson, D. R. & Chinnaiyan, A. M. 2013. Identification of targetable FGFR gene fusions in diverse cancers. *Cancer Discov,* 3**,** 636-47.

Yamamoto, Y., Matsui, J., Matsushima, T., Obaishi, H., Miyazaki, K., Nakamura, K., Tohyama, O., Semba, T., Yamaguchi, A., Hoshi, S. S., Mimura, F., Haneda, T., Fukuda, Y., Kamata, J. I., Takahashi, K., Matsukura, M., Wakabayashi, T., Asada, M., Nomoto, K. I., Watanabe, T., Dezso, Z., Yoshimatsu, K., Funahashi, Y. & Tsuruoka, A. 2014. Lenvatinib, an angiogenesis inhibitor targeting VEGFR/FGFR, shows broad antitumor activity in human tumor xenograft models associated with microvessel density and pericyte coverage. *Vasc Cell,* 6**,** 18.

Yamanaka, T., Harimoto, N., Yokobori, T., Muranushi, R., Hoshino, K., Hagiwara, K., Gantumur, D., Handa, T., Ishii, N., Tsukagoshi, M., Igarashi, T., Tanaka, H., Watanabe, A., Kubo, N., Araki, K. & Shirabe, K. 2020. Nintedanib inhibits intrahepatic cholangiocarcinoma aggressiveness via suppression of cytokines extracted from activated cancer-associated fibroblasts. *Br J Cancer,* 122**,** 986-994.

7. Explanation of own contribution

Die Arbeit wurde im Universitätsklinikum Tübingen in der Medizinischen Klinik – Innere Medizin I (Gastroenterologie, Gastrointestinale Onkologie, Hepatologie, Infektiologie und Geriatrie) unter Betreuung von Professor Dr. Michael Bitzer und Dr. Stephan Spahn durchgeführt.

Die Konzeption der Studie erfolgte durch Professor Dr. Michael Bitzer, Stellv. Ärztlicher Direktor und Dr. Stephan Spahn, Assistenzarzt.

Die klinischen Verläufe der Patient*innen wurden nach Anleitung durch Dr. Stephan Spahn von mir selbst aufgearbeitet.

Das Design der Plasmide erfolgte durch Dr. Stephan Spahn und Dr. Bui Khac Cuong.

Die *in vitro* Versuche wurden nach Einarbeitung durch die Labormitglieder Dr. Stephan Spahn, Louise Kaldjob-Heinrich und Christine Geisler von mir eigenständig durchgeführt.

Die statistische Auswertung wurde nach Anleitung durch Dr. Stephan Spahn von mir selbst durchgeführt.

Ich versichere, das Manuskript selbständig verfasst zu haben und keine weiteren als die von mir angegebenen Quellen verwendet zu haben.

Teile dieser Arbeit sind in einem Artikel mit dem Titel „The molecular interaction pattern of lenvatinib enables inhibition of wild-type or kinase-mutated FGFR2-driven cholangiocarcinoma“ im Journal „Nature Communications“ veröffentlicht worden (s.u.).

Tübingen, den 18.03.2025

8. Own publications

Spahn, S.*, **Kleinhenz, F.***, Shevchenko, E., Stahl, A., Rasen, Y., Geisler, C., Ruhm, K., Klaumuenzer, M., Kronenberger, T., Laufer, S. A., Sundberg-Malek, H., Bui, K. C., Horger, M., Biskup, S., Schulze-Osthoff, K., Templin, M., Malek, N. P., Poso, A. & Bitzer, M. 2024. The molecular interaction pattern of lenvatinib enables inhibition of wild-type or kinase-mutated FGFR2-driven cholangiocarcinoma. *Nat Commun,* 15**,** 1287

https://doi.org/10.1038/s41467-024-45247-6

*These authors contributed equally: Stephan Spahn, Fabian Kleinhenz

9. Acknowledgements

Mein besonderer Dank gilt meinem Doktorvater Prof. Dr. Michael Bitzer, der mir dieses spannende Thema anvertraut hat und mir durch seine freundliche Art einen sehr angenehmen Einstieg in die Welt der Forschung bereitet hat. Durch stets konstruktive Kritik, passende Anregungen und weiterführende Ideen konnte ich rasch und nachhaltig die Begeisterung für translationale Forschung teilen.

Ganz herzlich möchte ich meinem Betreuer Dr. Stephan Spahn für die rundum ausgezeichnete Betreuung danken. Ohne Ihn wäre diese Arbeit und die eingereichte Veröffentlichung nicht möglich gewesen. Er hat mich in alle Aspekte der Forschung eingearbeitet und stand mir auch trotz zeitweiser großer örtlicher Distanz bei allen Fragen stets zur Seite.

Außerdem möchte ich mich bei Christine Geisler und Louise Kaldjob-Heinrich bedanken, die mich in zahlreiche Labormethoden eingeführt haben und mir im Laboralltag eine unglaubliche Hilfe waren. Dank Ihnen war die Arbeit im Labor außerdem immer von guter Laune und Leichtigkeit geprägt.

Allen Mitgliedern der Arbeitsgruppen Bitzer und Malek danke ich für die angenehme Arbeitsatmosphäre und die ständige Bereitschaft mir mit Rat und Tat auszuhelfen.

Dem IZKF Promotionskolleg danke ich für deren finanzielle Unterstützung und deren ausgesprochen gutes Betreuungsprogramm.

Ein großer Dank gilt meinen Freunden Daniel, Johannes, Felix und Henning für die willkommene Ablenkung in meiner Freizeit.

Zuletzt danke ich vor allem meinen Eltern, meinen Geschwistern und meiner Freundin Annalena für die unvergleichliche Unterstützung zu jeder Zeit und in jeder erdenklichen Hinsicht.